

KRISTIAN SEMJONOV

Development of pharmaceutical
quench-cooled molten and
melt-electrospun solid dispersions for
poorly water-soluble indomethacin



KRISTIAN SEMJONOV

Development of pharmaceutical
quench-cooled molten and
melt-electrospun solid dispersions for
poorly water-soluble indomethacin



Institute of Pharmacy, Faculty of Medicine, University of Tartu, Estonia

This dissertation has been accepted for the commencement of the degree of Doctor of Philosophy in Pharmacy on August 29, 2018 by the Council of the Faculty of Medicine, University of Tartu, Estonia.

Supervisors: Professor Jyrki Heinämäki, PhD (Pharm)
Institute of Pharmacy, Faculty of Medicine
University of Tartu, Estonia

Associate Professor Karin Kogermann, PhD (Pharm)
Institute of Pharmacy, Faculty of Medicine
University of Tartu, Estonia

Senior Research Fellow Ivo Laidmäe, PhD (Pharm)
Institute of Pharmacy, Faculty of Medicine
University of Tartu, Estonia

Reviewed by: Professor Ursel Soomets, MSc, PhD (Neurochem)
Department of Biochemistry, Institute of Biomedicine and
Translational Medicine, Faculty of Medicine
University of Tartu, Estonia

Associate Professor Uno Mäeorg, MSc, PhD (Chem)
Institute of Chemistry, Faculty of Science and Technology
University of Tartu, Estonia

Opponent: Professor Ingunn Tho, MSc, PhD (Pharm)
Department of Pharmacy
University of Oslo, Norway

Commencement: October 26, 2018

This study was supported by the European Union through the European Social Fund (grants ETF7980, PUT1088, SF0180042s09 and IUT-34-18).

ISSN 1024-395X
ISBN 978-9949-77-846-1 (print)
ISBN 978-9949-77-847-8 (pdf)

Copyright: Kristian Semjonov, 2018



University of Tartu Press
www.tyk.ee

CONTENTS

LIST OF ORIGINAL PUBLICATIONS	7
ABBREVIATIONS	8
1. INTRODUCTION	10
2. LITERATURE REVIEW	12
2.1. Challenges of poorly water-soluble drugs	12
2.1.1. Theory of solubility/dissolution rate	12
2.1.2. Effect of solid-state form on the solubility/dissolution behavior of drug	13
2.1.3. Methods to improve drug solubility and dissolution rate	14
2.2. Solid dispersions	15
2.2.1. Preparation methods of solid dispersions	17
2.2.1.1. Quench cooling of the melt	18
2.2.1.2. Melt-electrospinning	18
2.2.2. Characterization of solid dispersions	21
2.2.3. Physical stability of solid dispersions	22
2.2.4. Pharmaceutical application of solid dispersion	23
3. SUMMARY OF THE LITERATURE	24
4. AIMS OF THE STUDY	25
5. EXPERIMENTAL	26
5.1. Materials	26
5.1.1. Indomethacin	26
5.1.2. Soluplus®	26
5.1.3. Xylitol	26
5.2. Methods for fabricating physical mixtures and solid dispersions	27
5.2.1. Preparation of physical mixtures (I–II)	27
5.2.2. Preparation of solid dispersions by melt quench cooling (I–II)	27
5.2.3. Melt-electrospinning (III)	27
5.3. Characterization of physical mixtures and solid dispersions	28
5.3.1. Scanning electron microscopy (I–III)	28
5.3.2. X-ray powder diffraction (I–III)	28
5.3.3. Fourier-transform infrared spectroscopy (I–III)	28
5.3.4. Near-infrared spectroscopy (III)	28
5.3.5. Nuclear magnetic resonance spectroscopy (III)	29
5.3.6. Differential scanning calorimetry (I–III)	29
5.3.7. Thermogravimetric analysis (II)	29
5.3.8. High-performance liquid chromatography (III)	30
5.3.9. Karl-Fischer titration (II)	30
5.3.10. Moisture sorption and contact angle measurements (II)	30

5.3.11. Powder flow test (II)	31
5.3.12. Dissolution test (II–III).....	31
5.4. Storage stability studies (I).....	31
5.5. Data analysis.....	32
6. RESULTS AND GENERAL DISCUSSION	33
6.1. Classification of solid dispersions (I–III)	33
6.2. Quench-cooled molten solid dispersions of indomethacin and Soluplus® (I, II).....	34
6.2.1. Physical solid state drug-carrier interactions (I).....	34
6.2.2. Particle size, shape and surface morphology (I, II).....	37
6.2.3. Powder flow (II).....	38
6.2.4. Moisture content, sorption and wetting properties (II).....	39
6.3. Quench-cooled molten solid dispersions of indomethacin and xylitol (I, II)	42
6.3.1. Physical solid state and drug-carrier interactions (I).....	42
6.3.2. Particle size, shape and surface morphology (I, II).....	42
6.3.3. Powder flow (II).....	43
6.3.4. Moisture content, sorption and wetting properties (II).....	44
6.4. Melt-electrospun fibrous solid dispersions of indomethacin and Soluplus® (III).....	45
6.4.1. Physical solid state and drug-carrier interactions (III).....	45
6.4.2. Fiber diameter, shape and surface morphology (III).....	47
6.4.3. Moisture content (II)	49
6.4.4. Chemical and thermal stability (III).....	49
6.5. Dissolution in vitro (II–III).....	51
6.6. Physical storage stability of solid dispersions (I)	53
7. SUMMARY AND CONCLUSIONS.....	56
REFERENCES	57
SUMMARY IN ESTONIAN	66
ACKNOWLEDGEMENTS	71
PUBLICATIONS	73
CURRICULUM VITAE	110
ELULOOKIRJELDUS.....	111

LIST OF ORIGINAL PUBLICATIONS

Given thesis is based on the following original publications referred to in the text by Roman numerals (I–III):

- I **Semjonov, K.**, Kogermann K., Laidmäe I., Antikainen O., Strachan C. J., Ehlers H., Yliruusi J., Heinämäki J., 2017. The formation and physical stability of two-phase solid dispersion systems of indomethacin in supercooled molten mixtures with different matrix formers. *European Journal of Pharmaceutical Sciences*, 97, 237–246.
- II **Semjonov, K.**, Salm M., Lipiäinen T., Kogermann K., Lust A., Laidmäe I., Antikainen O., Strachan C. J., Ehlers H., Yliruusi J., Heinämäki J., 2018. Interdependence of particle surface properties and bulk powder behavior of indomethacin in quench-cooled molten two-phase solid dispersions. *International Journal of Pharmaceutics*, 541, 188–197.
- III **Semjonov, K.**, Lust A., Kogermann K., Laidmäe I., Maunu S. L., Hirvonen S. P., Yliruusi J., Nurk G., Lust E., Heinämäki J., 2018. Melt-electro-spinning as a method to improve the dissolution and physical stability of a poorly water-soluble drug. *European Journal of Pharmaceutical Sciences*, 121, 260–268.

Contribution of Kristian Semjonov to original publications (I–III):

Publication I: participation in study design; performing the experiments and data analysis; writing the paper.

Publication II: participation in study design; performing the experiments and data analysis; writing the paper.

Publication III: participation in study design; performing the experiments and data analysis; writing the paper.

ABBREVIATIONS

3D	Three-dimensional
API	Active pharmaceutical ingredient
ATR-FTIR	Fourier transform infrared spectroscopy equipped with attenuated total reflection
aw	Water activity
BCS	Biopharmaceutics Classification System
CD	Cyclodextrins
CDER	Center for Drug Evaluation and Research
Ct	Concentration at time t
dC/dt	Change in concentration with time
DSC	Differential scanning calorimetry
FDA	Food and Drug Administration
GFA	Glass forming ability
GI	Gastrointestinal tract
GS	Glass stability
HSM-PLM	Hot-stage microscopy coupled with polarized light microscope
HPMC	Hydroxypropylmethylcellulose
HPMCAS	Hydroxypropylmethylcellulose acetate succinate
ICH	International Conference on Harmonisation
IND	Indomethacin
KF	Karl-Fischer
LBF	Lipid based formulations
MES	Melt-electrospinning
MSF	Melt-electrospun fiber
NIR	Near-infrared
NMR	Nuclear magnetic resonance spectroscopy
PCL	Polycaprolactone
PEG	Polyethyleneglycole
Ph. Eur.	European Pharmacopoeia
PM	Physical mixture
PVP VA	Polyvinylpyrrolidone vinyl acetate
PWS	Poorly water soluble
QC	Quench cooling
RH	Relative humidity
RT	Room temperature
SD	Solid dispersion
SOL	Soluplus [®]
Tg	Glass transition temperature
TGA	Thermogravimetric analysis

T _m	Melting point
USP	United States Pharmacopeia
w _f	Weight of the sample after storage
w _i	Weight of the sample before storage
VT-XRPD	Variable-temperature X-ray powder diffraction
XYL	Xylitol

1. INTRODUCTION

Pharmaceutical dosage form design and product development requires a wide range of expertise and background knowledge. The working process starts from a disease target identification, active substance identification following with pharmacological/toxicological investigations, preformulation, final formulation development, and clinical trials in order to prove the safety and efficacy of the final product. Regulatory guidelines are intended for the pharmaceutical industry to support the product development and to assure the quality, safety and efficacy issues (CDER/FDA, 2015; CDER/FDA, 2007; ICH 2015). For example, extensive dissolution tests and stability studies are crucial for a successful product development and a drug product approval process.

Oral administration remains the main route for drug delivery. It is a simple, rapid, convenient and painless way of drug administration for a wide range of dosage forms, thus making it the most attracting one for the patients and pharmaceutical industry. It is generally known that aqueous solubility and gastrointestinal (GI) permeability are the key parameters controlling the rate and extent of drug absorption, although the onset of drug action is also affected by the complexation on target receptors. European Pharmacopoeia classifies the solubility without any solvent specification in terms of quantification, a soluble compound requires less than 1 ml or up to 30 ml of a solvent to be dissolved (“very soluble” / “freely soluble” / “soluble”), and compounds that need over 30 ml or more than 10 000 ml of a solvent have been termed as „sparingly soluble” / “slightly soluble” / “very slightly soluble” / “practically insoluble” (Ph. Eur. 9.0). Based on US Food and Drug Administration (FDA) guideline and classification, a drug is considered highly soluble when the highest dose strength is soluble in 250 mL or less of aqueous medium over the pH range of 1 to 6.8 (CDER/FDA, 2015). European Medicine Agency defines highly water-soluble drugs as drugs with a dose/solubility volume of less than or equal to 250 ml over a pH range of 1.2 to 6.8. Drugs not fulfilling these requirements are considered poorly water-soluble (European Medicines Agency, 2000). According to the Biopharmaceutics Classification System (BCS), drugs are categorized into the following four groups based on the abovementioned two parameters: high solubility-high permeability (BCS I); poor solubility-high permeability (BCS II); high solubility-poor permeability (BCS III); poor solubility-poor permeability (BCS IV) (Amidon et al., 1995). According to the literature, only 5% of new active substances can be placed in BCS I while 90% of such drugs are considered as poorly water-soluble (PWS) (BCS II and IV) (Williams et al., 2016). It has been reported that over 75% of drugs under the development or in the product pipeline are classified as PWS (Di et al., 2009). The development of advanced formulations, new excipients and manufacturing methods will foster the understanding of how to improve the aqueous solubility and dissolution rate of drugs, and hence the bioavailability of PWS drugs.

In the present PhD thesis, the principal hypothesis was that amorphous solid dispersions (SDs) prepared with Soluplus[®] (SOL) and xylitol (XYL) and using different methods of preparation improve the dissolution rate and stabilize an amorphous PWS drug (indomethacin, IND as a model drug). SOL is a novel amphiphilic graft co-polymer which was originally designed for hot-melt extrusion (BASF, 2010). XYL is a small molecule sugar polyol, which has just recently found its position as a pharmaceutical excipient. Quench cooling (QC) of the melt is a common approach along with the solvent evaporation method for SDs preparation. In addition to QC, melt-electrospinning (MES) can be regarded as another modification of traditional melting/fusion method for SD preparation. In the present study, MES was studied as a novel approach to prepare the advanced drug delivery systems for PWS drugs. Physicochemical characteristics and drug release from QC mixtures with different carriers SOL/XYL were investigated. The melt-electrospun fibers (MSFs) with their unique properties were investigated, and the key question was, whether they could accelerate the dissolution rate of such drug and improve its physicochemical stability within a novel dosage form. We showed that the produced MSFs of a PWS drug (IND) were physically stable and presented immediate drug release.

2. LITERATURE REVIEW

2.1. Challenges of poorly water-soluble drugs

The adoption of new formulation strategies for PWS drugs are currently of great interest, since the majority of new drug candidates emerging from the drug development pipeline are PWS compounds (Brough and Williams, 2013). The major reasons behind this phenomenon are an increased application of combinatorial chemistry, desire to achieve site-specific drug targeting, and high-throughput screening in non-aqueous media (Lipinski, 2000). According to Takagi et al. (2006), among top 200 drug products (parenteral and modified release excluded) 30–40% were composed of an active substance(s) categorized as practically insoluble (solubility <0.1 mg/ml). This leads to a number of concerns, since such drugs have extremely low absorption in the GI tract resulting in low oral bioavailability, and hence a limited therapeutic effect. To mitigate this problem, most often a time-consuming and expensive formulation development is needed. Promising formulation approaches are the formation of salts, cyclodextrins, polymorphs and co-crystal, particle size reduction, and use of surfactants, co-solvents and lipid based formulations (Brough and Williams, 2013; Gursoy and Benita, 2004; Hörter and Dressman, 1997; Jermain et al., 2018; Williams et al., 2016). As a separate technological approach, solid dispersions (SD) can be prepared, and to date SDs have found uses in many commercially marketed products (Table 2) and will be discussed in more detail in the following chapters. Herein, in this thesis, SDs prepared via melting/co-fusion showed its potential as a means for improving the aqueous solubility of PWS drugs.

2.1.1. Theory of solubility/dissolution rate

Aqueous solubility of active pharmaceutical ingredient (API) is a key parameter to be resolved in the pharmaceutical product development and in the subsequent preclinical and clinical settings. The solubility of API is affected by the intermolecular and intramolecular forces, lipophilicity, ion charges, and H-bonding with a dissolution medium (Lipinski, 2000). The dissolution rate is driven by the concentration gradient between the concentration on the particle surface and concentration in the bulk medium (Williams et al., 2013). Solubility and dissolution rate relationship is characterized by Noyes-Whitney (1987) equation (Eq. 1):

$$\frac{dC}{dt} = \frac{DA}{h} (C_s - C_t) \quad (\text{Eq. 1})$$

where dC/dt is the dissolution rate, D the diffusion coefficient, A the surface area, h the diffusion layer thickness, C_s the saturation solubility of the drug in

medium and C_t the amount of drug in solution at time t (Noyes and Whitney, 1897).

According to Eq. 1, PWS drugs have low solubility (C_s), and consequently, this results in a low concentration gradient ($C_s - C_t$) and low dissolution rate. Furthermore, PWS drugs possess a poor *in vitro*/ *in vivo* correlation and these drugs are also prone to interact with food (Gu et al., 2007).

2.1.2. Effect of solid-state form on the solubility/dissolution behavior of drug

The API may exist in crystalline (usually with different crystal modifications) or amorphous form. In crystalline solids, molecules have a three dimensional (3D) long-range order and are packed very tightly, with a repeating unit cell. The strong intermolecular interactions within the crystal lattice result in the reduced mobility of the molecules and higher physical stability (lower solubility, dissolution and disintegration rate) (Zhang et al., 2004). Crystalline APIs can exist as polymorphs, solvates or hydrates. Furthermore, the co-crystals and salts of APIs may be prepared. Polymorphic systems are usually divided into two groups, enantiotropic and monotropic (Burger and Ramberger, 1979a). In enantiotropic systems, reversible transitions can occur between polymorphs at defined transition temperature below melting point (T_m). In monotropic systems, no reversible transitions between polymorphs can take place below melting point (e.g., indomethacin, IND). It is also known that the most stable polymorph at specified environmental conditions has higher density values (Burger and Ramberger, 1979b). Polymorphs show also different physico-chemical properties such as chemical and physical stability, flowability, hygroscopicity and tableting behavior, solubility, and dissolution rate (Haleblian and McCrone, 1969). The human studies have shown that polymorphism affects the bioavailability, oral drug absorption and hence drug therapy efficacy (Singhal and Curatolo, 2004). Common ways for preparing the amorphous form of API are solvent and fusion/melting methods, which will be discussed in more detailed in the following sub-chapters. Amorphous materials lack highly ordered three dimensional (3D) crystal structure, thus these materials possess lower intermolecular interactions. Due to a higher free energy level, the API in an amorphous form has higher apparent solubility, but it is less stable (solution or solid-state mediated) resulting in the recrystallization of less soluble crystal form (Burger & Ramberger 1979b). The present stability changes are solution or solid state mediated. The risk is especially high with narrow therapeutic window APIs (e.g., carbamazepine) which undergo transformation during the dissolution to a metastable form (from anhydrate to hydrate), compromising solubility, dissolution rate and therapeutic efficiency (Edwards et al., 2001; Murphy et al., 2002). In case of carbamazepine this may lead to epilepsy treatment failures. Three mechanisms are involved in solution mediated transformations namely (1) dissolution of metastable form, (2) molecular

rearrangement to stable phase, (3) and subsequent growth of stable phase (Murphy et al., 2002). Solid state mediated transformation may occur during the manufacturing or storage. The mechanical stress (grinding, compression) applied to crystal structure, producing amorphous regions results in improved dissolution rate (Mosharraf and Nyström, 1995). Amorphous solids prepared by different methods will have different glass transition temperature (T_g), relaxation times and kinetics affecting their chemical and physical stability (Shalaev and Zografi, 2002). In order to avoid the unwanted solid-state phase transformation of amorphous solid, the addition of stabilizing carrier is often used to prevent or limit the nuclei formation and subsequent crystal growth in the system (Brough and Williams, 2013). Amorphous solids formulated with or without stabilizing carrier differ from each other in terms of physical (incl. mechanical) and chemical properties (Vippagunta et al., 2001). Therefore, it is paramount to select the most suitable solid state form for the pharmaceutical product development.

2.1.3. Methods to improve drug solubility and dissolution rate

One of the common and most effective ways to improve the solubility of PWS APIs is a salt formation for weak bases and weak acids. However, this is quite challenging since only 20–30% of new chemical entities are able to form a salt (Serajudin & Pupipeddi, 2008). The complex formation with cyclodextrins (CD) is another option with hydrophilic outer exterior and hydrophobic inner cavity (Stella and He, 2008). Cyclic structure of CD allows to entrap the drug inside the CD cavity forming water-soluble inclusion complexes. Today, drug-CD complexes can be found in over 35 marketed pharmaceutical products (Davis and Brewster, 2004; de Oliveira Makson et al., 2015). The aqueous solubility and dissolution of APIs are also dependent on polymorphism, and there is a considerable difference between the solubility and dissolution rate of different polymorphs. Tawashi (1968) reported that the dissolution rate of aspirin polymorphic form II was 50% faster compared to form I. Pudipeddi & Serajuddin (2005) studied the solubility ratios of total 55 compounds (actually 81, due to several forms for some compounds) and revealed that an average solubility ratio for different polymorphs was 1.7 (Pudipeddi and Serajuddin, 2005). However, it would be incorrect to draw conclusions regarding the bioavailability of such compounds. Solubility ratio of amorphous form is usually higher (e.g., glibenclamide 14) (Hancock and Parks, 2000). Co-crystal formation is another approach towards improved solubility and dissolution rate of APIs, where a target API is combined with a coformer crystal by non-covalent and non-ionic forces. Co-crystals have shown solubility advantage over crystalline polymorphs and similar or above the amorphous form (Good and Rodriguez-Hornedo, 2009).

Particle size reduction of APIs leads to increased surface area available for solvation and dissolution. Particles can be obtained in micron and nano sized

range. Nanoparticles have several fold higher specific surface area compared to micron sized particles, thus leading to even higher dissolution rates. It has been shown that over 80% ibuprofen nanocrystals prepared by comminution dissolved within only 2 min (Plakkot et al., 2011). Surfactants are able to solubilize PWS APIs through micelle formation, which improves wetting and are commonly used in (nano)suspensions for stabilizing purpose (Williams et al., 2013).

In co-solvent systems organic solvents such as ethanol, glycerol, propylene glycol, polyethylene glycol 300/400, dimethyl sulfoxide, dimethylacetamide are mostly used (Williams et al., 2013). Organic solvents are increasing the solubility of PWS APIs by reducing the polarity of the bulk solvent. Co-solvents are commonly combined with surfactants in self-emulsifying formulations, but toxicity issues and risk of drug precipitation upon dilution limits the use of such systems (Lukyanov and Torchilin, 2004; Williams et al., 2016). The application of more safer lipid systems comes from the dietary lipids, which are well absorbed across the GI tract. Lipid based formulations (LBF) are good choice for lipophilic PWS drugs with dissolution rate as a limiting step. In most cases, LBFs are combinations of surfactants, co-solvents and natural or synthetic oils. After mixing with GI fluids and dilution effect, LBFs form oil-in-water (o/w) emulsions or microemulsions, which are readily absorbed from a GI tract (Gursoy and Benita, 2004). Recent advancement in co-amorphous systems, where two small molecules combined together (ratios 1:1, 1:2, 2:1), has resulted in increased apparent solubility, dissolution rate and provided good physical stability. Such approach could be an alternative to polymer based amorphous SD (Korhonen et al., 2017).

All these strategies are aimed (1) to reduce the intermolecular forces in solid state, (2) to increase the lipophilicity and solubilization, and (3) to increase the surface area which will be in contact with the solvent. However, the influence of the manufacturing method on the physicochemical stability of drug should be assessed to avoid the risks related with the thermal degradation, formation of chemical decomposition products, and polymorphic or other unwanted solid state transformations during processing (Janssens et al., 2010; Jermain et al., 2018; Van Den Mooter, 2012; Williams et al., 2013).

2.2. Solid dispersions

Solid dispersion (SD) is a broad term describing drug dispersion in a carrier matrix, where usually a hydrophobic drug is dispersed in a hydrophilic carrier (sugar, polymer). There are different ways how SDs have been classified. Firstly, SDs have been classified based on material type, physical state of ingredients and miscibility (Brough and Williams, 2013; C. Brown et al., 2014; Van Den Mooter, 2012). These types are crystalline SD, amorphous SD, and amorphous solid solution (Figure 1). The crystalline SD is a multiphase-immiscible system, with crystalline and separate carrier phase. Amorphous SD

is also a multiphase system with discrete amorphous drug distributed in an amorphous carrier manifesting in multiple glass transitions (Tg). Amorphous solid solution is a miscible, one-phase system, where the drug is homogeneously dispersed within the carrier phase. In such systems, differential scanning calorimetry (DSC) shows only single Tg.

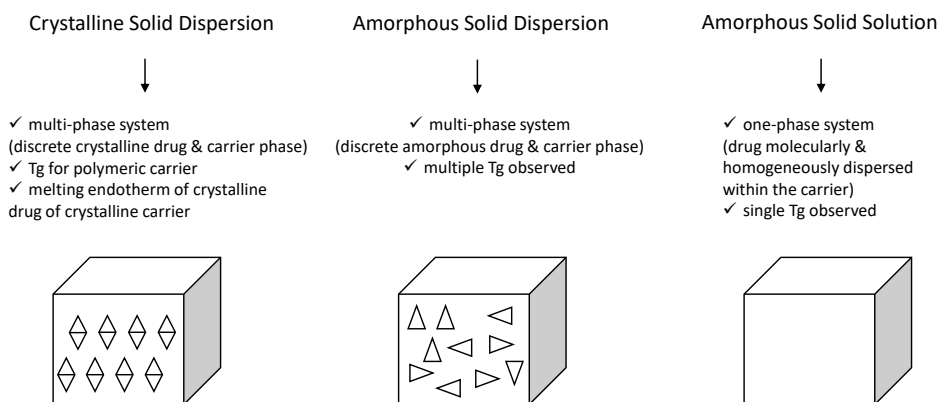


Fig. 1. Solid dispersion classification based on phases and different states. Key: Tg – glass transition temperature (modified from Williams et al., 2016).

Secondly, Thommes et al (2011, 2012) have classified SDs into subtypes based on the solid-state form of the drug/carrier (crystalline/amorphous) and number of phases (Table 1). In one-phase systems, the drug is molecularly dispersed within the carrier and both components exist in the amorphous phase (or co-crystal) (Thommes, 2012; Thommes et al., 2011). Such formulations are widely considered as the most desired ones for PWS drugs. The application of one-phase systems, however, is challenging due to the limitations related to the drug loading and manufacturing. Furthermore, the dissolution of one-phase SDs may be even worse compared to a pure drug, if the intermolecular binding between the drug and matrix material is too strong. For example, impaired dissolution has been reported recently with one-phase IND and SOL containing SDs (Surwase et al., 2015). With these factors in mind, one can also consider two-phase systems. In two-phase systems, the components can be present as independent crystalline and/or crystalline/amorphous phases. Thommes et al. (2011) prepared a crystalline suspension by using a hot-melt extrusion (HME) method, where crystalline drug was physically mixed with crystalline sugar. Interestingly, such HME crystalline suspension is like a physical mixture with an exception that it has significantly improved dissolution properties compared to that of a conventional physical mixture (Thommes et al., 2011; Thommes, 2012).

Those amorphous SDs where the drug is in an amorphous form have higher apparent solubility and faster dissolution rate compared to their crystalline counterpart (Di et al., 2009; Hasegawa et al., 2005; Newman et al., 2012). Due to the high tendency of recrystallization associated with thermodynamically

unstable amorphous drugs, proper carrier molecules with desired functionality are of utmost importance. The key mechanisms by which carrier materials provide physical stabilization for amorphous drug within SD include (1) the reduction in molecular mobility via increasing local viscosity, (2) intermolecular interactions between the drug and carrier, and (3) the prevention of a crystal nucleation (Hancock and Zografi, 1997; Marsac et al., 2008a; Van Den Mooter, 2012)

Table 1. Classification of pharmaceutical solid dispersions, SDs (I) (modified from the classification system introduced by Thommes, 2012).

	Solid Solution	Glassy Solid Solution	Compound Complex Formation	Solid Crystal Suspension	Eutectic Mixture	Amorphous Precipitation	Glassy Suspension
Phase	1	1	1	2	2	2	2
API	molecularly dispersed	molecularly dispersed	molecularly dispersed	crystalline	crystalline	amorphous	amorphous crystalline
Carrier	crystalline	amorphous	crystalline amorphous	crystalline	crystalline	crystalline	amorphous

Key: API, active pharmaceutical ingredient

2.2.1. Preparation methods of solid dispersions

As mentioned earlier, generally methods can be divided into solvent and thermal melting/fusion methods. SDs prepared by a solvent evaporation method require a common solvent, where both the drug and carrier are dissolved followed by solvent evaporation. Secondary drying step is needed to reduce the residual amount of solvent below acceptable limits. Traces of solvent, acting as a plasticizer could negatively impact the physiochemical properties of the SDs (Janssens and Van den Mooter, 2009). Solvent evaporation method is a better option for thermolabile drugs, but potential organic solvent residues and high cost of the manufacturing are still a major concern. Moreover, critical process parameters such as temperature, evaporation rate, and solvent type affect the physical state of the SDs (Janssens and Van den Mooter, 2009; Jermain et al., 2018; Williams et al., 2016). Spray drying is a common solvent method for fabricating pharmaceutical SDs. In spray drying, the drug-polymer solution is atomized to tiny droplets, which are immediately dried upon contact with hot gas, and the subsequent drug-polymer precipitate in the form of particles is collected (Van Den Mooter, 2012).

In case with thermal methods, SD is formed through heating the drug and carrier above their melting point followed by rapid cooling. Afterwards, material is pulverized to obtain the powder. Industrial version of thermal method is HME, where the powder mixture is supplied through the hopper into the heated barrel with screw elements for mixing/kneading and conveying the molten mass

through the die shaping the final melt into granules, ribbons, or pellets (Janssens and Van den Mooter, 2009; Williams et al., 2016). Advantage of thermal method is the avoidance of any organic solvents and a drying step. However, the chemical stability of drug(s) should be kept in mind, since there is a significant risk for chemical decomposition and for the formation of chemical degradation products resulting in an impaired drug-carrier miscibility (Forster et al., 2001). Most of the commercial amorphous SDs are prepared either by spray-drying or HME (Table 2). Other non-conventional methods for SDs preparation for pharmaceutical applications include supercritical fluid, electrospinning (solvent/melt), and more recent a microwave irradiation method (Doreth et al., 2017; Janssens and Van den Mooter, 2009; Vasconcelos et al., 2007; Brough and Williams, 2013).

2.2.1.1 Quench cooling of the melt

Quench cooling (QC) of a drug-carrier melt followed by pulverization is a common technique for manufacturing pharmaceutical SDs (Janssens and Van den Mooter, 2009; Vasconcelos et al., 2007). The current trend is to first heat up a carrier material, and subsequently suspend the drug inside a molten carrier matrix (Vasconcelos et al., 2007). In order to prevent spontaneous recrystallization, the addition of a stabilizing carrier is of critical importance (Vasconcelos et al., 2007). In QC, the cooling rate of a melt should be faster than recrystallization rate for preventing any molecular mobility and retaining an amorphous structure (Brough and Williams, 2013). For example, ice bath and liquid nitrogen are applicable for rapid cooling of the system in QC.

2.2.1.2 Melt-electrospinning

Electrospinning (ES), also called as “electrostatic drawing”, is a nano and micro-fabrication method, in which a continuous liquid jet from a polymer solution or melt under syringe pump force is electrostatically directed onto a grounded collector. Melt-electrospinning (MES) is a thermal modification of ES, and MES can be carried out in both horizontal and vertical positions. Modified MES constitutes from tuned process environment, where electrospinning is carried out under vacuum with higher electrical fields overcoming viscosity and elasticity of the polymers. Main limitations is that in vacuum radiation cooling can be used only and hence solidification takes longer time, posing a risk for fusion of MSFs (Reneker and Yarin, 2008). Suitable heating systems for MES are e.g., thermostated circulating fluids, lasers, radiant heating systems, heated air or electrical heating systems (Hutmacher and Dalton, 2011). The critical process and material parameters of MES include e.g., melt viscosity, process temperature, spinneret diameter, flow rate, voltage, collection distance, and a collector type (Brown et al., 2016). These parameters can greatly affect the fiber alignment and morphological properties of the final MSFs. The flow rate and polymer molecular weight are directly related to fiber diameter

and voltage to fiber uniformity (Brown et al., 2011; Brown et al., 2014; Detta et al., 2010). According to the literature, the MSFs are smooth, with a small inter-fiber diameter deviation, and the fiber size typically ranges from 270 nm to 500 μm (Dalton et al., 2006; Lyons et al., 2004). This also shows a great flexibility of the process.

The carriers intended for QC, MES and HME must be chemically and physically stable with sufficient thermoplasticity, and they need to support the drug release through solubilizing the released drug or stabilizing the super-saturated drug solution. Excipient functionality should be maintained throughout the manufacturing process, storage and *in vivo*. Thermal methods pose a significant risk for the degradation of drug and carrier. Therefore, the selection of a suitable thermostable carrier material is of crucial importance. Carriers with high Tg-s are preferred and functional groups for intermolecular interaction (hydrogen bonding) with drug are desirable. Carriers should also provide proper miscibility with drug, since drug solubility in the polymer mixture determines the upper limit of the drug concentration, showing no phase separation and crystallization. If the drug amount exceeds the solubility limit (above miscibility), phase separation with following crystallization may occur and solubility advantages of SDs will be lost (Marsac et al., 2006; Marsac et al., 2008b). Hence, the assessment of drug-carrier miscibility is important. Fourier transform spectroscopy (FTIR), microscopy and differential scanning calorimetry (DSC) could be used as fast screening tools. In MES, polymers should have also suitable viscosity to pass through a MES spinneret. The molecular weight of the carrier has been shown to have the most significant impact on the fiber diameter (Brown et al., 2011; Brown et al., 2014). In the present thesis, amphiphilic graft copolymer, Soluplus[®], SOL (BASF, 2010), was investigated as a novel carrier in MES. Originally, SOL was developed as a carrier material for HME and hot-melt granulation processes, but due to its unique material properties (thermal behavior, solubilizing properties, binding effects, etc.) it has also been tested in other pharmaceutical manufacturing processes. Xylitol (XYL) is a small-molecular carrier investigated for SD fabrication. It is crystalline sugar alcohol used as a matrix of SDs for improving the solubility of PWS drugs (Mummaneni and Vasavada, 1990; Sjökvist and Nyström, 1991; Singh et al., 2011). Common polymers used for thermal methods and in the marketed products are listed in Table 2.

MES has number of advantages over conventional solution-based ES and SD preparation methods: (1) the use of organic solvent(s) can be avoided; (2) the yield is exceptionally high (often 100%); (3) the size of fibers is uniform (diameter $\pm 5\%$), and (4) MES can be readily extended to 3D direct writing mode for preparing the scaffolds for tissue engineering (analogue for 3D printing). MES fibers made without any organic solvents comply more easily to medical device regulations, which also reduces the time for product development and marketing authorisation approval (Mitchell, 2015). The major limitations of MES are related to the thermal stability of the compounds.

Table 2. Currently marketed amorphous solid dispersion (SD) products (modified from Jermain et al., 2018; Qiu et al., 2017)

Product	API	Company	BCS class	Carrier	Dispersion process
Afeditab®	Nifedipine	Elan/Watson	2	Poloxamer or PVP	Melt/absorb on carrier
Certican (non-US)	Everolimus	Novartis	3	HPMC	Melt or spray drying
Cesamet®	Nabilone	Valeant Pharmaceuticals	2 or 4	PVP	Melt extrusion
Fenoglide®	Fenofibrate	LifeCycle Pharma	2	PEG	Spray melt
Gris-PEG®	Griseofulvin	Novartis/Penidol	2	PEG	Melt extrusion
Ibuprofen®	Ibuprofen	Soliqs	2	various	Melt extrusion
Incivek® (US)	Telaprevir	Vertex Pharmaceuticals	2 or 4	HPMCAS	Spray drying
Incivo® (Europe)	Telaprevir	Janssen Pharmaceuticals	2 or 4	HPMCAS	Spray drying
Intelence®	Etravirine	Janssen Pharmaceuticals	4	HPMC	Spray drying
Isoptin SRE-240	Verapamil	Abbvie Inc	2	HPC/HPMC	Melt extrusion
Kalydeco®	Ivacaftor	Vertex	2 or 4	HPMCAS	Spray drying
Kaletra®	Lopinavir ritonavir	AbbVie	2 and 4	PVP VA	Melt extrusion
LCP-Tacro®	Tacrolimus	LifeCycle Pharma/Veloxis	2	HPMC	Melt granulation
Nimotop®	Nimodipine	Bayer	2	PEG	Spray drying/fluid bed
Norvir®	Ritonavir	AbbVie	4	PVP VA	Melt extrusion
Noxafil®	Posaconazole	Merck	2	HPMCAS	Melt extrusion
Onmel®	Intraconazole	GlaxoSmithKline/ Stiefel	2	PVP VA	Melt extrusion
Orkambi®	Lumacaftor/ Ivacaftor	Vertex	2 and 4	PVP/HPMC CAS	Spray drying
Prograf®	Tacrolimus	Astellas Pharma Inc	2	HPMC	Spray drying/fluid bed
Sporonox®	Intraconazole	Janssen Pharmaceuticals	2	HPMC	Spray layering (fluid granulation)
Venclexta™	Venetoclax	Abbvie	4	PVP VA	Melt extrusion
Zelboraf®	Vemurafenib	Roche	4	HPMCAS	Antisolvent precipitation
Zortress® (US)	Everolimus	Novartis Pharmaceuticals	3	HPMC	Melt or spray drying
Zepatier®	Elbasvir/ Grazoprevir	Merck	4 and 2	PVP VA/HPMC	Spray drying
Mavyret™	Glecaprevir/ Pibrentasvir	AbbVie	4	PVP VA/HPMC	Melt extrusion

Key: API, active pharmaceutical ingredient; BCS, Biopharmaceutics Classification System; PVP, polyvinylpyrrolidone; HPMC, hydroxypropylmethylcellulose; PEG, polyethylene glycol; HPMCAS, hydroxypropylmethylcellulose acetate succinate; PVP VA, polyvinylpyrrolidone vinyl acetate

MES is a novel technique which is intensively studied in biomedical and pharmaceutical fields. Today, the main application areas of MES include tissue engineering constructs and scaffolds. Several studies with osteoprogenitors, osteoblasts and fibroblasts showed that MSF polycaprolactone (PCL) scaffolds can support the cell growth and extracellular matrix formation (Henkel and Hutmacher, 2013; Hutmacher and Dalton, 2011; Thibaudeau et al., 2014). There are number of successful animal models, where PCL based scaffolds were used for bone bridging and regeneration (Henkel and Hutmacher, 2013). The flexibility of MES allows to adjust the mechanical properties of fibers, pore size, surface morphology and fibers deposition. The application of MES in the pharmaceutical field is in its infancy. To date, only few studies have been published on the application of MES as a method for improving the solubility and dissolution rate of PWS drugs (Balogh et al., 2014; Lian and Meng, 2017; Nagy et al., 2013).

2.2.2. Characterization of solid dispersions

Many characterization methods used for the solid state analysis can be utilized for analyzing the SDs. The physicochemical properties and stability of SDs immediately after preparation and during storage are generally investigated. X-ray powder diffraction (XRPD) is a golden tool for polymorphic screenings (sharp reflections) and amorphicity detection („halo“) of drugs and excipients. Freshly prepared amorphous SDs should not have any crystalline reflections and show only an amorphous halo on their diffractograms. When two-phase (crystalline-amorphous) systems are investigated, elevated baseline with reduced and broaden crystalline reflections are detected. However, XRPD alone might not be sensitive enough to differentiate between discrete amorphous-amorphous phases, and consequently, other analytical techniques are needed. Vibrational spectroscopy methods (infrared (IR), near-infrared (NIR), Raman) can be used for the solid-state characterization and quantification (Aaltonen et al., 2003). Vibrational spectroscopy methods are fast, non-destructive and precise providing chemical and physical data and NIR and Raman spectroscopy can be easily coupled with devices for in-line or spatially resolved analysis (flow through cells, microscopes, array detectors) (Fraser-Miller et al., 2016). Thermal methods such as differential scanning calorimetry (DSC), thermogravimetric analysis (TGA), hot-stage microscopy (HSM), are widely used to study the miscibility of the systems, recrystallization and moisture content. In case of amorphous solids, there is no melting endotherm of a drug observed. Regarding with miscibility, only one T_g value for miscible systems and two T_g values for immiscible systems (less stable formulations) will be detected (Qian et al., 2010). With the TGA, a weight loss of MSF can be observed, thus indicating the dehydration and potential thermal decomposition of the system.

2.2.3. Physical stability of solid dispersions

In order to sustain pharmaceutical quality and functionality, the drug-loaded SDs must be chemically and physically stable. The SDs must be formulated and stored in a way which enables to reduce the risk of product degradation or polymorphic changes. Environmental factors affecting the formulation stability are humidity, temperature, light, and oxygen. All these factors may change the mechanical properties and disintegration time of dosage form, induce polymorphic transformation of API to less water-soluble form, accelerate chemical degradation and/or impair the physical appearance of the final product. In addition, SD fabrication methods have their own limitations and challenges. For example, drug and excipients are subjected to a high temperature in HME or MES, which can result in the decomposition of drug/excipient. With solvent evaporation methods, the traces of organic solvent residuals can induce the polymorphic transformations resulting in variable solubility, dissolution rate and bioavailability of the drug. The use of organic solvent also rises the toxicity issues and safety hazard during the handling process. Hence if solid phase is sensitive to heat, solvent evaporation methods must be chosen and *vice versa*.

In order to stabilize amorphous form, the inclusion of a proper excipient in the system is needed. However, unique physical and chemical properties of carrier(s) can significantly limit the formulation stability. It has been shown that some polymers (e.g., polyethylene glycol, PEG) are prone to recrystallization on the course of storage, thus resulting in the reduced dissolution rate of the final product (Bley et al., 2010). Moreover, hygroscopicity of the polymers is disrupting the interactions between the drug and carrier, lowering the solubility or miscibility of the drug in the carrier, increasing the molecular mobility and favoring the phase separation leading to crystallization (Marsac et al., 2008b). As an example, the storage of hydrophobic drugs ((nifedipin, griseofulvin, polyvinyl pyrrolidone (PVP)) SDs at high relative humidity led to an amorphous-amorphous phase separation, and subsequently the crystallization of the drugs (Rumondor et al., 2009). With amorphous SDs, both absorption and adsorption phenomena can occur, where water is attracted into internal site or on the surface of the system, respectively. Therefore, amorphous SDs show higher sorption values (absorption plus adsorption) compared to the corresponding physical mixtures (PM) (Crowley and Zografí, 2002). As mentioned earlier, SOL has proved to have stabilizing (recrystallization retardation/inhibition) and solubility enhancing properties with pharmaceutical SDs, thus resulting in improved wettability and dissolution of PWS (Linn et al., 2012; Shamma and Basha, 2013). Yamashita et al. (2003) investigated the effect of polymeric precipitation inhibitors ((PEG6000, hydroxypropylmethyl cellulose (HPMC), PVP)) as a means for improving the absorption of PWS. Nevertheless, excipients with high T_g, will significantly reduce the molecular mobility and stabilize the supersaturated drug.

A complete miscibility of the components is desired to gain a stable formulation. For estimating the miscibility, a simple DSC scan can be used, where

miscibility between the drug and polymer during heating-cooling-heating cycle is assessed (Sarode et al., 2013). As mentioned earlier, a single T_g value confirms the miscibility, whereas two T_g values suggest partial miscibility. However, DSC does not take into account the heat induced co-fusion or recrystallization. Another interesting classification system for SDs was introduced by Baird and co-workers (2010) which relies on the glass forming ability (GFA) and glass stability (GS) assesment. In order to form a glassy SD, mixture must be QC below T_g to prevent the nuclei formation (GFA) and resistance of such material to crystallization upon cooling is known as GS. Intial DSC stability assessment based on fast screening was performed with total 51 APIs. According to Baird et al. (2010), the compounds which recrystallized upon cooling are weak glass formers (Class I) and those which crystallized upon reheating are strong glass formers (Class II). The strongest glass formers are regarded as those which did not show any recrystallization (Class III). The compounds belonging to Class I (e.g., carbamazepine, benzocaine, haloperidole) or Class II (e.g., acetaminophen, celecoxib, nifedipine) are categorized as high risk compounds in formulating stable amorphous SD. Whereas the Class III (e.g., ibuprofen, indomethacin, ketoprofen) compounds are considered as excellent candidates for formulating stable amorphous SDs. It was noted that high molecular weight and complex structure are the key properties for strong glass formers (Baird et al., 2010).

2.2.4. Pharmaceutical application of solid dispersion

Examples of currently marketed amorphous SDs are depicted in Table 2. As seen in Table 2, mostly they were prepared either by melt extrusion or spray drying. As an example, Sporanox[®] molecular disperison of PWS itraconazole within the HPMC and attached to sugar beads. Compared to the crystalline drug, the amorphous SDs showed significant improvement in bioavailability (Eerdenbrugh et al., 2009). The number of marketed amorphous SDs is relatively low, however positive increasing trend has been seen for recent years. The reason for small number of marketed products is the instability of amorphous system, which tend to recrystallize during manufacture, storage, or drug release, and which result in loss of favorable dissolution profile. Also, limited number of suitable pharmaceutical excipients with reasonable solubility in organic solvents for solvent based techniques and appropriate viscosity and thermal stability of thermal methods is a concern.

3. SUMMARY OF THE LITERATURE

As it can be concluded, poorly water-soluble drugs remain a big challenge for pharmaceutical industry, hindering bringing to market efficient therapeutical agents. The number of such drugs are expected to grow in following years. Limited solubility and/or dissolution rate coming from physicochemical properties of chemical entity, raises the need for novel methods or optimizing existing ones. Also, limited number of suitable pharmaceutical excipients is slowing the development process. Solid dispersion preparation technique has shown its potential in numerous marketed products. However, miscibility/stability of the formulation is still a significant challenge. The application of modified thermal methods coupled with potentially new pharmaceutical excipients could be a new solution for an old problem.

4. AIMS OF THE STUDY

The aim of the present thesis was to investigate and gain understanding of the effects of two thermal pharmaceutical solid dispersions fabrication methods on the physicochemical properties, physical stability and dissolution behavior of a poorly water-soluble drug indomethacin.

The specific objectives were:

- to investigate the solid-state stabilization properties of the solid dispersions with two matrix formers (Soluplus[®]/xylitol)
- to investigate the particle and bulk powder properties, wetting and dissolution of the quench cooled molten two-phase solid dispersions of a poorly water-soluble indomethacin and selected two matrix formers
- to elucidate the impact of polymeric and crystalline carrier properties on the formulation and performance of SDs with a major emphasis on the dissolution studies
- to develop novel drug-loaded melt-electrospun fibers using MES for improving the dissolution rate of a poorly water-soluble drug
- to gain understanding of the physical solid-state changes, drug-carrier polymer interactions, and dissolution rate associated with melt-electrospun fibers

5. EXPERIMENTAL

Complete description of materials and methods the reader should refer to original publications (I–III).

5.1. Materials

5.1.1. Indomethacin

Indomethacin (IND) is a widely-used non-steroidal anti-inflammatory drug, and is a commonly used model drug in the development of amorphous systems for PWS drugs (Hart and Boardman, 1963; Ewing et al., 2014; Dimensional et al., 2015). IND has two crystalline polymorphs (α and γ forms) and an amorphous form (Atef et al., 2012; Savolainen et al., 2007; Clare J Strachan et al., 2007). Recently, Surwase et al. (2013) discovered and characterized several new polymorphs (ε , ζ , η) for IND, which were prepared under different crystallization conditions (Surwase et al., 2013). In the present thesis, IND (γ -IND) (NLT 97.5%, *Acros Organics, England and Hawkins, USA*) was used as a PWS model drug. The preparation of α -polymorph and amorphous forms of a model drug IND can be found in the original publications (I–III).

5.1.2. Soluplus®

Soluplus® (SOL) is a new amphiphilic graft copolymer for pharmaceutical applications (BASF, 2010). Chemically SOL is a graft copolymer consisting of polyvinyl caprolactam-polyvinylacetate-polyethylene. SOL has been regarded as a bifunctional polymer having matrix forming and solubilizing properties for PWS drugs (Shamma and Basha, 2013). Originally, SOL was developed as a carrier material for HME and hot-melt granulation processes (BASF, 2010). In the present study, SOL was received as a gift from BASF SE (Pharma Ingredients & Services, Germany) and it was used as a solubilizing polymeric matrix former in both the QC molten and MES SDs (I–III).

5.1.3. Xylitol

Xylitol (XYL) is a sugar alcohol, which is widely used as a non-cariogenic sugar substitute in confectionary and dental hygienic products (Salli et al., 2016). To date, it has gained attention in the pharmaceutical use as a small-molecular matrix of SDs for improving the solubility of PWS drugs (Mummaneni and Vasavada, 1990; Singh et al., 2011; Sjökvist and Nyström, 1991). In the present thesis, XYL (Ph. Eur.) was obtained from Yliopiston Apteekki (Helsinki, Finland), and it was used as a small-molecule freely soluble SD matrix former (I, II).

5.2. Methods for fabricating physical mixtures and solid dispersions

5.2.1. Preparation of physical mixtures (I-II)

The physical mixtures (PMs) of a drug and carrier were prepared by mixing the components with a pestle in a mortar and using a geometric dilution. PMs were prepared with SOL/XYL and both IND polymorphs (γ -IND and α -IND). Samples were sieved using a mesh of 450 μm , and the fraction passing through was collected for further use (**I**). The drug:carrier weight ratios used in the PMs were 1:3, 1:6 and 1:9 (w/w) (drug:polymer) (**I**). In the subsequent studies, pure materials were sieved (150 μm) prior to use and characterization (**II**, **III**).

5.2.2. Preparation of solid dispersions by melt quench cooling (I-II)

For preparing the solid dispersions (SDs) by melt quench cooling (QC), the traditional QC method, explained in the Literature review under paragraph 2.2.1. Preparation methods of solid dispersions (SDs), was modified in the present study. In the present PhD thesis, two-phase drug-carrier systems were prepared with an unorthodox and modified QC method, where the drug (not carrier) was molten first followed by the addition of the carrier (**I**). QC co-melted SD mixtures were prepared by melting the γ -IND in a stainless steel dish at approximately 175 $^{\circ}\text{C}$ and then adding SOL/XYL. Therefore, the molten mass was solidified by pouring liquid nitrogen onto the stainless steel dish. The molten mass was then gently ground in a mortar. All samples were sieved using the same fraction as PMs. The SDs with the weight ratios 1:3, 1:6, 1:9 (w/w) (drug:polymer) were investigated (**I**). In the subsequent studies, SDs at the weight ratio 1:3 (w/w) (drug:polymer) were used (**II-III**).

5.2.3. Melt-electrospinning (III)

Prior to use, the drug and carrier polymer were manually sieved through a 150- μm size sieve. The PMs were prepared as described in the original publication (**I**). The batch size of each PM was 6.0 g. The PM1 and PM3 consisted of crystalline γ -IND and SOL (1:3). The PM2 consisted of amorphous IND prepared by QC of a melt and subsequently mixed with SOL at a drug-polymer weight ratio of 1:3. The PMs 1 and 2 were used as reference samples and PM3 was used as a binary pretreated mixture for the MES experiments (**III**). Pretreatment was performed by storing the PM of γ -IND and SOL (1:3) at high relative humidity (approx. 90% RH) for 24 h prior MES.

5.3. Characterization of physical mixtures and solid dispersions

5.3.1. Scanning electron microscopy (I–III)

Scanning electron microscope (SEM) (Zeiss EVO MA 15, Germany) was exploited for imaging the particle/fiber size, shape, surface porosity and morphology of the samples. The samples were attached on a carbon tape, and sputter coated with platinum (3–5 nm) in an argon atmosphere. The measurements were carried out under low vacuum. Martin's diameter of 50 randomly selected particles was determined in vertical direction from SEM images and particle size was measured by Image J (NIH, USA).

5.3.2. X-ray powder diffraction (I–III)

The X-ray powder diffraction (XRPD) patterns of rotating samples were collected with a Bruker D8 Advance diffractometer (Bruker Corporation, Germany) using Cu radiation $\lambda=1.5418 \text{ \AA}$ and operated at 40 kV and 40 mA. For data gathering, theta–theta geometry in the range of 5° – $35^{\circ} 2\theta$ (with the step size of $0.0195^{\circ} 2\theta$) and a LynxEye positive sensitive detector, were applied. Variable-temperature XRPD (VT-XRPD) was used for tracking the heat induced solid-state transitions and understanding the miscibility of the systems and revealing the presence of multi-phase system. Data were collected from 8 to $22.5^{\circ} 2\theta$, with a step size of $0.0195^{\circ} 2\theta$. The heating process started from RT at a rate of $0.5^{\circ}\text{C}/\text{min}$ and the first scan was taken at 30°C and other scans were measured at intervals of 10°C up to 150°C for IND:SOL systems and after every 5°C until 160°C for all systems. The heated samples were then cooled down to 30°C and remeasured.

5.3.3. Fourier-transform infrared spectroscopy (I–III)

Fourier transform infrared spectroscopy (FT-IR) spectra of samples were collected with IR Prestige-21 Spectrophotometer (Schimadzu Corp., Kyoto, Japan) and Specac Golden Gate Single attenuated total reflection (ATR) crystal (Specac Ltd., Orpington, United Kingdom). Operating range was 4000 – 600 cm^{-1} .

5.3.4. Near-infrared spectroscopy (III)

Near-infrared spectroscopy (NIR) spectra (1200 – 2200 nm) were measured with AvaSpec-NIR256-2.2 (Avantes, The Netherlands), equipped with 256 pixel in GaAs detector and tungsten halogen lamp as a light source (AvaLight-HAL). The final spectrum was the mean of total four scans, and each sample was measured in pentaplicate.

5.3.5. Nuclear magnetic resonance spectroscopy (III)

Nuclear magnetic resonance spectroscopy (NMR) with ^1H and ^{13}C FT-NMR-spectra in CDCl_3 (Eur-isotop 99.80% containing 0.03% TMS) solution together with ^{13}C CP-MAS spectra in solid state were recorded using Bruker Avance III 500 MHz spectrometer (Bruker, UK Limited, United Kingdom). Solution spectra were recorded in 5-mm glass tubes and solid state spectra in 4-mm rotors. All spectra were recorded at 23 °C. In order to calculate the approximate domain size, equation 2 (Brettmann et al., 2012) was used:

$$L = (6DT_i)^{1/2} \quad (\text{Eq. 2})$$

where L is the magnetization diffusion length, D is the spin diffusion coefficient and T_i is the relaxation time. In this study, approximate values of D , $8.0 \times 10^{-16} \text{ m}^2/\text{s}$ for rigid systems and $0.5 \times 10^{-16} \text{ m}^2/\text{s}$ for mobile systems were used reported earlier by Spiegel et al. (1994). Because the rigidity/flexibility of the system is not precisely known the domain sizes were presented as a range and the result gives upper limits for the domain size.

5.3.6. Differential scanning calorimetry (I-III)

Differential scanning calorimetry (DSC) 4000 (Perkin Elmer Ltd., Shelton, CT, USA) was used for the thermal analysis of samples in an aluminum pans with pinholes in a lid and under a dry nitrogen flow. The key parameters used in the DSC experiments were as follows: sample size (2–8 mg), heating rate (10 °C/min), and operating temperature range (20–200 °C). The DSC system was calibrated with indium.

Hot-stage microscopy (HSM) was performed with a Mettler Toledo F82 (Switzerland) and visualized with a polarized light microscope (Leica DM/LM, Germany) under $5\times$ magnification (HSM-PLM). The temperature range and heating rate were 30–200 °C and 20 °C/min, respectively.

5.3.7. Thermogravimetric analysis (II)

Moisture content and thermal stability was assed with thermogravimetric analysis (TGA) performed with a NETZSCH STA 449 F3 Jupiter® (NETZSCH-Gerätebau GmbH, Germany) simultaneous thermal analyzer. Air was used as a purge gas at the flow rate of 60 ml/min. Samples (25–35 mg) were placed in corundum sample holders. The sample was heated from 20 °C to 350 °C at the rate of 10 °C/min and held isothermally at 350 °C for 10 min. Data were processed with NETZSCH Proteus® Software for Thermal Analysis. Thermal changes up to 150 °C were taken as a dehydration process.

5.3.8. High-performance liquid chromatography (III)

The content and chemical stability of IND in MSFs (three different batches, n=8) was assayed by high-performance liquid chromatography (HPLC) (254 nm) using slightly modified European Pharmacopeia (Ph. Eur. 9.0) method. HPLC system (Shimadzu Prominence LC20 with PDA detector SPD-M20A) controlled by software LC solution was used. The standard of IND (~0.15 mg/ml) was dissolved in acetonitrile:water solution (1:1). A Phenomenex Luna2 C18 column was used with the flow rate of 1.0 ml/min and injection volume 10 µl at the temperature of 50 °C. The following mobile phases were used: (A) 10 g/l solution of 30% (m/V) acetic acid in water, (B) 10 g/l solution of 30% (m/V) acetic acid in acetonitrile. HPLC was also used to confirm the results of drug release from MSFs obtained by UV-Vis spectrophotometer (Specord® 200 Plus, Analytik Jena AG, Germany).

5.3.9. Karl-Fischer titration (II)

Karl-Fischer (KF) titration (Mettler Toledo V30 Volumetric KF Titrator, Mettler-Toledo GmbH, Schwerzenbach, Switzerland) was used for determining the total water content of materials. The KF titrations (n = 2–3) were carried out at 21 °C temperature / 22% relative humidity (RH).

5.3.10. Moisture sorption and contact angle measurements (II)

The moisture sorption of the drug, carrier materials, PMs and SDs was investigated by storing the pre-weighed samples in open petri dishes. The petri dishes were kept at a constant temperature (25 °C) and RH 95% for 7 days. All samples were kept at 30 °C for 24 h before the first weighing. The moisture sorption was calculated from the weight gain using the following equation (Eq. 3) (Maddineni et al., 2015):

$$G = [(w_f - w_i)/S] \times 100 \quad (Eq. 3)$$

where S is the initial mass of the sample, w_i is the total original mass of a petri dish and the sample, and w_f is the total end mass of a petri dish and the sample. Total three parallel determinations were performed.

Contact angle measurements (CAM200, ver. 4.1, KSV Instruments, Finland) were performed with the flat-faced compacts ($m = 300$ mg) prepared using a table top hydraulic press with a 13-mm die. Each compact was pressed using 100 MPa of pressure for 30 s. A purified water drop (MilliQ, EMD Millipore Corporation, Billerica, MA, USA) was used as the testing liquid. Images were taken within 40 ms after the liquid drop touched the surface of the compact, and both angles were recorded.

5.3.11. Powder flow test (II)

The powder flow was determined using a novel in-house flow testing device (Fig. 1; **II**). The flow testing device has a sample cuvette mounted on a stepper motor, which was controlled with a custom-made software. The cuvette consisted of two vertically positioned chambers separated by a 3 mm orifice. The powder was placed in the left chamber, and the cuvette was subjected to a specific acceleration profile, consisting of a slow acceleration and rapid deceleration when moving to the right and a rapid acceleration and slow deceleration when moving to the left. As a result of the acceleration profile and based on Newtonian mechanics, the powder is able to gradually move to the opposite chamber through the orifice. When the powder was completely transferred to the opposite chamber, the measurement was terminated. The result was expressed as the amount of powder transferred per movement (mg/movement). The acceleration profile was programmed using MATLAB (The MathWorks, Inc., Natick, MA, USA). The testing method was validated with known excipients and against comparable powder flow measurements found in the literature (Seppälä et al., 2010).

5.3.12. Dissolution test (II-III)

The dissolution tests were carried out using an USP paddle method (Distek Dissolution system 2100B, Distek, Inc., NJ, U.S.A). A table-top UV-VIS spectrophotometer (Specord 200 plus, AnalyticJena, Germany) was used at the analytical wavelength of 370 nm for the analysis of the PM and SD samples ($n = 3$). Prior to experiments, it was verified that neither SOL nor XYL showed any absorption at this specific wavelength. The two buffer solutions (Ph. Eur. 9.0), pH 1.2 and pH 6.8, were used as dissolution media at 37.0 ± 0.5 °C. The total volume of the medium in each dissolution vessel was 500 ml. The rotation speed of the paddles was set at 100 rpm. At regular time intervals (10, 20, 30, 60, 360, and 1440 min), the samples of 5 ml were manually collected with a syringe and replaced accordingly with the pure buffer solution in a dissolution vessel. The samples were filtered using a 25-mm syringe filter (VWR, USA) and through cellulose filters with a pore size of 45 µm. The first 2 ml of the filtrated solution was not included in the quantitative analysis with a UV-VIS spectrophotometer.

5.4. Storage stability studies (I)

For assessing the physical stability of prepared multi-phase SD systems and revealing possible phase transitions and/or polymorphic changes, the QC molten SDs were stored in open glass petri dishes at 0% RH, 50% RH and 75% RH at RT (23 ± 2 °C) for up to 2 months. The samples of the aged SDs stored under

50% and 75% RH were taken periodically every 24 h during the first week, and subsequently after 10 days, 14 days, 21 days and 27 days. The samples stored at 0% RH were monitored for up to 2 months. In addition, the SD of IND with XYL (a drug-carrier weight ratio 1:3) was taken for the short accelerated stability testing and stored only at 50% RH/RT up to 4 days.

5.5. Data analysis

ImageJ (version 1.50b) software was used to measure the particle size (Martin's diameter) and particle size variation. OriginPro (versions 9.1 and 8.5) software was used for plotting figures. Particle size normality distribution was analyzed with a Shapiro-Wilk test. ChemBioDraw Ultra (version 13.0) drawing program was used for structure generation. The statistical analysis ($p < 0.05$) of contact angle results was performed with a ANOVA one-way test and Tukey test.

6. RESULTS AND GENERAL DISCUSSION

Summary of present thesis has been depicted in Fig. 2. Modified quench cooling (QC) of the melt and melt-electrospinning carried out with different carriers resulted in one-phase/multi-phase system solid dispersions (SD). As a result, improved dissolution rate with SD was achieved.

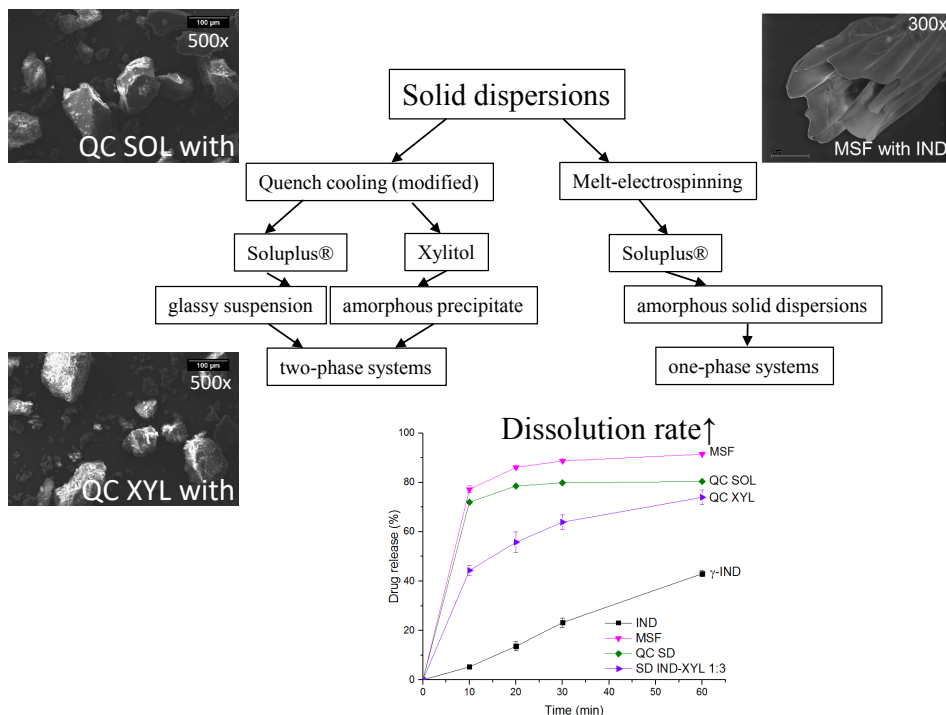


Fig. 2. Schematic illustration of solid dispersion preparations used in this thesis and the key results. Key: MSF – melt-spun fiber, QC – quench cooled, SOL – Soluplus®, XYL – xylitol, IND – indomethacin.

6.1. Classification of solid dispersions (I-III)

The formulation of pharmaceutical SDs does not always result in molecularly dispersed one-phase systems and different multi-phase SDs have been classified according to the solid state of the components and their stability (Thommes et al. 2012). In the present doctoral study, it was of interest to understand the relative stability of two-phase systems compared to the corresponding PMs and one-phase amorphous SDs systems. Furthermore, the crystallinity of the carrier material may effect the formulation of SDs and its properties. The use of crystalline and semicrystalline carriers, such as freely water-soluble sugars,

promotes ingress of hydration media into the SD. With amorphous polymer carriers, drug crystallization is prevented through intermolecular interactions with the polymer. However, large bulk volumes of polymer need to be used to reduce the mobility and increase local viscosity. The hygroscopicity of the polymer can also destabilize the amorphous system (Löbmann et al., 2013; Williams et al., 2013). Compared to amorphous carrier, crystalline carrier can act as a nucleation surface for the crystallization of drug followed by nucleation and crystal growth (Duong et al., 2015). Based on the phase separation and physical solid-state form of drug (IND) and carriers (SOL, XYL), the QC molten SDs were classified into different categories as shown in Table 1 (I). The fresh QC molten amorphous SDs of IND with SOL were two-phase *glassy suspensions* in which the drug is in amorphous form within the amorphous polymer matrix. After a short-term aging, the amorphous SDs may still contain the drug (IND) in an amorphous form or partially crystalline form depending on the storage conditions. The fresh QC molten SDs systems of IND with XYL were characterized as two-phase *amorphous precipitation systems* in which the drug is in an amorphous form in the crystalline sugar alcohol matrix. However, a short-term aging of the present SDs systems results in the formation of a two-phase solid crystal suspension in which IND is in a crystalline form together with crystalline XYL. The fibrous SD (MSFs) prepared by MES with SOL can be apparently regarded as an amorphous glassy solution or amorphous SD with a superior dissolution rate.

6.2. Quench-cooled molten solid dispersions of indomethacin and Soluplus® (I, II)

6.2.1. Physical solid state drug-carrier interactions (I)

Understanding of the thermal phase behavior and polymer-drug interactions of the two-phase binary system is of key importance for the selection of the most suitable carrier. Thermal stability of the fresh QC molten SDs at the weight ratio of 1:3 (drug:polymer) as well as drug-polymer miscibility was studied using DSC, MT-DSC, HSM and VT-XRPD. As a reference, the thermal behavior of all pure materials and corresponding PMs were studied. In line with the XRPD results, the absence of a melting endotherm on the DSC thermograms of freshly prepared QC SDs with IND:SOL provided evidence of the formation/presence of amorphous systems (Table 1, I). Upon heating no heat-induced recrystallization was observed in the DSC thermograms. Due to the broad endothermic artifact from 30–100 °C in the conventional DSC, the T_g-s of amorphous IND and SOL were indistinguishable and it was impossible to understand the presence or absence of multiple phases of this drug-carrier system. In order to investigate this further and unambiguously identify the T_g-s as well as classify the SDs according to their structure (one or multi-phase systems), MT-DSC experiments were conducted. The MT-DSC with QC SDs of IND:SOL (1:3)

system showed a two-phase SDs system, where on a reversing thermogram two Tg-s were clearly observed: the first one at 40.3 °C for amorphous IND and the second one at approximately 88 °C for SOL (Fig. 4, I). Clear shift in Tg-s of IND-SOL SDs compared to the pure materials confirmed some level of drug polymer miscibility important for the stability of amorphous systems.

HSM-PLM was also used to visualize the DSC/MT-DSC results and get more insight into the phenomena occurring at the interfaces within SD and PM mixtures (Fig. 3). The QC molten IND:SOL mixtures were heterogeneous and consisted of darker particles and more yellowish particles, hence no birefringence was observed confirming the presence of two-phase amorphous SDs system (Fig. 3). Upon heating no crystals were observed in these systems, only the drug dissolution into a polymer melt was detected. Similar phenomenon has been described by Fini and co-workers (2008) with ibuprofen and diclofenac, when they investigated the interactions between these two drugs with different types of PVP in PMs and SDs.

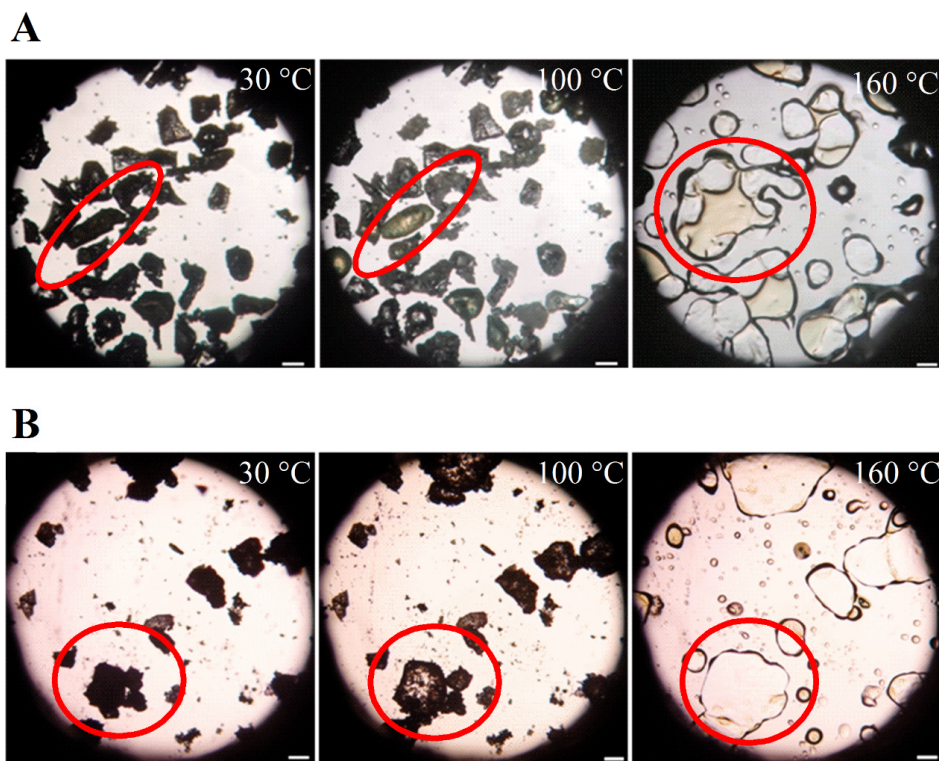


Fig. 3. Photomicrographs of indomethacin (IND) fresh solid dispersion systems (SDs) and their respective physical mixtures (PMs) with γ -IND. A. SDs with Soluplus® (SOL) IND:SOL in weight ratio of 1:3 (drug:polymer); B. PMs with Soluplus (SOL) γ -IND:SOL in weight ratio of 1:3 (drug:polymer). Scale bar of 100 μ m.

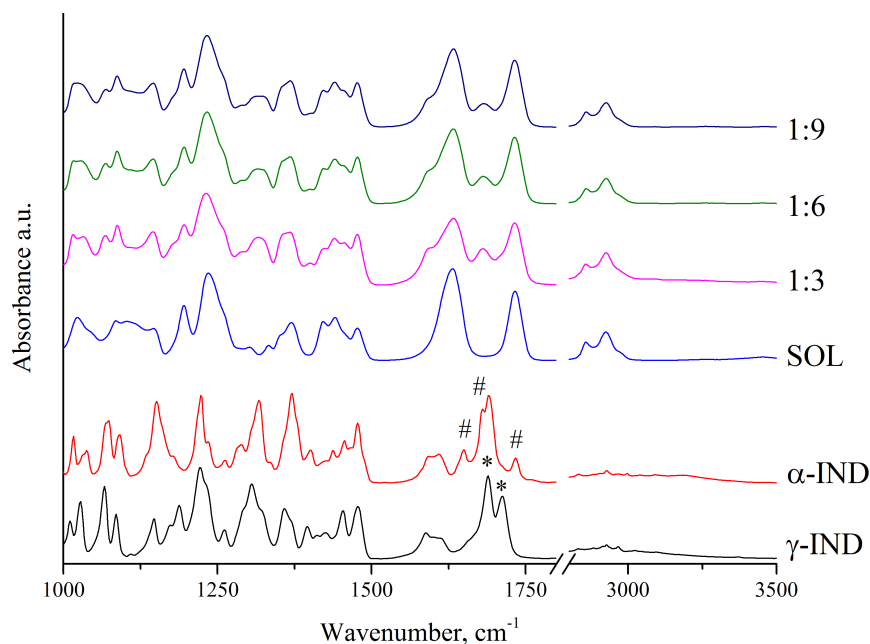


Fig. 4. Attenuated total reflection Fourier Transform Infrared (ATR-FTIR) spectra of indomethacin (IND) fresh solid dispersion systems (SDs) with γ -IND. SDs with Soluplus® (SOL) IND:SOL in different weight ratios (1:3, 1:6, 1:9 (drug:polymer)). The (*) and (#) marks denote the reflections unique to γ -IND and α -IND, respectively.

Interestingly, VT-XRPD results showed that the amorphous SDs of IND and SOL started to recrystallize as α -IND at 70 °C (Fig. 5A, I). The most pronounced reflections of α -IND were detected at 100 °C (denoted with # on Fig. 5B, I). This confirmed that SOL is not able to entirely prevent the heat-induced phase separation and recrystallization of α -IND. Differences between VT-XRPD and other thermal techniques (DSC, MT-DSC, HSM-PLM) can be explained with much longer measurement time in the VT-XRPD experiments, which may induce more pronounced changes in the sample upon heating (Mirza et al., 2006).

Since thermal analysis revealed that IND-SOL SD has some mixing between the components, the ATR-FTIR spectroscopy was used to examine further the possible molecular-level interactions between the drug and carrier in SD systems. The pure material spectra matched with the reported spectra in the literature (Bahl and Bogner, 2006; Lan et al., 2010; Shamma and Basha, 2013; Clare J. Strachan et al., 2007). The ATR-FTIR spectra of IND-SOL amorphous SDs at all drug:polymer weight ratios showed strong absorption peaks at 1630 cm^{-1} and 1732 cm^{-1} (Fig. 4) which belong to SOL molecular vibrations (carbonyl groups of block sequences – polyvinylacetate $\text{O}-\text{C}=\text{O}-\text{CH}$ and

caprolactam C=O–N vibrations, respectively). Since the pure amorphous IND also showed shoulder band at 1734 cm^{-1} and strong vibrations at 1689 cm^{-1} and 1679 cm^{-1} , the spectral overlap with strong SOL vibrations covered several amorphous IND peaks. However, as evidenced by the MT-DSC results (shift in T_g of IND-SOL SDs compared to pure materials), some hydrogen-bond formation at the molecular level may have occurred between SOL and IND molecules during SD preparation (peak observed at 1680 cm^{-1}). Zhang et al. (2013) described similar interaction with the SDs composed of itraconazole and SOL.

6.2.2. Particle size, shape and surface morphology (I, II)

Comparison of the SEM results of pure materials with those obtained with the QC molten SDs can help to indicate the influence of the method of preparation and carrier on the particle size, shape and surface morphology. All mixtures (1:3, 1:6, 1:9) were initially prepared, but only 1:3 was tested further. Fig. 5 illustrates the SEM images of the particles representing the solid-state forms of IND (A-C) and the two carrier materials studied (D, E).

The γ -form of IND displayed pointed and plate-like particles (Fig. 5, A), whereas the particles of α -IND were clearly needle-like in shape (Fig. 5, B). SOL had the largest particles ranging from 100 to 200 μm in diameter, and γ -IND the smallest ones with a size range below 50 μm . The PMs showed clearly distinguishable γ -IND particles and larger carrier particles and in SDs fused drug particles on polymer surface can be detected (Fig. 6).

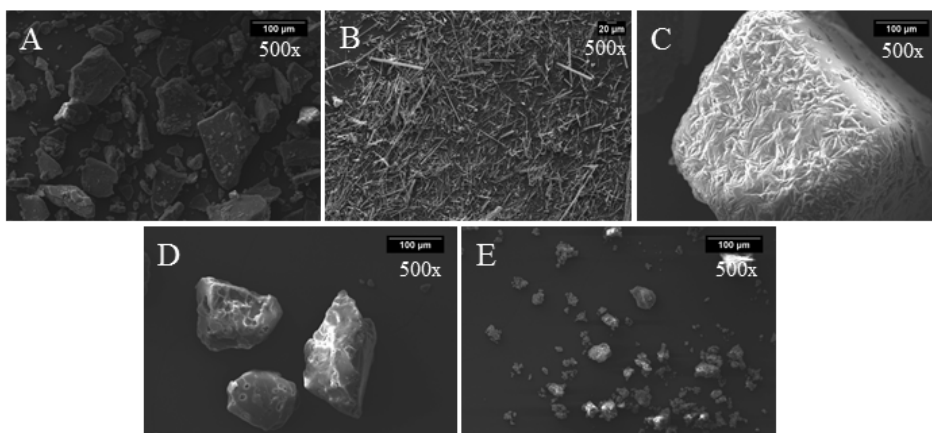


Fig. 5. SEM micrographs of pure materials. Key: A – γ -IND; B – α -IND; C – amorphous IND; D – SOL; E – XYL. Key: IND = indomethacin; SOL = Soluplus[®]; XYL = xylitol. Magnification: $\times 100$ and $\times 500$.

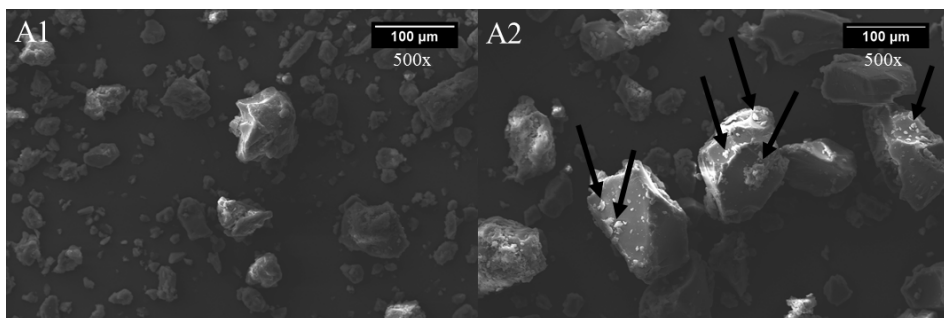


Fig. 6. SEM micrographs of physical mixtures (PMs) and quench cooled (QC) molten solid dispersions (SDs). Key: A1 – PMs of γ -IND and SOL (1:3); A2 – SDs of IND and SOL (1:3). Key: IND = indomethacin; SOL = Soluplus[®]. Magnification: $\times 500$. Drug particles are indicated by arrows.

6.2.3. Powder flow (II)

Characterization of powder flow is an important aspect in formulating efficient pharmaceutical product. Hence, the powder flow of pure materials, PMs and SDs were evaluated using an in-house automated cuvette rheometer designed for testing in a small scale (Fig. 1, II). Fig. 7 shows the dependence of the number of cuvette movements and the sample mass in the chambers, thus quantifying the powder flow rate (mg/movement) of the sample. As expected, the powder flow of pure γ -IND was very poor due to the morphology and size of particles (rectangular, sharp edged particles). Both carrier materials (SOL/XYL) presented free flowing powder behavior. Similar results have been shown previously (Seppälä et al., 2010; Reginald-Opara et al., 2015).

When the amount of the carrier material was increased, the powder flow of the PMs significantly improved (Fig. 7). The PMs of γ -IND and SOL with the highest drug-polymer weight ratio (1:9) showed the highest powder flow rate (21.2 mg/movement), while the powder flow rate of the PMs (3:1) was the poorest (6.0 mg/movement) (Fig. 7). The 1:9 PMs (drug-sugar alcohol ratio) showed a good powder flow (20.0 mg/movement) and 3:1 PMs exhibited very poor powder flow (6.2 mg/movement) (Fig. 7).

According to the literature, some established polymeric carriers (PVP, HPMC, chitosan) can advance the powder flow of crystalline IND in PMs (Yadav and Yadav, 2009). The powder flow of IND in these PMs was evidently improved due to the contact (drug particles) with round shaped polymeric/non-polymeric carriers. Li et al. (2015) reported that the powder flow properties of paracetamol in PMs with SOL was improved since the drug crystals formed a thin coating layer on the surface of the polymer (SOL) particles (Li et al., 2015). The powder flow of the SDs of IND and SOL was superior compared to that of the corresponding PMs with the powder flow rate values of 17.6 mg/movement and 12.9 mg/movement, respectively (Fig. 7). This could be explained by the

larger average particle size and more spherical shape (oval) of the SDs compared to that of PMs (Fig. 6). Djuris et al. (2013) showed that the SDs of SOL advanced the powder flow properties of carbamazepine. Dabbagh and Taghipour (2007) reported that the SDs of ibuprofen and PEG have superior powder flow properties over the corresponding PMs, and the authors suggested that SDs can be used for promoting the bulk powder flow of the drug. In the present study, the moisture content of SD (SOL) was somewhat smaller than that observed with the respective PMs (Fig. 8). Nevertheless, it is evident, that the difference in particle size and morphology is the major factor leading to the differences in the powder flow of SDs and PMs.

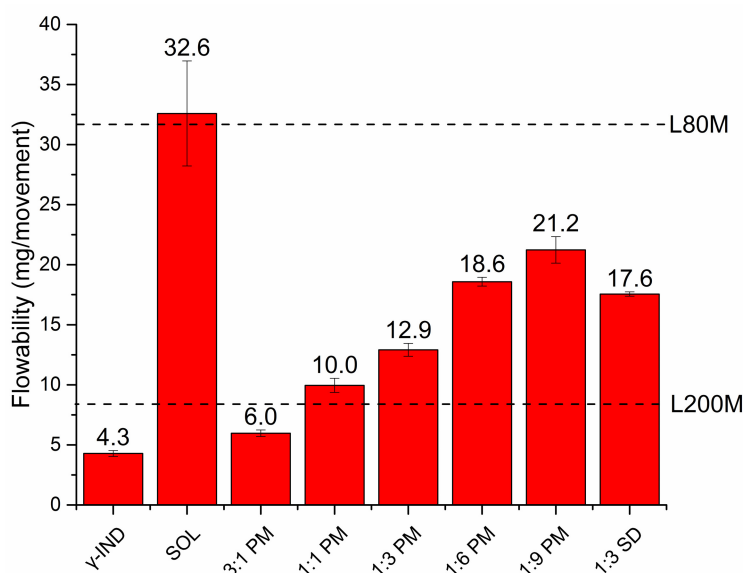


Fig. 7. Powder flow of pure materials (γ -IND, SOL), physical mixtures (PMs) and quench cooled (QC) molten SDs with SOL ($n = 3$). Key: IND = indomethacin; SOL = Soluplus[®]. Reference materials for a powder flow test: Lactose 80M – 31.72 ± 1.31 mg/movement (= good flowability), Lactose 200M – 8.37 ± 0.27 mg/movement (= poor flowability) (dotted lines).

6.2.4. Moisture content, sorption and wetting properties (II)

The moisture content and wetting of pharmaceutical powders can essentially affect the bulk powder behavior, manufacturing, performance and stability of a final pharmaceutical dosage form. Fig. 8 shows the residual water content of pure materials, PMs and SDs. The water contents for the drug and SOL were 0.24% and 2.49%, respectively. These results are in line with the values presented in the literature (Priemel et al., 2013b). The hydrophobic IND had a low water content, and this was verified also in the moisture sorption studies. SOL is an amorphous polymer known to be able to absorb water vapor from the

environment, and the polymer chains most likely interact more readily with water compared to XYL molecule (crystalline material). Different polymers behave differently, and the water may exist in different states within the material-bound *vs* free water which also affects the behavior of polymers in the presence of drug molecules (Williams et al., 2013). As shown in Fig. 8, the differences in the water content of PMs and SDs consisting of either SOL or XYL, are evident. With the PMs of γ -IND and SOL, the water content increased as the amount of polymer was increased (Fig. 8). The moisture content of the SDs of IND and SOL (1:3) was smaller than that observed with the respective PMs. Most likely this is due to the fact that within the glassy suspension of IND and SOL, the hydrogen bonding between the drug and polymer reduces the potential of H-bonding of the water to either component.

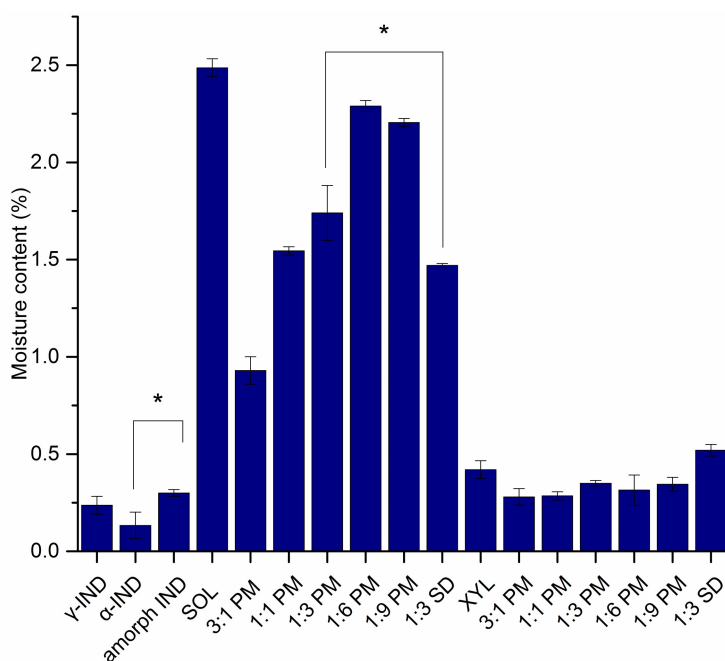


Fig. 8. Water content (w/w %) of pure materials (γ -IND, SOL, XYL), physical mixtures (PMs), and quench cooled (QC) molten solid dispersions (SDs) ($n = 3$). Key: IND = indomethacin; SOL = Soluplus[®]; XYL = xylitol. The symbol (*) indicates the statistical significant difference ($p < 0.05$).

As expected, the moisture sorption of amorphous IND was found to be higher (1.3–2% increase in weight gain) than the moisture sorption of γ -IND. The corresponding increase in weight gain for SOL was 13–18%. The pure materials were exposed to high 95% RH for 7 days, but the equilibrium was reached already within 96 h. The PMs of IND and SOL (1:3) exhibited slightly higher values for weight gain (water vapor sorption) compared to the respective SDs. This result is in line with the water content measurement results. The moisture

sorption of SDs of IND and SOL (1:3) was much higher compared to that of pure IND forms (γ , α , amorphous IND). Most likely, the inclusion of SOL between IND molecules in regions of molecular-level mixing makes the interior of the SD particles more hygroscopic, thus resulting in increased water vapor uptake compared to pure forms. SOL containing PMs and SDs were less prone to water sorption. Punčochová and co-workers (2014) reported that the water sorption of SOL stored at 90% RH resulted in a 25% mass gain. In their study, the PMs and SDs of valsartan and SOL (1:3) were subjected to dynamic water sorption (0–95% RH). Interestingly, both PMs and SDs (the latter assumed to include molecular-level mixing) showed identical sorption isotherms with approximately 16% of a mass gain, which is in line with our findings. The reason for such phenomenon is obviously strong drug-polymer interactions and the blockage of H-bonding functional groups for water sorption. Nevertheless, the SDs showed faster dissolution (pH 6.8) kinetics than respective PMs (Punčochová et al., 2014).

Formulating the drug in PMs and SDs usually results in improved wet-ability, which is correlated with the improved intrinsic dissolution rate of the model drug (Chokshi et al., 2007). In the present study, the contact angle values for the SDs containing different carrier material were $54.9^\circ \pm 8.0$ (IND and SOL 1:3). The difference in contact angle values, however, were not statistically significant. It is evident that amorphous IND in the SDs absorbs water more readily compared to the crystalline γ - and α -IND (as verified in Fig. 9), thus resulting in decreased and more uniform contact angle values obtained with the SDs with different carrier materials (Fig. 9, II).

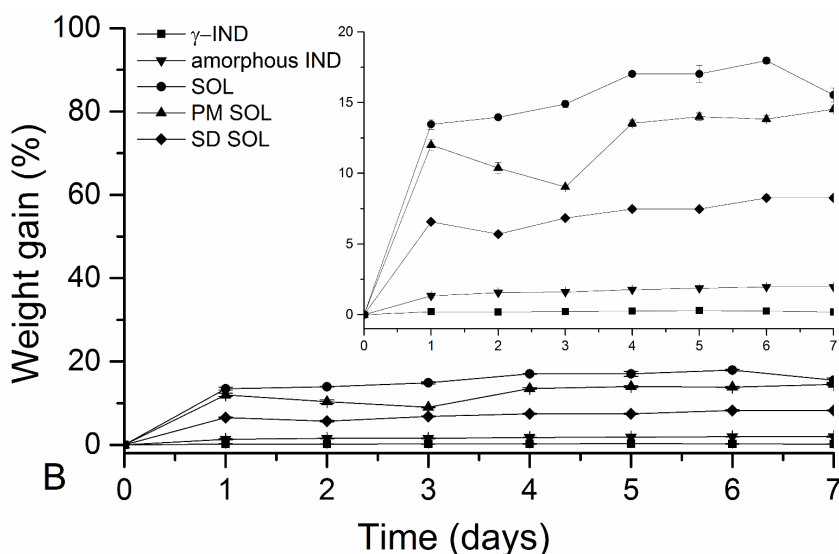


Fig. 9. Moisture sorption of pure materials (γ -IND, amorphous IND, SOL), physical mixtures (PMs) and quench cooled (QC) molten solid dispersions (SDs) ($n = 3$). Key: IND = indomethacin; SOL = Soluplus®.

6.3. Quench-cooled molten solid dispersions of indomethacin and xylitol (I, II)

6.3.1. Physical solid state and drug-carrier interactions (I)

The DSC and MT-DSC thermograms of QC molten IND:XYL SDs showed two endothermic events (one for XYL at 89 °C and one for α -IND at 152 °C) and no change in T_g compared to pure materials, thus suggesting the presence of a poorly miscible two-phase drug-carrier system (Table 1, I). Since the recrystallization of IND was also detected at 124 °C, it is evident that XYL was not able to prevent the heat induced solid-state changes of IND in these SDs. Furthermore, also VT-XRPD results using IND:XYL SDs (Figs. 5C and D, I) verified the DSC/MT-DSC results showing a two-phase system (Fig. 4, I).

The specific spectral regions of interest for the IND and XYL related interactions in SDs and PMs are at 1714 cm^{-1} and 1689 cm^{-1} (both C=O of IND) and 3421 cm^{-1} , 3359 cm^{-1} , and 3293 cm^{-1} (OH groups of XYL). The FT-IR spectra showed limited compatibility between those two components, since instead of the peak shift only intensity changes were detected in carbonyl and hydroxyl group vibrations. Several studies have shown limited ability of XYL to form chemical interaction with the active ingredients (Mummaneni and Vasavada, 1990; Sjökvist and Nyström, 1991; Suzuki and Sunada, 1997; Madgulkar et al., 2015).

6.3.2. Particle size, shape and surface morphology (I, II)

Xylitol (XYL) possessed smaller agglomerates or particles with an uneven shape and size as amorphous IND and SOL (Figs 3, C, D, E). The average particle size of IND quench cooled (QC) molten mixtures of IND and XYL was alike to corresponding PM and SD of SOL. Interestingly, the larger particles in the PMs of γ -IND and XYL were layered with tiny drug particles (Fig. 10).

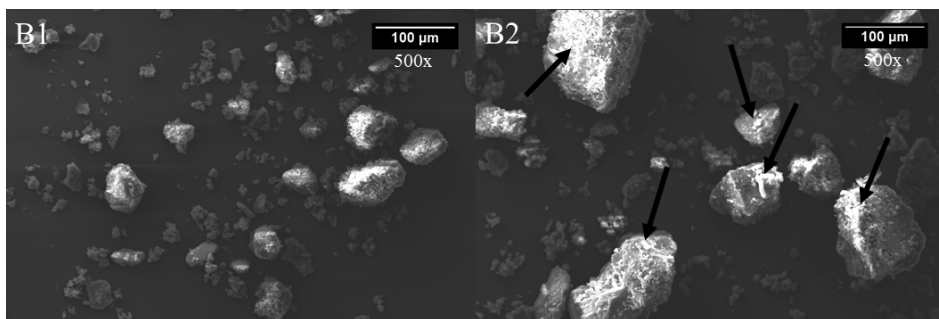


Fig. 10. SEM micrographs of physical mixtures (PMs) and quench cooled (QC) molten solid dispersions (SDs). Key: B1 – PMs of γ -IND and XYL (1:3); B2 – SDs of IND and XYL (1:3). IND = indomethacin; XYL = xylitol. Magnification: $\times 500$. Drug particles are indicated by arrows.

The corresponding micrographs of SDs containing IND and XYL at the weight ratio of 1:3 showed similar results, thus indicating that the drug particles were dispersed in a XYL matrix (Fig. 2C).

6.3.3. Powder flow (II)

The powder flow of XYL containing mixtures showed that it is a carrier driven process. As with SOL, those PMs of γ -IND and XYL with the highest drug polymer weight ratio (1:9) showed the highest powder flow rate, and the poorest flow with the highest drug loading (3:1). Sugars with a low water activity possess good powder flow properties (Seppälä et al., 2010). The powder flow properties of the SDs of IND and XYL (1:3), and the corresponding PMs were very similar (Fig. 11). This could be explained by the crystallization of XYL from the SDs resulting in the SD bulk powder with similar properties as PMs.

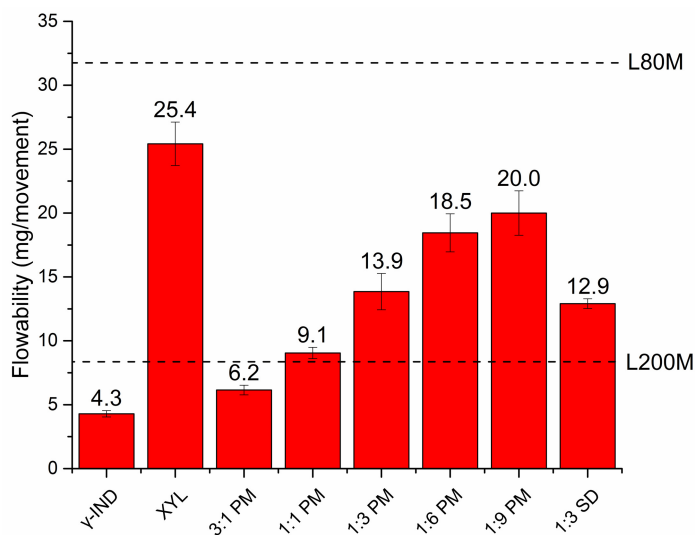


Fig. 11. Powder flow of pure materials (γ -IND, XYL), physical mixtures (PMs) and quench cooled (QC) molten SDs with XYL ($n = 3$). Key: IND = indomethacin; XYL = xylitol. Reference materials for a powder flow test: Lactose 80M – 31.72 ± 1.31 mg/movement (= good flowability), Lactose 200M – 8.37 ± 0.27 mg/movement (= poor flowability) (dotted lines).

The water content of the samples showed only small differences and moisture sorption was also alike. Indeed, the particles of the SDs were larger compared to those of the PMs, but the adhesion of IND particles to the surface of XYL particles in the PMs unified the surface roughness of the PM and SD particles. The particles with smooth surfaces were observed with both PMs (XYL) and SDs (XYL) (as shown in Fig. 10) which could explain their similar flow properties. According to the literature, the adhesion and friction forces between

the drug and carrier material are greatly dependent on the surface roughness of the particles (Podczek, 1998). Genina and co-workers (2009) revealed that the particle surface engineering with an ultrasonic water mist improved the powder flow of lactose due to the particle surface smoothing and loss of fines. In the present study, it appeared that the inclusion of SOL or XYL in the PMs and SDs clearly promotes the powder flow of poorly flowing IND. It was found that the bulk powder flow properties of both PMs and SDs were directly related to the amount of carrier polymer used, and the SDs of the drug and carrier material presented equal powder flow as the corresponding PMs. In the PMs and SDs with XYL, drug particles were adhered or fused onto the surface of XYL, which unified also the powder flow of these systems. Moisture sorption most probably does not play any significant role in such systems, since XYL does not absorb much water below 80% RH (Rowe et al., 2009).

6.3.4. Moisture content, sorption and wetting properties (II)

The water content for XYL was 0.42%. XYL is a small-molecule nonporous sugar alcohol, and it possesses much lower water content due to its crystalline structure. With the PMs of γ -IND and XYL, the water content was virtually independent of the amount of the carrier used (Fig. 6). With the SDs of IND and XYL (1:3), the moisture content was higher (0.52%) compared to that of PMs (0.35%). This small difference in water content could be explained by the more hygroscopic nature of amorphous IND dispersed in a crystalline hydrophilic XYL matrix in two-phase SDs (amorphous precipitation system). Since the surface of the PMs and SDs of IND and XYL samples was covered with drug particles (confirmed by SEM, Fig. 10), the adsorption of water on crystalline XYL is most likely largely depended on the solid state of the drug. The moisture studies showed a significant weight gain for XYL (34–89%). XYL was rapidly absorbing moisture for up to 144 h (89%). As seen in Fig. 12, the SDs of IND and XYL (1:3) showed a similar weight gain (water vapor sorption) as its respective PMs. SDs containing XYL showed highly hydrophilic properties, with contact angle of $46.4^\circ \pm 5.7$ (IND and XYL 1:3). Rapid changes in the weight gain of both PM and SD samples occurred within the first 24 h (25.2–35.5% increase in weight gain). The SDs of IND and XYL (1:3) dissolved partially in sorbed water and formed transparent droplets. According to the literature, the water sorption of sugars ranges typically 3–5 mg/g, and water activity (a_w) of XYL is 0.6 (25 °C) (Weisser et al., 1982). At the a_w levels of 0.6–0.7, water molecules are adsorbed on the crystal surface, but at the a_w values higher than 0.7, the amount of absorbed water rises steadily resulting in the dissolution of the crystals (Demertzis et al., 1989). As IND and XYL were in two separate phases in both SDs and PMs, the overall effect of the hydrophobic small molecule on the moisture sorption was negligible. In summary, the PMs and SDs of IND with XYL can sorb water vapor more readily compared to the corresponding PMs and SDs of IND with SOL.

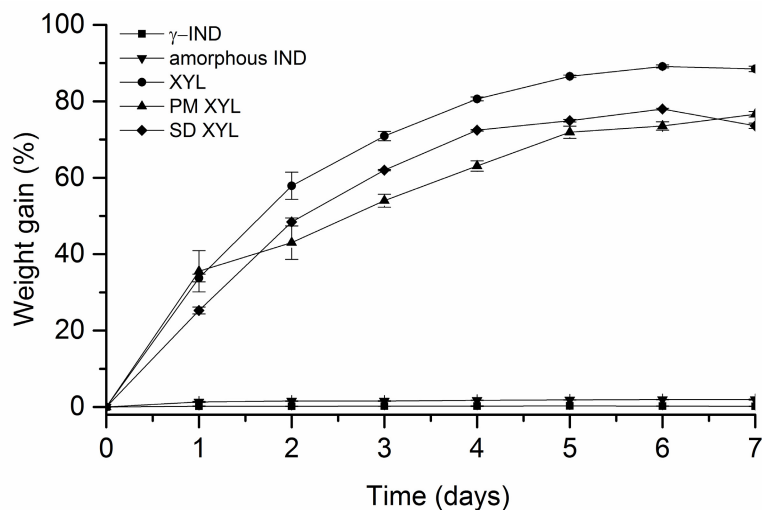


Fig. 12. Moisture sorption of pure materials (γ -IND, XYL), physical mixtures (PMs) and quench cooled (QC) molten solid dispersions (SDs) ($n = 3$). Key: IND = indomethacin; XYL = xylitol.

6.4. Melt-electrospun fibrous solid dispersions of indomethacin and Soluplus® (III)

6.4.1. Physical solid state and drug-carrier interactions (III)

The XRPD was used to detect physical solid-state changes of the components in a MES process. The list of prepared formulations are depicted in Table 3. The drug (IND) in the PM1 preserved its γ -IND crystalline form after mixing with SOL (a slightly elevated baseline of amorphous SOL can be also seen). As expected, the PM of amorphous IND and SOL (PM2) showed only an amorphous halo. In case of the PM3 (the PM was stored at RH 90%), the XRPD pattern showed minor intensity changes, but the γ -IND reflections were clearly distinguishable. The polymorphic transformation of an amorphous IND to α -IND, however, was not detected at high RH in the present study, and this finding differs from the results on the physical stability of IND reported in the literature (Shalaev and Zograf, 2002). Evidently, the addition of polymer (SOL) can significantly alter the crystallization behavior of an amorphous material. The MSFs of IND and SOL (originated from the PM3) showed the XRPD pattern with a clear amorphous halo, thus confirming the formation of an amorphous SD (Fig. 4, III).

Table 3. Formulations used in melt-electrospinning (MES) studies

Formulations	Composition
PM1	physical mixture of crystalline γ -IND and SOL at the weight ratio 1:3 (drug:polymer)
PM2	physical mixture of amorphous IND and SOL at the weight ratio 1:3 (drug:polymer)
PM3	PM1 stored at high RH (90%)
MSF	melt-electrospun fibers prepared from PM3

Key: PM – physical mixture, MSF – melt-electrospun fiber, SOL – Soluplus[®], RH – relative humidity.

FTIR, spectroscopy was used to investigate the potential drug-carrier polymer interactions during MES. In the present study, a special attention was paid to the region between 1650 cm^{-1} and 1750 cm^{-1} which is characteristic to IND carbonyl (C=O) stretching bands (Ewing et al., 2014). As seen in (Fig. 5, III), the FTIR spectrum of γ -IND contains two bands in this region. The peaks at 1688 cm^{-1} and 1711 cm^{-1} were assigned to the benzoyl C=O and assymmetric stretch of the carbocyclic acid bands, respectively. The present results are in accordance with the wavenumbers reported for C=O bands in the literature (Ewing et al., 2014; Lin et al., 2015; Terife et al., 2012). The spectra of PM1 and PM3 are quite similar. Both contain the benzoyl C=O vibration band at 1688 cm^{-1} . Due to spectral overlapping with the SOL ester C=O band at 1732 cm^{-1} , the band assigned to assymmetric stretch of the carbocyclic acid is located at 1715 cm^{-1} in the spectra of PM1 and PM3. The benzoyl C=O vibration band appears at 1682 cm^{-1} in the spectra of MSFs and PM2. According to the literature, the band at this wavenumber is specific to amorphous IND (Ewing et al., 2014; Lin et al., 2015; Terife et al., 2012). The spectrum of PM2 contains a shoulder to the SOL ester C=O band at 1709 cm^{-1} that has been assigned to the hydrogen bonded carboxylic acid C=O in amorphous IND molecules arranged as chains or dimers (Ewing et al., 2014; Lin et al., 2015; Terife et al., 2012). This feature is lacking in the spectrum of MSFs. This difference in the spectra could indicate at least partial hydrogen bonding between IND and SOL molecules in MSFs.

We also recorded the ^1H -spectra of PM1 and MSFs which were recorded after dissolving the materials in deuteriochloroform. The NMR spectra of electrospun mixture includes a combination of IND and SOL chemical shifts, thus confirming the lack of thermal degradation (Fig. 13A).

^{13}C FT-NMR spectroscopy (^{13}C CP-MAS-spectra) was carried out to study more intimate mixing of the drug:carrier (SOL) and their chemical stability. ^{13}C -CP-MAS-spectrum of the PM1 shows the chemical shifts of both substances as a direct superposition of the spectra of the pure materials (Fig. 13B). In the PM1, IND is still in the γ -form as indicated by the lack of splitting of the signals (Masuda et al., 2006). For the MSFs, the chemical shifts show a marked change as in general the signals from γ -IND are broadened significantly

and nearby signals are merged together. As the signals from pure SOL are already quite broad, similar changes were not observed for SOL in MSFs. This change in the IND spectrum suggests more intimate mixing of the substances during a MES process (Fig. 13B).

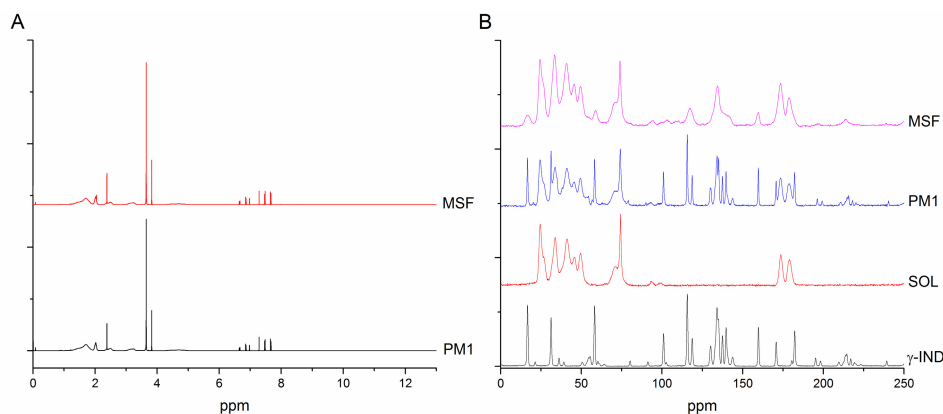


Fig 13. Overlay of ^1H -spectrum of physical mixture (PM1) and melt-electrospun fibers (MSFs) (A) and ^{13}C CP-MAS-spectra of starting materials, physical mixture (PM1) and melt-electrospun fibers (MSFs) (B). Key: γ -IND – indomethacin, SOL – Soluplus[®], PM1 – the physical mixture of crystalline γ -IND and SOL at the weight ratio 1:3 (drug:polymer), MSF – melt-electrospun fibers prepared from PM3 (the PM1 stored at high RH (90%).

In order to get more information about the difference of IND in the PM1 and MSFs, the relaxation time $T_1(^1\text{H})$ was recorded. Signals in the approximate region of 63–76 ppm originate exclusively from SOL and 125–138 ppm from IND. The measured $T_1(^1\text{H})$ of SOL (63–76 ppm) is 2.061 s for the PM1 and 2.067 s for the MSFs, and they can be considered to be practically the same. However, the measured $T_1(^1\text{H})$ of IND (125–138 ppm) in the PM is 4.524 s compared to that of 2.165 s for the MSFs. This gives IND a domain size range of 25–100 nm for the MSFs. The very similar values of $T_1(^1\text{H})$ for both IND and SOL in the MSFs can be considered as a strong indication of significantly smaller domain size of the IND in the SOL matrix compared to the PM1. The $T_{1\rho}^1\text{H}$, which would give information about the domain size within the range of 2–20 nm, could not be measured as the long spin-lock times would have seriously damaged the probe.

6.4.2. Fiber diameter, shape and surface morphology (III)

The fiber size and morphology of drug-loaded melt-electrospun fibers (MSFs) of IND and SOL at the weight ratio of 1:3 and the corresponding blank MSFs are presented in Fig. 14. The diameter of drug loaded MSFs ranged from

300 μm to 400 μm and the diameter of blank MSFs ranged from 200 μm to 400 μm . As reported elsewhere, the diameter of fibers prepared by MES can vary even from 270 nm (i.e., nano-scale) to 500 μm (micro-scale) (Dalton et al., 2006; Lyons et al., 2004). Such a wide size range option in fiber diameters shows the flexibility of MES. In the present study, the large micro-scale size of MSFs could be explained by the high molecular weight of SOL (90 000 – 140 000 g/mol) (BASF, 2010). According to the literature, the molecular weight of a thermal carrier polymer is a critical factor determining the final fiber diameter in MES (Lyons et al., 2004).

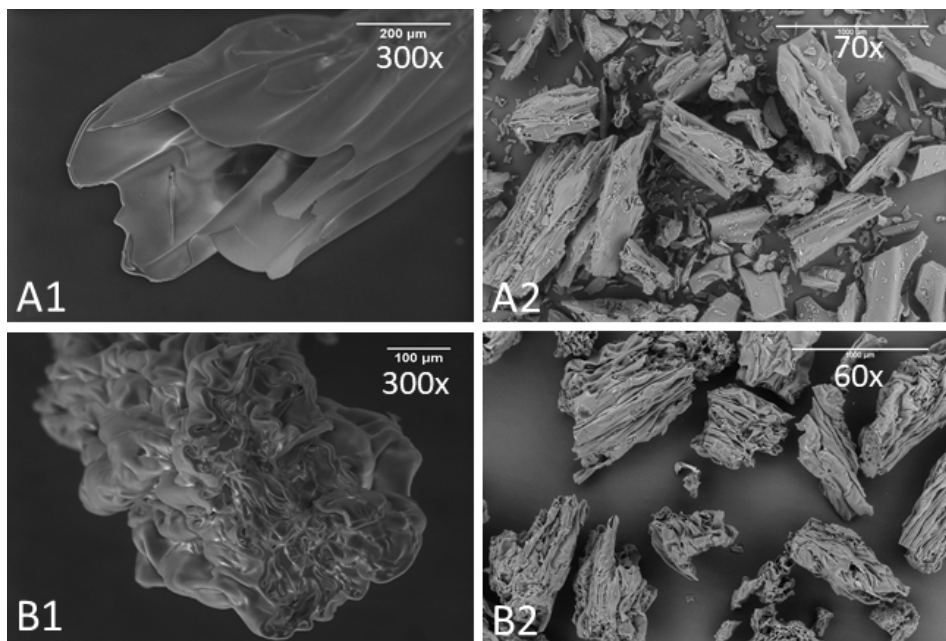


Fig. 14. The SEM images of (A1) intact melt-electrospun fibers (MSF) of γ -IND and SOL at the weight ratio of 1:3 (drug to polymer), (A2) the corresponding ground MSFs, (B1) blank MSFs, and (B2) the corresponding ground blank MSFs. Key: γ -IND = indomethacin, SOL = Soluplus®.

The surface morphology of the present MSFs (Fig. 14) was smooth without any voids or pores, but clearly shrunken and billowy for the whole fiber area. This could be explained by a thermal shock induced by the temperature difference during MES when the fibers are produced and collected. The shrinking was more pronounced with blank MSFs (Fig. 14B), thus showing a higher polymer chain mobility compared to the drug loaded MSF. It is well known that higher surface area results in higher dissolution rate (Noyes and Whitney, 1897). Hence the major advantage of shrunken and billowy MSFs compared to the smooth fibers is a larger specific surface area, and thus their dissolution rate should be faster compared to the smooth surfaced fibers/particles.

The SEM image on the cross-section of drug-loaded MSFs (Fig. 14A1) shows a non-uniform structure of the fiber. At some places, the fibers are hollow and at others they do not have any inner voids at all. The cross-section of blank fiber (as shown in Fig. 14B1) consisted of primarily intact solid surface with very small voids. The difference in the fiber morphology of the drug-loaded and blank MSFs could be related to the different molecular mobility and rigidity of the IND containing SOL and pure SOL during MES process. As mentioned earlier, the instability of a MES process could also partially explain the formation of MSFs with such a complicated structure. Fig. 14 shows also the SEM images of drug-loaded (A2) and blank (B2) MSFs in a powder form after grinding. The partially hollow structure of the original MSFs can be still seen even after grinding (Fig. 14A2). These cavities are evidently the former water vapor channels inside a fiber matrix, and they are formed as water is evaporated from the matrix or extrudate (Miladinov and Hanna, 1999).

6.4.3. Moisture content (II)

Due to the high viscosity of the melt, it was necessary to decrease the temperature of the process to avoid the chemical degradation of the drug (IND) and carrier (SOL). Pre-storing the samples at high humidity (above 90% RH) in dessiccator prior MES experiments was used in order to plasticize the PM1. The latter enabled to lower the processing temperature of MES by 40 °C (to 180 °C). Hence, the addition of plasticizer (in our case water) was of critical importance. In addition, water vapor heated up to 180 °C created additional pressure that probably helped to overcome the high viscosity of the polymer melt.

In our system, water acted as a plasticizer reducing the viscosity of the melt and improving the performance of a MES. The plasticizing effect of water has been previously shown for starches prior extrusion into the foams (Shogren, 1996; Sjöqvist and Gatenholm, 2005). In the case of starch extrusion, water added in the system is entrapped inside the cavities of the extrudate, and after leaving extruder, it evaporates and forms channels in the matrix (Miladinov and Hanna, 1999). It is evident that similar interaction with water also occurs in the present MES process, thus resulting in the formation of partially hollow MSF structures.

6.4.4. Chemical and thermal stability (III)

Like in HME, on the course of MES the materials are subjected to a short-term high temperature and pressure during the process. These conditions can cause the chemical degradation of drug, polymer or both. According to the literature, thermal decomposition of IND is a one-step phenomenon within the range of 236–338 °C (Tita et al., 2009). IND has a good safety margin for thermal processing at lower temperatures. According to Forster et al. (2001), the chemical

stability of IND in PVP/IND dispersions at different weight ratios (1:1 and 4:1) after HME at 170 °C was good, since only less than 1% of drug was decomposed. Melt extrusion of acrylic polymers/IND (30% drug concentration) showed that IND is chemically stable after exposure to high temperature (140 °C) (Zhu et al., 2006). SOL is thermally stable up to 220 °C showing no changes in the chemical composition or degree of polymerization (BASF, 2010; Kolter et al., 2012). Weight loss of the samples up to 150 °C was assigned to the desorption of water. Given values were used to estimate the amount of water absorbed by SOL and PMs. SOL contained 2.37% and the PM1 contained 1.56% of water by weight. After storage at high RH (90%), the PM3 contained 7.41% of water by weight. IND was found to be a thermally stable compound at the temperature that was used for MES (only 0.11% of weight loss at 180 °C was detected). The thermal degradation of IND and SOL started at 197.1 °C and 218.2 °C, respectively. According to the literature, the thermal degradation of IND occurs approximately at 236 to 338 °C (with T_{\max} 314 °C) (Tita et al., 2009). The present results are in agreement with those reported in the literature, where a 2.5% weight loss of SOL was detected at low temperatures, and the degradation of the material started approximately at 250 °C (Kolter et al., 2012). In summary, TGA results suggest that MES performed at 180 °C is a non-destructive process and does not cause (or causes only minimal) thermal degradation for the present materials. A long-term exposition of materials to MES process, however, will most likely result in thermal degradation of the materials.

The TGA results were in line with the DSC results, where γ -IND showed a sharp melting endotherm at 161.8 °C (without any water desorption), and SOL showed a broad water evaporation endotherm until 76.3 °C (indicating also a substantial amount of water in the samples) (Fig. 15, B). The DSC thermographs of PM1 showed broad water evaporation endotherm derived from SOL within PMs and a broad fusion endotherm of γ -IND into SOL starting at 115.7 °C. The fusion endotherm ended with a minor sharp endotherm at 160.1 °C, which was attributed to the melting of residual γ -IND. The PM2 containing amorphous IND and SOL at the weight ratio 1:3 (drug:polymer) presented the T_g of IND at 50.6 °C and a water evaporation endotherm. In addition, a small exothermic peak was recorded at 83.8 °C, and it was assigned to the crystallization of IND. The onset temperature of the subsequent fusion endotherm for recrystallized IND was recorded at 107.0 °C. The PM3 (stored at high RH 90%) thermogram mirrored the results of PM1. As expected, the thermal behavior of PMs revealed the behavior of the pure materials alone (Fig. 15, B). The DSC thermograph of MSF indicates the formation of amorphous SD, since no signs of the IND melting point were detected, which obviously indicated at least partial mixing of a drug in a molten polymer (Fig. 15, B).

Total drug content of MSFs after preparation was assayed/verified by HPLC. Three different MES batches were analysed in duplicate or triplicate (theoretical drug content was 25%). The following drug content for different MSF batches

were measured: $23.2 \pm 0.15\%$ ($n=3$) for batch 1; $23.8 \pm 0.6\%$ ($n=3$) for batch 2 and $23.5 \pm 0.4\%$ ($n=2$) for batch 3. These values were in close proximity to the theoretical drug content values confirming that the present MES process is stable and reproducible resulting in small drug content variation.

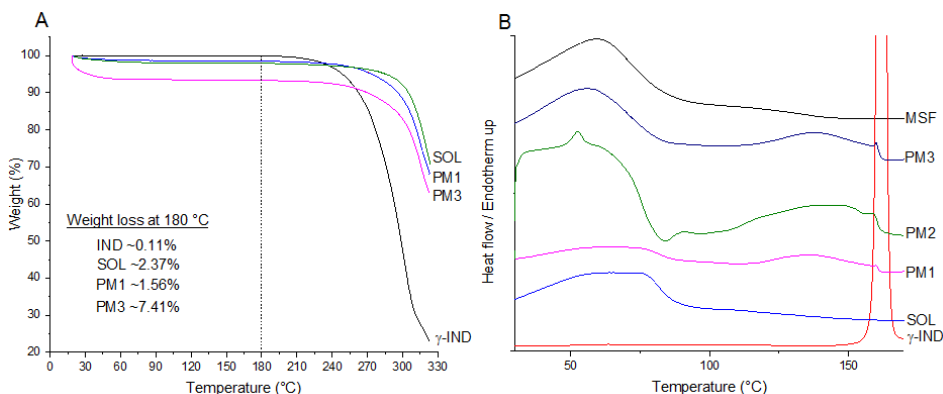


Fig. 15. Thermogravimetric analysis (TGA) (A) and differential scanning calorimetry (DSC) thermograms (B) of starting materials, physical mixtures (PMs) and melt-electrospun fibers (MSF). Key: γ -IND – indomethacin, SOL – Soluplus[®], PM1 – the physical mixture of crystalline γ -IND and SOL at the weight ratio 1:3 (drug:polymer), PM2 – the physical mixture of amorphous IND and SOL at the weight ratio 1:3 (drug:polymer), PM3 – the PM1 stored at high RH (90%), MSF – melt-electrospun fibers prepared from PM3. The actual process temperature of MES (180 °C) is indicated with a solid line in the figure.

6.5. Dissolution in vitro (II–III)

The BCS deploys IND among the class II drugs, which are characterized by slow or partial dissolution and fast absorption *in vivo* (Amidon et al., 1995). Accordingly, with the BCS class II drugs dissolution is a critical attribute governing their oral bioavailability and therapeutic effect. Craig (2002) reported that the dissolution of drug-loaded SDs can be primarily either (1) the carrier-controlled dissolution (especially at low drug loadings), or (2) drug-dependent dissolution. The prevalence of the release mechanism is dependent on the miscibility and solubility of the components in the concentrated solution of the polymer (Craig, 2002). In addition, several processes competing with one another take place simultaneously during the dissolution of SDs, and both the drug and carrier polymer properties affect the total drug release (Kogermann et al., 2013).

We found that the SDs of IND and SOL form a two-phase glassy suspension where the amorphous IND is thoroughly mixed with amorphous SOL (Fig. 2). This enhanced dissolution is obviously as a result of improved wetting of IND and inhibited crystallization of the drug from amorphous form or from solution

to α form by SOL. Furthermore, over 85% of the drug was released from the SDs of IND and SOL within 60 min of the dissolution test (Fig. 16). According to Surwase et al. (2015), molecular mixing between IND and SOL in one-phase SD completely inhibited the drug release. Interestingly in the present study, the release of IND from the corresponding PMs was hindered due to the gelling properties of the polymeric carrier and very poor wettability of PMs and γ -IND (Fig. 5). Since γ -IND is hydrophobic, the amphiphilic SOL molecules tend to adhere onto the IND crystals, thus decreasing the effective dissolution surface area. The present results are consistent with the earlier studies showing that the PMs of IND and SOL exhibit a slower dissolution rate because of the gel formation and strong H-bonding (Terife et al., 2012).

According to the results, the SDs of IND and XYL are two-phase systems in which IND is in amorphous form in a crystalline XYL matrix (Fig. 2). The drug release was improved with XYL containing PMs and SDs (Fig. 16) without reaching plateau as with SOL SDs. Excipient intrinsic properties are of critical importance in enhancing the solubility and dissolution rate of PWS drugs. Most likely on the course of rapid dissolution of XYL, the IND particles did not adhere to each other and higher effective surface area was achieved. XYL as a carrier material is freely water-soluble polyalcohol with no gel forming ability (Rowe et al., 2009).

The MSFs of IND and SOL were prepared to assess their drug releasing behavior and compare with to the respective QC SDs. It was found that the dissolution rate of MSFs and PM2 (amorphous IND) was significantly higher than that of crystalline γ -IND powder (Fig. 16). The PM1 showed the slowest drug release, probably due to gel formation of the polymer (SOL). Almost complete drug release of MSFs was observed within 30 min ($88.7 \pm 0.5\%$), while the dissolution of drug released from crystalline drug and respective PMs was much slower and limited. The improved release rate of IND from MSFs is evidently due to the amorphous state and smaller domain size of IND compared to PM1 and PM2. Furthermore, MSFs in a powder form provide a higher effective surface area compared to other solid state forms. This is due to a specific morphology of the powder particles obtained by grinding the present MSFs (i.e., partially plate shaped particles). These properties have been reported to have a significant effect on the release rate of PWS drugs (Hancock and Parks, 2000; Hughey et al., 2013; Merisko-Liversidge and Liversidge, 2011). These observations are in accordance with those reported by Balogh et al. (2014) and Nagy et al. (2013), who found that the drug release of MSF is comparable to the fibers fabricated by solvent-based ES and superior to PMs and drug alone (Balogh et al., 2014; Nagy et al., 2013).

Drug dissolution rate from MSFs was higher than from QC SDs or respective PMs. The XYL containing PMs showed different release profile but by 60 min the total amount of drug in the solution was similar to MSF. Our findings suggest that MES can be viable option for improving the solubility of PWS drugs and regarded as alternative SD preparation technique to QC and HME.

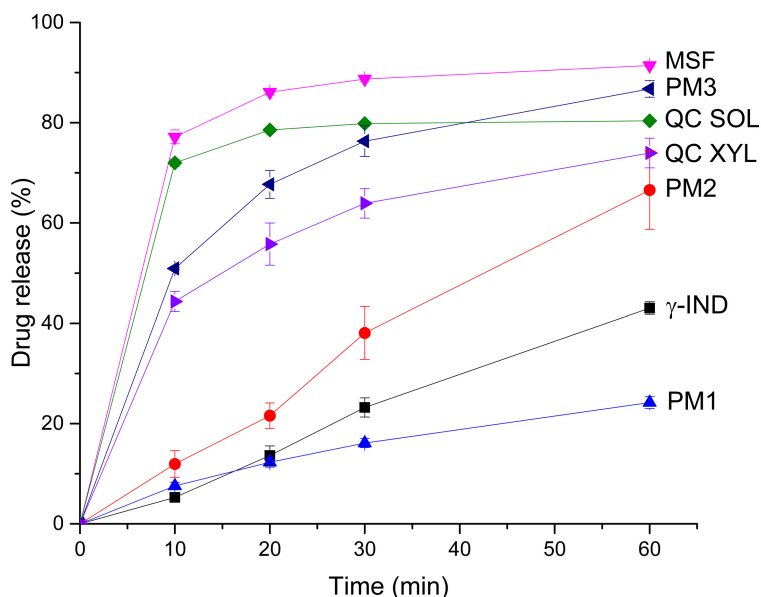


Fig. 16. *In vitro* dissolution profiles of γ -IND, physical mixtures (PMs) and melt-electrospun fibers (MSF) at the weight ratio 1:3 (drug:polymer) in pH 6.8 phosphate buffer (n=3). Key: γ -IND – indomethacin, PM1 – the physical mixture of crystalline γ -IND and SOL at the weight ratio 1:3 (drug:polymer), PM2 – the physical mixture of amorphous IND and SOL at the weight ratio 1:3 (drug:polymer), PM3 – the physical mixture of amorphous IND and SOL at the weight ratio 1:3 (drug:polymer) stored at 90% RH, QC SOL – quench cooled solid dispersion of IND and SOL at the weight ratio 1:3 (drug:polymer), QC XYL – quench cooled solid dispersion of IND and XYL at the weight ratio 1:3 (drug:polymer), MSF – powdered melt-electrospun fibers. The error bars indicate the standard deviations (n = 3).

6.6. Physical storage stability of solid dispersions (I)

According to the literature, molecularly dispersed single-phase solid dispersions (SDs) are the most stabilized systems against crystallization (Williams et al., 2013). Hence, the degree of miscibility between the drug and polymer is important for the formation of a physically stable amorphous system. Aging under different humidity conditions can change the physical solid-state properties and performance of two-phase SDs systems. In the present study, the physical stability of the two-phase systems was investigated to understand their potential stabilizing mechanisms (I). The physical storage stability of the aged QC molten SDs of IND:SOL and IND:XYL was investigated by means of XRPD, DSC and ATR-FTIR spectroscopy. Interestingly, different analytical methods revealed somewhat different level of physical stability in these two-phase SD systems, thus providing a further proof that complementary analysis methods are needed to obtain complete insight into the complex recrystalli-

zation behavior. According to XRPD, the QC molten SDs (with a IND:SOL weight ratio of 1:3) were stable up to 2 months when stored at 0% RH/RT, and at least 1 week when stored at 50% RH/RT (no sign of recrystallization observed). However, storing the present SDs at 75% RH/RT provided only temporary stability. Due to the high noise and low intensity, it was very difficult to fully confirm the origin of the present IND reflection by XRPD (the peak is in close proximity of both γ - (21.8° 2 θ) and α -IND (22.0° 2 θ). The DSC results revealed that a partial recrystallization of α -IND during storage was observed (melting endotherm at 153 °C). According to Andronis et al (1997), amorphous IND stored at 30 °C and 56% RH crystallized into α -IND and amorphous IND stored at 0% was stable at least for 100 days. Whilst during storage at temperatures below the T_g and at low RH usually the recrystallization of γ -IND is favored and above T_g and high RH metastable α -IND is formed (Shalaev and Zografi, 2002). It is known that the method of preparation as well as the presence of stabilizing molecule may change the physical stability of IND samples (Vasconcelos et al., 2007; Surwase et al., 2015). With two-phase amorphous SDs, the level of miscibility (like with one-phase systems), steric hindrance and reduced interface molecular mobility are crucial affecting the physical stability. It has been shown with the PMs of Eudragit® E and pure amorphous IND that the polymer reduces the molecular mobility and possibly mechanical obstruction at the surface of amorphous IND, thus stabilizing amorphous IND (Priemel et al., 2013a). However, due to the large particle size differences between the drug and polymer (SOL), SOL was unable to cover the surface of IND and inhibit its surface-biased nucleation and growth at low RH (22%, 43% RH) and temperature (Priemel et al., 2013a). More recently, Surwase and co-workers (2015) investigated the physical stability of amorphous IND in aqueous suspension with different polymers. The SD of IND and SOL showed the latest crystallization onset (>28 days) compared to other systems, which was explained by the reduced molecular mobility of SD (higher T_g) compared to pure amorphous IND, and by formation of hydrogen bonding or other intermolecular interactions between the components (Surwase et al., 2015). The prepared two-phase IND:SOL SDs showed that two amorphous components with different T_g have separate phases, but are stable enough to prevent the surface-based crystallization at least at low RH. Most likely, the same stabilization mechanism (as described by Surwase and co-workers) governs and plays an important role with our SDs as well. It is possible that some hydrogen bonding interactions between amorphous IND and SOL in the QC molten two-phase amorphous SDs were present thus stabilizing the SDs. However, the stability of a two-phase system may be associated to physical stabilization of multiple phases.

The physical stability of QC molten IND:XYL SDs (50% RH/RT) was very limited. It has been shown that the co-milling of IND and aminoacids (eg., low molecular weight molecules), results in stable co-amorphous systems which are physically stable up to 6 months of storage at 40 °C (Löbmann et al., 2013). However, in the present study two-phase amorphous precipitation system was

obtained instead of co-amorphous form with specific molecular interactions. For our two-phase SDs amorphous suspensions, the proposed stabilization mechanisms are as follows: (1) Internal stabilization, where amorphous IND rich phase is contaminated with SOL leading to reduced molecular mobility due to increased local viscosity. With IND:XYL SD where amorphous drug was precipitated in a crystalline matrix, this is not so evident. The phase contamination in IND:SOL SD was confirmed by the change in T_g compared to pure materials. (2) Interface stabilization which could be related to the hydrogen bond formation at the phase boundary between the drug-polymer, thus preventing crystallization by the formation of drug-drug interactions. In case with SOL, it has functional groups (C=O and -OH) with capacity to bind to IND. Drug XYL combination has limited functional groups and bone rigidity to support the intermolecular interaction within the system. Priemel and co-workers (2013a) have shown that IND crystallized from the surface at temperature below T_g , and reduced molecular mobility at the surface and mechanical inhibition can improve the physical stability.

7. SUMMARY AND CONCLUSIONS

The QC molten two-phase SDs of a PWS drug indomethacin with two different matrix formers (amorphous copolymer *vs* crystalline sugar alcohol) exhibit significant differences in particle properties and bulk powder behavior. Both carrier materials studied here can advance the powder flow properties of a cohesive IND powder, and this improvement is directly related to the amount of a carrier material used in PMs or SDs. The inclusion of a carrier material (SOL/XYL) in both PMs and SDs improves also the wetting properties of an IND powder, where XYL mixtures showed higher moisture sorption compared to SOL ones. The *in-vitro* drug release of the present SDs and PMs has a carrier-controlled release mechanism at pH 6.8. The enhanced drug dissolution from the SDs with SOL is due to improved wetting and inhibited crystallization of IND. XYL as a freely water-soluble polyalcohol advances the dissolution rate of IND most likely through improving the wetting properties and providing the hydrophilic environment in the solution.

Furthermore, it was shown that MES is an auspicious novel method for fabricating amorphous SDs for PWS drug. Only minimal thermal degradation of a model drug (IND) is associated with the fabrication of MSFs in a MES process. Solid-state analysis suggests more intimate mixing between IND and an amorphous stabilizing carrier material (SOL) in the present MSFs. The MSFs of IND and SOL provided significantly faster drug dissolution compared to QC SDs, corresponding PMs and crystalline drug.

In summary, the MSFs produced by MES could be an alternative strategy to traditional or modified QC and HME in improving the dissolution, and consequently the oral bioavailability of PWS drugs. Further studies are needed to confirm if current findings would lead to better absorption rate and bioavailability *in vivo*.

REFERENCES

- Aaltonen, J., Rantanen, J., Siiria, S., Karjalainen, M., Jørgensen, A., Laitinen, N., Savolainen, M., Seitavuopio, P., Louhi-kultanen, M., Yliruusi, J., 2003. Polymorph screening using near-infrared spectroscopy. *Anal. Chem.* 75, 5267–5273. <https://doi.org/10.1021/ac034205c>
- Amidon, G.L., Lennernäs, H., Shah, V.P., Crison, J.R., 1995. A theoretical basis for a biopharmaceutic drug classification: the correlation of in vitro drug product dissolution and in vivo bioavailability. *Pharm. Res.* 12, 413–420. <https://doi.org/10.1023/A:1016212804288>
- Andronis, V., Yoshioka, M., Zograf, G., 1997. Effects of sorbed water on the crystallization of indomethacin from the amorphous state. *J. Pharm. Sci.* 86, 346–357. <https://doi.org/10.1021/js9602711>
- Atef, E., Chauhan, H., Prasad, D., Kumari, D., Pidgeon, C., 2012. Quantifying solid-state mixtures of crystalline indomethacin by Raman spectroscopy comparison with thermal Analysis. *ISRN Chromatogr.* 2012, 1–6. <https://doi.org/10.5402/2012/892806>
- Bahl, D., Bogner, R.H., 2006. Amorphization of indomethacin by co-grinding with Neusilin US2: amorphization kinetics, physical stability and mechanism. *Pharm. Res.* 23, 2317–2325. <https://doi.org/10.1007/s11095-006-9062-x>
- Baird, J.A., Van Eerdenbrugh, B., Taylor, L.S., 2010. A classification system to assess the crystallization tendency of organic molecules from undercooled melts. *J. Pharm. Sci.* 99, 3787–3806. <https://doi.org/10.1002/jps.22197>
- Balogh, A., Drávavölgyi, G., Faragó, K., Farkas, A., Vigh, T., Sóti, P.L., Wagner, I., Madarász, J., Pataki, H., Marosi, G., Nagy, Z.K., 2014. Plasticized drug-loaded melt electrospun polymer mats: characterization, thermal degradation, and release kinetics. *J. Pharm. Sci.* 103, 1278–1287. <https://doi.org/10.1002/jps.23904>
- BASF, 2010. BASF. Safety data sheet, Soluplus®. BASF, Pharma Ingredients Serv. 1–7.
- Bley, H., Fussnegger, B., Bodmeier, R., 2010. Characterization and stability of solid dispersions based on PEG/polymer blends. *Int. J. Pharm.* 390, 165–173. <https://doi.org/10.1016/j.ijpharm.2010.01.039>
- Brettmann, B., Bell, E., Myerson, A., Trout, B., 2012. Solid-state NMR characterization of high-loading solid solutions of API and excipients formed by electrospinning. *J. Pharm. Sci.* 101, 1538–1545. <https://doi.org/10.1002/jps.23032>
- Brough, C., Williams, R.O., 2013. Amorphous solid dispersions and nano-crystal technologies for poorly water-soluble drug delivery. *Int. J. Pharm.* 453, 157–66. <https://doi.org/10.1016/j.ijpharm.2013.05.061>
- Brown, C., DiNunzio, J., Eglesia, M., Forster, S., Lamm, M., Lowinger, M., Marsac, P., McKelvey, C., Meyer, R., Schenck, L., Terife, G., Troup, G., Smith-Goettler, B., Starbuck, C., 2014. HME for solid dispersions: scale-up and late-stage development, in: Shah, N., Sandhu, H., Choi, D.S., Chokshi, H., Malick, A.W. (Eds.), *Amorphous solid dispersions: theory and practice*. Springer New York, New York, NY, pp. 231–260. https://doi.org/10.1007/978-1-4939-1598-9_7
- Brown, T.D., Dalton, P.D., Hutmacher, D.W., 2016. Melt electrospinning today: an opportune time for an emerging polymer process. *Prog. Polym. Sci.* 56, 116–166. <https://doi.org/10.1016/j.progpolymsci.2016.01.001>
- Brown, T.D., Dalton, P.D., Hutmacher, D.W., 2011. Direct writing by way of melt electrospinning. *Adv. Mater.* 23, 5651–5657. <https://doi.org/10.1002/adma.201103482>

- Brown, T.D., Edin, F., Detta, N., Skelton, A.D., Hutmacher, D.W., Dalton, P.D., 2014. Melt electrospinning of poly (ϵ -caprolactone) scaffolds: phenomenological observations associated with collection and direct writing. *Mater. Sci. Eng. C* 45, 698–708. <https://doi.org/10.1016/j.msec.2014.07.034>
- Burger, A., Ramberger, R., 1979a. On the polymorphism of pharmaceuticals and other molecular crystals. I. *Mikrochim. Acta* 2, 259–271. <https://doi.org/10.1007/BF01197379>
- Burger, A., Ramberger, R., 1979b. On the polymorphism of pharmaceuticals and other molecular crystals. II. *Mikrochim. Acta* 2, 273–316. <https://doi.org/10.1007/BF01197380>
- CDER/FDA, 2015. Guidance for Industry, Waiver of in vivo bioavailability and bioequivalence studies for immediate release solid oral dosage forms based on a biopharmaceutics classification system. *Cent. Drug Eval. Res.* 1–2.
- Chokshi, R.J., Zia, H., Sandhu, H.K., Shah, N.H., Malick, W.A., 2007. Improving the dissolution rate of poorly water soluble drug by solid dispersion and solid solution—pros and cons. *drug deliv.* 14, 33–45. <https://doi.org/10.1080/10717540600640278>
- Craig, D.Q., 2002. The mechanisms of drug release from solid dispersions in water-soluble polymers. *Int. J. Pharm.* 231, 131–144. [https://doi.org/10.1016/S0378-5173\(01\)00891-2](https://doi.org/10.1016/S0378-5173(01)00891-2)
- Crowley, K.J., Zograf, G., 2002. Water vapor absorption into amorphous hydrophobic drug / poly (vinylpyrrolidone) dispersions. *J Pharm Sci.* 91, 2150–2165.
- Dabbagh, M.A., Taghipour, B., 2007. Investigation of solid dispersion technique in improvement of physicochemical characteristics of ibuprofen powder. *Iran J Pharm Sci.* 3, 69–76
- Dalton, P.D., Lleixà Calvet, J., Mourran, A., Klee, D., Möller, M., 2006. Melt electrospinning of poly-(ethylene glycol-block- ϵ -caprolactone). *Biotechnol. J.* 1, 998–1006. <https://doi.org/10.1002/biot.200600064>
- Davis, M.E., Brewster, M.E., 2004. Cyclodextrin-based pharmaceuticals: past, present and future. *Nat. Rev. Drug Discov.* 3, 1023–1035. <https://doi.org/10.1038/nrd1576>
- de Oliveira Makson, G., Guimarães, A.G., Araújo Adriano, A., Quintans Jullyana, S., Santos, M.R., Quintans-Júnior, L.J., 2015. Cyclodextrins: improving the therapeutic response of analgesic drugs: a patent review. *Expert Opin. Ther. Pat.* 25, 897–907. <https://doi.org/10.1517/13543776.2015.1045412>
- Demertzis, P.G., Riganakos, K.A., Kontominas, M.G., 1989. Water sorption isotherms of crystalline raffinose by inverse gas chromatography. *Int. J. Food Sci. Technol.* 24, 629–636. <https://doi.org/10.1111/j.1365-2621.1989.tb00689.x>
- Detta, N., Brown, T.D., Edin, F.K., Albrecht, K., Chiellini, F., Chiellini, E., Dalton, P.D., Hutmacher, D.W., 2010. Melt electrospinning of polycaprolactone and its blends with poly(ethylene glycol). *Polym. Int.* 59, 1558–1562. <https://doi.org/10.1002/pi.2954>
- Di, L., Kerns, E.H., Carter, G.T., 2009. Drug-like property concepts in pharmaceutical design. *Curr. Pharm. Des.* 15, 2184–2194. <https://doi.org/10.2174/138161209788682479>
- Djuris, J., Nikolakakis, I., Ibric, S., Djuric, Z., Kachrimanis, K., 2013. Preparation of carbamazepine–Soluplus® solid dispersions by hot-melt extrusion, and prediction of drug–polymer miscibility by thermodynamic model fitting. *Eur. J. Pharm. Biopharm.* 84, 228–237. <https://doi.org/10.1016/j.ejpb.2012.12.018>

- Doreth, M., Hussein, M.A., Priemel, P.A., Grohgan, H., Holm, R., Lopez de Diego, H., Rades, T., Löbmann, K., 2017. Amorphization within the tablet: using microwave irradiation to form a glass solution in situ. *Int. J. Pharm.* 519, 343–351. <https://doi.org/10.1016/j.ijpharm.2017.01.035>
- Duong, T. Van, Van Humbeeck, J., Van den Mooter, G., 2015. Crystallization kinetics of indomethacin/polyethylene glycol dispersions containing high drug loadings. *Mol. Pharm.* 12, 2493–2504. <https://doi.org/10.1021/acs.molpharmaceut.5b00299>
- Edwards, A.D., Shekunov, B.Y., Forbes, R.T., Grossmann, J.G., York, P., 2001. Time-resolved X-ray scattering using synchrotron radiation applied to the study of a polymorphic transition in carbamazepine. *J. Pharm. Sci.* 90, 1106–1114.
- Eerdenbrugh, B. Van, Speybroeck, M. Van, Mols, R., Houthoofd, K., Martens, J.A., Froyen, L., Humbeeck, J. Van, Augustijns, P., den Mooter, G. Van, 2009. Itraconazole/TPGS/Aerosil®200 solid dispersions: characterization, physical stability and in vivo performance. *Eur. J. Pharm. Sci.* 38, 270–278. <https://doi.org/https://doi.org/10.1016/j.ejps.2009.08.002>
- European Medicines Agency, 2000. ICH Topic Q6 A. ICH Guidel. 1–32. [https://doi.org/10.1016/S0140-6736\(10\)60785-4](https://doi.org/10.1016/S0140-6736(10)60785-4)
- European Pharmacopoeia Comisson, 2017. European Pharmacopoeia 9.0. European Directorate for the Quality of Medicines, Strasbourg.
- Ewing, A.V., Clarke, G.S., Kazarian, S.G., 2014. Stability of indomethacin with relevance to the release from amorphous solid dispersions studied with ATR-FTIR spectroscopic imaging. *Eur. J. Pharm. Sci.* 60, 64–71. <https://doi.org/10.1016/j.ejps.2014.05.001>
- FDA, 2007. Guidance for industry ANDAs: pharmaceutical solid polymorphism. Cent. Drug Eval. Res. 13.
- Fini, A., Cavallari, C., Ospitali, F., 2008. Raman and thermal analysis of indomethacin/PVP solid dispersion enteric microparticles. *Eur. J. Pharm. Biopharm.* 70, 409–420. <https://doi.org/10.1016/j.ejpb.2008.03.016>
- Forster, A., Hempenstall, J., Tucker, I., Rades, T., 2001. Selection of excipients for melt extrusion with two poorly water-soluble drugs by solubility parameter calculation and thermal analysis. *Int. J. Pharm.* 226, 147–161. [https://doi.org/https://doi.org/10.1016/S0378-5173\(01\)00801-8](https://doi.org/https://doi.org/10.1016/S0378-5173(01)00801-8)
- Fraser-Miller, S.J., Saarinen, J., Strachan, C.J., 2016. Vibrational spectroscopic imaging. *Analytical techniques in the pharmaceutical sciences*. Springer New York, New York, NY, 523–589. https://doi.org/10.1007/978-1-4939-4029-5_17
- Genina, N., Räikkönen, H., Heinämäki, J., Antikainen, O., Siirä, S., Veski, P., Yliruusi, J., 2009. Effective modification of particle surface properties using ultrasonic water mist. *AAPS PharmSciTech* 10, 282–288. <https://doi.org/10.1208/s12249-009-9208-3>
- Good, D.J., Rodriguez-Hornedo, N., 2009. Solubility advantage of pharmaceutical crystals. *Cystalal Growth Des.* 9, 2252–2264. <https://pubs.acs.org/doi/abs/10.1021/cg801039j>
- Gu, C.H., Li, H., Levons, J., Lentz, K., Gandhi, R.B., Raghavan, K., Smith, R.L., 2007. Predicting effect of food on extent of drug absorption based on physicochemical properties. *Pharm. Res.* 24, 1118–1130. <https://doi.org/10.1007/s11095-007-9236-1>
- Gursoy, R.N., Benita, S., 2004. Self-emulsifying drug delivery systems (SEDDS) for improved oral delivery of lipophilic drugs. *Biomed. Pharmacother.* 58, 173–182. <https://doi.org/10.1016/j.biopha.2004.02.001>
- Haleblian, J., McCrone, W., 1969. Pharmaceutical applications of polymorphism. *J. Pharm. Sci.* 58, 911–929. <https://doi.org/10.1002/jps.2600580802>

- Hancock, B.C., Parks, M., 2000. What is the true solubility advantage for amorphous pharmaceuticals? *Pharm. Res.* 17, 397–404.
<https://doi.org/10.1023/A:1007516718048>
- Hancock, B.C., Zografi, G., 1997. Characteristics and significance of the amorphous state in pharmaceutical systems. *J. Pharm. Sci.* 86, 1–12.
<https://doi.org/10.1021/js9601896>
- Hasegawa, S., Hamaura, T., Furuyama, N., Kusai, A., Yonemochi, E., Terada, K., 2005. Effects of water content in physical mixture and heating temperature on crystallinity of troglitazone-PVP K30 solid dispersions prepared by closed melting method. *Int. J. Pharm.* 302, 103–112. <https://doi.org/10.1016/j.ijpharm.2005.06.021>
- Henkel, J., Hutmacher, D.W., 2013. Design and fabrication of scaffold-based tissue engineering. *BioNanoMaterials* 14, 171–193.
<https://doi.org/10.1515/bnm-2013-0021>
- Hörter, D., Dressman, J.B., 1997. Influence of physicochemical properties on dissolution of drugs in the gastrointestinal tract. *Adv. Drug Deliv. Rev.* 25, 3–14.
[https://doi.org/10.1016/S0169-409X\(96\)00487-5](https://doi.org/10.1016/S0169-409X(96)00487-5)
- Hughey, J.R., Keen, J.M., Miller, D.A., Kolter, K., Langley, N., McGinity, J.W., 2013. The use of inorganic salts to improve the dissolution characteristics of tablets containing Soluplus®-based solid dispersions. *Eur. J. Pharm. Sci.* 48, 758–766.
<https://doi.org/10.1016/j.ejps.2013.01.004>
- Hutmacher, D.W., Dalton, P.D., 2011. Melt electrospinning. *Chem. Asian J.* 6, 44–56.
<https://doi.org/10.1002/asia.201000436>
- Janssens, S., De Zeure, A., Paudel, A., Van Humbeeck, J., Rombaut, P., Van Den Mooter, G., 2010. Influence of preparation methods on solid state supersaturation of amorphous solid dispersions: a case study with itraconazole and eudragit E100. *Pharm. Res.* 27, 775–785. <https://doi.org/10.1007/s11095-010-0069-y>
- Janssens, S., Van den Mooter, G., 2009. Review: physical chemistry of solid dispersions. *J. Pharm. Pharmacol.* 61, 1571–1586.
<https://doi.org/10.1211/jpp.61.12.0001>
- Jermain, S.V., Brough, C., Williams, R.O., 2018. Amorphous solid dispersions and nanocrystal technologies for poorly water-soluble drug delivery – An update. *Int. J. Pharm.* 535, 379–392. <https://doi.org/10.1016/j.ijpharm.2017.10.051>
- Kogermann, K., Penkina, a, Predbannikova, K., Jeeger, K., Veski, P., Rantanen, J., Naelapää, K., 2013. Dissolution testing of amorphous solid dispersions. *Int. J. Pharm.* 444, 40–6. <https://doi.org/10.1016/j.ijpharm.2013.01.042>
- Kolter, E., Karl, M., Gryczke, A., 2012. Hot-Melt Extrusion with BASF Pharma Polymers.
- Korhonen, O., Pajula, K., Laitinen, R., 2017. Rational excipient selection for co-amorphous formulations. *Expert Opin. Drug Deliv.* 14, 551–569.
<https://doi.org/10.1080/17425247.2016.1198770>
- Lan, Y., Ali, S., Langley, N., 2010. Characterization of Soluplus® by FTIR and Raman spectroscopy results and discussion. *CRS 2010 Annu. Conf.* 5–8.
<https://doi.org/DOI:10.13140/2.1.3771.6805>
- Li, M., Gogos, C.G., Ioannidis, N., 2015. Improving the API dissolution rate during pharmaceutical hot-melt extrusion I: effect of the API particle size, and the co-rotating, twin-screw extruder screw configuration on the API dissolution rate. *Int. J. Pharm.* 478, 103–112. <https://doi.org/10.1016/j.ijpharm.2014.11.024>

- Lian, H., Meng, Z., 2017. Melt electrospinning of daunorubicin hydrochloride-loaded poly (ϵ -caprolactone) fibrous membrane for tumor therapy. *Bioact. Mater.* 2, 96–100. <https://doi.org/10.1016/j.bioactmat.2017.03.003>
- Lin, S.Y., Lin, H.L., Chi, Y.T., Huang, Y.T., Kao, C.Y., Hsieh, W.-H., 2015. Thermo-analytical and Fourier transform infrared spectral curve-fitting techniques used to investigate the amorphous indomethacin formation and its physical stability in Indomethacin-Soluplus® solid dispersions. *Int. J. Pharm.* 496, 457–465. <https://doi.org/10.1016/j.ijpharm.2015.10.042>
- Linn, M., Collnot, E., Djuric, D., Hempel, K., Fabian, E., Kolter, K., Lehr, C., 2012. Soluplus® as an effective absorption enhancer of poorly soluble drugs in vitro and in vivo. *Eur. J. Pharm. Sci.* 45, 336–343. <https://doi.org/10.1016/j.ejps.2011.11.025>
- Lipinski, C.A., 2000. Drug-like properties and the causes of poor solubility and poor permeability. *J. Pharmacol. Toxicol. Methods* 44, 235–249. [https://doi.org/10.1016/S1056-8719\(00\)00107-6](https://doi.org/10.1016/S1056-8719(00)00107-6)
- Löbmann, K., Grohgan, H., Laitinen, R., Strachan, C., Rades, T., 2013. Amino acids as co-amorphous stabilizers for poorly water soluble drugs-Part 1: preparation, stability and dissolution enhancement. *Eur. J. Pharm. Biopharm.* 85, 873–81. <https://doi.org/10.1016/j.ejpb.2013.03.014>
- Lukyanov, A.N., Torchilin, V.P., 2004. Micelles from lipid derivatives of water-soluble polymers as delivery systems for poorly soluble drugs. *Adv. Drug Deliv. Rev.* 56, 1273–1289. <https://doi.org/10.1016/j.addr.2003.12.004>
- Lyons, J., Li, C., Ko, F., 2004. Melt-electrospinning part I: processing parameters and geometric properties. *Polymer*. 45, 7597–7603. <https://doi.org/10.1016/j.polymer.2004.08.071>
- Madgulkar, A., Bandivadekar, M., Shid, T., Rao, S., Madgulkar, A., Bandivadekar, M., Shid, T., Rao, S., 2015. Sugars as solid dispersion carrier to improve solubility and dissolution of the BCS class II drug: clotrimazole. *Drug Dev. Ind. Pharm.* 1–11. <https://doi.org/10.3109/03639045.2015.1024683>
- Marsac, P.J., Konno, H., Rumondor, A.C.F., Taylor, L.S., 2008a. Recrystallization of nifedipine and felodipine from amorphous molecular level solid dispersions containing poly(vinylpyrrolidone) and sorbed water. *Pharm. Res.* 25, 647–656. <https://doi.org/10.1007/s11095-007-9420-3>
- Marsac, P.J., Li, T., Taylor, L.S., 2008b. Estimation of drug–polymer miscibility and solubility in amorphous solid dispersions using experimentally determined interaction parameters. *Pharm. Res.* 26, 139–151. <https://doi.org/10.1007/s11095-008-9721-1>
- Marsac, P.J., Shamblin, S.L., Taylor, L.S., 2006. Theoretical and practical approaches for prediction of drug-polymer miscibility and solubility. *Pharm. Res.* 23, 2417–26. <https://doi.org/10.1007/s11095-006-9063-9>
- Masuda, K., Tabata, S., Kono, H., Sakata, Y., Hayase, T., Yonemochi, E., Terada, K., 2006. Solid-state ^{13}C NMR study of indomethacin polymorphism. *Int. J. Pharm.* 318, 146–153. <https://doi.org/10.1016/j.ijpharm.2006.03.029>
- Merisko-Liversidge, E., Liversidge, G.G., 2011. Nanosizing for oral and parenteral drug delivery: A perspective on formulating poorly-water soluble compounds using wet media milling technology. *Adv. Drug Deliv. Rev.* 63, 427–440. <https://doi.org/10.1016/j.addr.2010.12.007>
- Miladinov, V.D., Hanna, M.A., 1999. Physical and molecular properties of starch acetates extruded with water and ethanol. *Ind. Eng. Chem. Res.* 38, 3892–3897. <https://doi.org/10.1021/ie990255p>

- Mirza, S., Heinämäki, J., Miroshnyk, I., Rantanen, J., Christiansen, L., Karjalainen, M., Yliruusi, J., 2006. Understanding processing-induced phase transformations in erythromycin-PEG 6000 solid dispersions. *J. Pharm. Sci.* 95, 1723–32. <https://doi.org/10.1002/jps.20640>
- Mitchell, G.R., 2015. *Electrospinning: principles, practice and possibilities*. Royal Society of Chemistry 2015.
- Mosharraf, M., Nyström, C., 1995. The effect of particle size and shape on the surface specific dissolution rate of micro-sized practically insoluble drugs. *Int. J. Pharm.* 122, 35–47. [https://doi.org/10.1016/0378-5173\(95\)00033-F](https://doi.org/10.1016/0378-5173(95)00033-F)
- Mummaneni, V., Vasavada, R.C., 1990. Solubilization and dissolution of famotidine from solid glass dispersions of xylitol. *Int. J. Pharm.* 66, 71–77. [https://doi.org/10.1016/0378-5173\(90\)90386-I](https://doi.org/10.1016/0378-5173(90)90386-I)
- Murphy, D., Rodríguez-Cintrón, F., Langevin, B., Kelly, R.C., Rodríguez-Hornedo, N., 2002. Solution-mediated phase transformation of anhydrous to dihydrate carbamazepine and the effect of lattice disorder. *Int. J. Pharm.* 246, 121–134. [https://doi.org/10.1016/S0378-5173\(02\)00358-7](https://doi.org/10.1016/S0378-5173(02)00358-7)
- Nagy, Z.K., Balogh, A., Drávavölgyi, G., Ferguson, J., Pataki, H., Vajna, B., Marosi, G., 2013. Solvent-free melt electrospinning for preparation of fast dissolving drug delivery system and comparison with solvent-based electrospun and melt extruded systems. *J. Pharm. Sci.* 102, 508–517. <https://doi.org/10.1002/jps.23374>
- Newman, A., Knipp, G., Zografi, G., 2012. Assessing the performance of amorphous solid dispersions. *J. Pharm. Sci.* 101, 1355–1377. <https://doi.org/10.1002/jps.23031>
- Noyes, A.A., Whitney, W.R., 1897. The rate of solution of solid substances in their own solutions. *J. Am. Chem. Soc.* 19, 930–934. <https://doi.org/10.1021/ja02086a003>
- Plakkot, S., De Matas, M., York, P., Saunders, M., Sulaiman, B., 2011. Comminution of ibuprofen to produce nano-particles for rapid dissolution. *Int. J. Pharm.* 415, 307–314. <https://doi.org/10.1016/j.ijpharm.2011.06.002>
- Podczek, F., 1998. Adhesion forces in interactive powder mixtures of a micronized drug and carrier particles of various particle size distributions. *J. Adhes. Sci. Technol.* 12, 1323–1339. <https://doi.org/10.1163/156856198X00461>
- Priemel, P. a., Laitinen, R., Barthold, S., Grohgan, H., Lehto, V.P., Rades, T., Strachan, C.J., 2013a. Inhibition of surface crystallisation of amorphous indomethacin particles in physical drug-polymer mixtures. *Int. J. Pharm.* 456, 301–306. <https://doi.org/10.1016/j.ijpharm.2013.08.046>
- Priemel, P. a., Laitinen, R., Grohgan, H., Rades, T., Strachan, C.J., 2013b. In situ amorphisation of indomethacin with Eudragit® e during dissolution. *Eur. J. Pharm. Biopharm.* 85, 1259–1265. <https://doi.org/10.1016/j.ejpb.2013.09.010>
- Pudipeddi, M., Serajuddin, A.T.M., 2005. Trends in solubility of polymorphs. *J. Pharm. Sci.* 94, 929–939. <https://doi.org/10.1002/jps.20302>
- Punčochová, K., Heng, J.Y.Y., Beránek, J., Štěpánek, F., 2014. Investigation of drug-polymer interaction in solid dispersions by vapour sorption methods. *Int. J. Pharm.* 469, 159–167. <https://doi.org/10.1016/j.ijpharm.2014.04.048>
- Qian, F., Huang, J., Zhu, Q., Haddadin, R., Gawel, J., Garmise, R., Hussain, M., 2010. Is a distinctive single T_g a reliable indicator for the homogeneity of amorphous solid dispersion? *Int. J. Pharm.* 395, 232–235. <https://doi.org/10.1016/j.ijpharm.2010.05.033>
- Qiu, Y., Chen, Y., Zhang, G.G., Yu, L., Mantri, R. V., 2017. *Developing Solid Oral Dosage Forms*.
- Reginald-Opara, J.N., Attama, A., Ofokansi, K., Umeyor, C., Kenekwuwu, F., 2015.

- Molecular interaction between glimepiride and Soluplus®-PEG 4000 hybrid based solid dispersions: Characterisation and anti-diabetic studies. *Int. J. Pharm.* 496, 741–750. <https://doi.org/10.1016/j.ijpharm.2015.11.007>
- Reneker, D.H., Yarin, A.L., 2008. Electrospinning jets and polymer nanofibers. *Polymer*. 49, 2387–2425. <https://doi.org/10.1016/j.polymer.2008.02.002>
- Rowe, R., Sheskey, P., Quinn, M., 2009. Handbook of Pharmaceutical Excipients. Sixth Ed. 786–789. [https://doi.org/10.1016/S0168-3659\(01\)00243-7](https://doi.org/10.1016/S0168-3659(01)00243-7)
- Rumondor, A.C.F., Marsac, P.J., Stanford, L.A., Taylor, L.S., 2009. Phase behavior of poly (vinylpyrrolidone) containing amorphous solid dispersions in the presence of moisture. *Mol. Pharm.* 86, 47–60. <https://doi.org/10.1021/mp900050c>
- Salli, K.M., Forssten, S.D., Lahtinen, S.J., Ouwehand, A.C., 2016. Influence of sucrose and xylitol on an early *Streptococcus mutans* biofilm in a dental simulator. *Arch. Oral Biol.* 70, 39–46. <https://doi.org/https://doi.org/10.1016/j.archoralbio.2016.05.020>
- Sarode, A.L., Sandhu, H., Shah, N., Malick, W., Zia, H., 2013. Hot melt extrusion (HME) for amorphous solid dispersions: predictive tools for processing and impact of drug-polymer interactions on supersaturation. *Eur. J. Pharm. Sci.* 48, 371–384. <https://doi.org/10.1016/j.ejps.2012.12.012>
- Savolainen, M., Heinz, A., Strachan, C., Gordon, K.C., Yliruusi, J., Rades, T., Sandler, N., 2007. Screening for differences in the amorphous state of indomethacin using multivariate visualization. *Eur. J. Pharm. Sci.* 30, 113–23. <https://doi.org/10.1016/j.ejps.2006.10.010>
- Seppälä, K., Heinämäki, J., Hataara, J., Seppälä, L., Yliruusi, J., 2010. Development of a new method to get a reliable powder flow characteristics using only 1 to 2 g of powder. *AAPS PharmSciTech* 11, 402–408. <https://doi.org/10.1208/s12249-010-9397-9>
- Serajuddin, A.T.M., Pudipeddi, M., 2008. Salt-selection strategies. In handbook of pharmaceutical salt properties, selection, and use. Weinheim. Wiley-VCH. 135–160
- Spiegel, K., Schmidt-Rohr, K., Boeffel, C., Spiess, W.H., 1994. ¹H spin diffusion coefficients of highly mobile polymers. *Polymer*. 21. 4566–4569. [https://doi.org/10.1016/0032-3861\(93\)90166-8](https://doi.org/10.1016/0032-3861(93)90166-8)
- Shalaev, E., Zografi, G., 2002. The concept of “structure” in amorphous solids from the perspective of the pharmaceutical sciences. *Amorph. Food Pharm. Syst.* 11–30. <https://doi.org/10.1039/9781847550118-00011>
- Shamma, R.N., Basha, M., 2013. Soluplus®: a novel polymeric solubilizer for optimization of carvedilol solid dispersions: formulation design and effect of method of preparation. *Powder Technol.* 237, 406–414. <https://doi.org/10.1016/j.powtec.2012.12.038>
- Shogren, R.L., 1996. Preparation, thermal properties, and extrusion of high-amylose starch acetates. *Carbohydr. Polym.* 29, 57–62. [https://doi.org/10.1016/0144-8617\(95\)00143-3](https://doi.org/10.1016/0144-8617(95)00143-3)
- Singh, G., Chhabra, G., Pathak, K., 2011. Dissolution behavior and thermodynamic stability of fused-sugar dispersions of a poorly water-soluble drug. *Dissolution Technol.* 18, 62–70. <https://doi.org/dx.doi.org/10.14227/DT180311P62>
- Singhal, D., Curatolo, W., 2004. Drug polymorphism and dosage form design: a practical perspective. *Adv. Drug Deliv. Rev.* 56, 335–347. <https://doi.org/10.1016/j.addr.2003.10.008>

- Sjökvist, E., Nyström, C., 1991. Physicochemical aspects of drug release. XI. Tableting properties of solid dispersions, using xylitol as carrier material. *Int. J. Pharm.* [https://doi.org/10.1016/0378-5173\(91\)90426-O](https://doi.org/10.1016/0378-5173(91)90426-O)
- Sjökvist, M., Gatenholm, P., 2005. The effect of starch composition on structure of foams prepared by microwave treatment. *J. Polym. Environ.* 13, 29–37. <https://doi.org/10.1007/s10924-004-1213-8>
- Stella, V.J., He, Q., 2008. Cyclodextrins. *Toxicol. Pathol.* 36, 30–42. <https://doi.org/10.1177/0192623307310945>
- Strachan, C.J., Rades, T., Gordon, K.C., 2007. A theoretical and spectroscopic study of γ -crystalline and amorphous indometacin. *J. Pharm. Pharmacol.* 59, 261–269. <https://doi.org/10.1211/jpp.59.2.0012>
- Surwase, S.A., Boetker, J.P., Saville, D., Boyd, B.J., Gordon, K.C., Peltonen, L., Strachan, C.J., 2013. Indomethacin: new polymorphs of an old drug. *Mol. Pharm.* 10, 4472–80. <https://doi.org/10.1021/mp400299a>
- Surwase, S.A., Itkonen, L., Aaltonen, J., Saville, D., Rades, T., Peltonen, L., Strachan, C.J., 2015. Polymer incorporation method affects the physical stability of amorphous indomethacin in aqueous suspension. *Eur. J. Pharm. Biopharm.* 96, 32–43. <https://doi.org/10.1016/j.ejpb.2015.06.005>
- Suzuki, H., Sunada, H., 1997. Comparison of nicotinamide, ethylurea, and polyethylene glycole as carriers for nifedipine solid dispersion systems. *Chem. Pharm. Bull.* 45, 1688–1693. <https://doi.org/10.1248/cpb.45.1688>
- Takagi, T., Ramachandran, C., Bermejo, M., Yamashita, S., Yu, L.X., Amidon, G.L., 2006. A provisional biopharmaceutical classification of the top 200 oral drug products in the United States, Great Britain, Spain, and Japan. *Mol Pharm.* 3, 631–643. <https://doi.org/10.1021/mp0600182>
- Tawashi, R., 1968. Aspirin: dissolution rates of two polymorphic forms. *Science.* 160, 76.
- Terife, G., Wang, P., Faridi, N., Gogos, C.G., 2012. Hot melt mixing and foaming of Soluplus[®] and indomethacin. *Polym. Eng. Sci.* 52, 1629–1639. <https://doi.org/10.1002/pen.23106>
- Thibadeau, L., Taubenberger, A. V., Holzapfel, B.M., Quent, V.M., Fuehrmann, T., Hesami, P., Brown, T.D., Dalton, P.D., Power, C.A., Hollier, B.G., Huttmacher, D.W., 2014. A tissue-engineered humanized xenograft model of human breast cancer metastasis to bone. *Dis. Model. Mech.* 7, 299–309. <https://doi.org/10.1242/dmm.014076>
- Thommes, M., 2012. Featured Article. *APV Drug Deliv. Focus Gr. Newsl.* – 1/2012 23, 3–4. <https://doi.org/10.1097/00132582-200301000-00002>
- Thommes, M., Ely, D.R., Carvajal, M.T., Pinal, R., 2011. Improvement of the dissolution rate of poorly soluble drugs by solid crystal suspensions. *Mol. Pharm.* 8, 727–735. <https://doi.org/10.1021/mp1003493>
- Tita, B., Fülías, A., Rusu, G., Tita, D., 2009. Thermal behaviour of indomethacin-active substance and tablets kinetic study under non-isothermal conditions. *Rev. Chim.* 60, 1210–1215.
- Van Den Mooter, G., 2012. The use of amorphous solid dispersions: a formulation strategy to overcome poor solubility and dissolution rate. *Drug Discov. Today Technol.* 9, 79–85. <https://doi.org/10.1016/j.ddtec.2011.10.002>
- Vasconcelos, T., Sarmiento, B., Costa, P., 2007. Solid dispersions as strategy to improve oral bioavailability of poor water soluble drugs. *Drug Discov. Today* 12, 1068–75. <https://doi.org/10.1016/j.drudis.2007.09.005>

- Vippagunta, S.R., Brittain, H.G., Grant, D.J.W., 2001. Crystalline solids. *Adv. Drug Deliv. Rev.* 48, 3–26. [https://doi.org/https://doi.org/10.1016/S0169-409X\(01\)00097-7](https://doi.org/https://doi.org/10.1016/S0169-409X(01)00097-7)
- Weisser, H., Weber, J., Loncin, M., 1982. Water vapour sorption isotherms of sugar substitutes in the temperature range 25 to 80 °C. *Int. Zeitschrift für Leb. und Verfahrenstechnik* 33, 89–97.
- Williams, H.D., Trevaskis, N.L., Charman, S. a, Shanker, R.M., Charman, W.N., Pouton, C.W., Porter, C.J.H., 2013. Strategies to address low drug solubility in discovery and development. *Pharmacol. Rev.* 65, 315–499. <https://doi.org/10.1124/pr.112.005660>
- Williams, R.O., Watts, A.B., Miller, D.A., 2016. Formulating poorly water soluble drugs. <https://doi.org/10.1007/978-3-319-42609-9>
- Yadav, V.B., Yadav, A. V., 2009. Enhancement of solubility and dissolution rate of indomethacin with different polymers by compaction process. *Int. J. ChemTech Res.* 1, 1072–1078.
- Yamashita, K., Nakate, T., Okimoto, K., Ohike, A., Tokunaga, Y., Ibuki, R., Higaki, K., Kimura, T., 2003. Establishment of new preparation method for solid dispersion formulation of tacrolimus. *Int. J. Pharm.* 267, 79–91. <https://doi.org/https://doi.org/10.1016/j.ijpharm.2003.07.010>
- Zhang, G.G.Z., Law, D., Schmitt, E.A., Qiu, Y., 2004. Phase transformation considerations during process development and manufacture of solid oral dosage forms. *Adv. Drug Deliv. Rev.* 56, 371–390. <https://doi.org/https://doi.org/10.1016/j.addr.2003.10.009>
- Zhang, K., Yu, H., Luo, Q., Yang, S., Lin, X., Zhang, Y., Tian, B., Tang, X., 2013. Increased dissolution and oral absorption of itraconazole/Soluplus extrudate compared with itraconazole nanosuspension. *Eur. J. Pharm. Biopharm.* 85, 1285–1292. <https://doi.org/10.1016/j.ejpb.2013.03.002>
- Zhu, Y., Shah, N., Waseem Malick, A., Infeld, M., McGinity, J., 2006. Controlled release of a poorly water-soluble drug from hot-melt extrudates containing acrylic polymers. *Drug Dev. Ind. Pharm.* 32, 569–583. <https://doi.org/10.1080/03639040500528996>

SUMMARY IN ESTONIAN

Vees halvasti lahustuva indometatsiini tahkete dispersioonide valmistamine farmatseutilisel eesmärgil sulami kiirjahutamisel ja sulami elektrospinnimisel

SISSEJUHATUS

Farmatseutilise ravimvormi disain ja väljatöötamine vajab laiahaardelisi erialaseid teadmisi ja tausta teavet. Tööprotsess algab haiguse identifitseerimisest, toimeaine leidmisest, järgnevad farmakoloogilised/toksikoloogilised uuringud, preformulatsiooni uuringud ja ravimvormi disain ning valmistamine. Kui prekliinilised uuringud on andnud positiivseid tulemusi, siis järgnevad kliinilised uuringud, kus tõestatakse ravimpreparaadi ohutus ja efektiivsus. Välja on töötatud regulatoorsed juhendid farmaatsiatööstusele, et toetada ravimpreparaatide väljatöötamist ning tagadaravimpreparaatide kvaliteeti, ohutust ja efektiivsust (CDER/FDA, 2015; CDER/FDA, 2007; ICH 2015). Näiteks laiaulatuslikud dissolutsioonitestid ja stabiilsuskatsed on vajalikud eduka toote väljatöötamiseks ja selle järgneva turule laskmiseks.

Suukaudne manustamine on jätkuvalt peamine ravimite kasutamise viis. See on lihtne, kiire, mugav ja valutu võimalus erinevate ravimvormide võtmiseks, tehes sellest kõige atraktiivsema ravimite manustamisviisi patsientidele. Samuti on tahke suukaudsed ravimvormid ühed levinumad ja lihtsamad valmistada ka farmaatsiatööstusele. Vesilahustuvus ja gastrointestinaalne permeaabelsus on teadaolevalt ühed võtmeparameetrid kontrollimaks toimeaine lahustuvuse ja imendumise ulatust organismis. Lähtuvalt Biofarmatseutilisest Klassifikatsiooni Süsteemist (BCS) ja eelpool nimetatud parameetritest, on ravimid jaotatud nelja rühma: hea lahustuvus-hea permeaabelsus (BCS I); halb lahustuvus-hea permeaabelsus (BCS II); hea lahustuvus-halb permeaabelsus (BCS III); ja halb lahustuvus-halb permeaabelsus (BCS IV) (Amidon et al., 1995). Kirjanduse andmetest lähtuvalt, ainult 5% uutest toimeainetest kuuluvad BCS I klassi ning 90% on klassifitseeritud kui halvasti lahustuvad (BCS II ja BCS IV) toimeained (Williams et al., 2016). On näidatud, et 75% toimeainetest väljatöötamise faasis või tootmise faasis klassifitseeritakse kui vees halvasti lahustuvad toimeained (Di et al., 2009). Uudsete ravimvormide, ravimkandursüsteemide ja abiainetega väljatöötamine ja tootmine võimaldab, parandada toimeainete vesilahustuvust, lahustumiskiirust ja seega ka vees halvasti lahustuvate toimeainete biosaadavust organismis.

Antud väitekirja hüpoteesiks on, et erinevate meetoditega valmistatud vees halvasti lahustuva toimeaine indometatsiini (IND) ja Soluplus®-i (SOL) ja/või ksülitooliga (XYL) tahked amorfsed dispersioonid tõstavad IND lahustusmiskiirust ja võimaldavad stabiliseerida tema amorfset vormi. SOL on uudne kopolümeer, mis oli esialgselt väljatöötatud kasutamiseks sulami-ekstrusioonis (BASF, 2010). XYL on suhkur polüool, mis alles hiljuti on leidnud kasutamist ka farmatseutilise abiaienena (Rowe et al., 2012). Koos solvendi aurustumise

meetodiga on sulami-kiirjahutamine üheks traditsiooniliseks tahkete dispersioonide valmistamisemeetodiks. Sulami-elektrospinnimist võib käsitleda traditsioonilise sulatamise/kokku-sulatamise edasiarendusena tahkete dispersioonide valmistamisel. Sulami-elektrospinnimine on üheks uudseks võimaluseks kaas-aegsete ravimkandursüsteemide arendamisel vees halvasti lahustuvate toimeainetele. Käesolevas väitekirjas uuriti erinevate abiainetega (SOL/XYL) kiirjahutatud amorfsete tahkete dispersioonide olulisi füsikokeemilisi omadusi ja toimeaine vabanemist ning tema stabiilsust. Uuriti sulami elektrospinnimise teel valmistatud ainulaadsete omadustega fiibreid, kus võtmeküsimus oli, kas antud omadused parandavad toimeaine lahustumiskiiruse ja antud ravimvormi füsikokeemilist stabiilsust. Töö tulemused näitasid, et sulami-elektrospinnimisel saadud vees halvasti lahustuva toimeainega (indometatsiin) fiibrid on füsikokeemiliselt stabiilsed ja tagavad toimeaine kiire vabanemise ja lahustumise.

EESMÄRGID

Antud väitekirja eesmärgiks oli aru saada kahe termilise tahke dispersiooni valmistamise meetodi ja kahe erineva abiaine mõjust vees halvasti lahustuva toimeaine indometatsiini (IND) füsikokeemilistele omadustele. Erilist tähelepanu pöörati just amorfsetes tahketes dispersioonides oleva toimeaine füüsikalise stabiilsuse ja toimeaine vabanemise- ja lahustumiskiiruse uuringutele.

Töö täpsemad eesmärgid:

- Uurida tahke aine vormi ja selle füüsikalist stabiilsust sulami-kiirjahutamisel valmistatud tahketes dispersioonides kahe maatriksit tekitava abiainega (SOL/XYL) (I).
- Uurida sulami-kiirjahutamisel valmistatud kahefaasiliste tahkete dispersioonide osakese ja pulbri taseme omadusi, märgumist ja toimeaine vabanemist ja lahustumiskiirust (II).
- Võrrelda polümeerse ja kristallilise abiaine mõju tahkete dispersioonide omadustele (nii molekulaarse taseme kui osakese ja pulbritaseme omadustele) ja selle mõjust toimeaine vabanemisele ja lahustumisele tahketest dispersioonidest (II).
- Valmistada sulami-elektrospinnimisel amorfne tahke dispersioon fiibris parandamaks vees halvasti lahustuva toimeaine lahustumiskiirust (III).
- Aru saada sulami-elektrospinnimisel valmistatud fiibris oleva toimeaine tahke aine vormi füüsikalistest muutustest, toimeaine-polümeerse abiaine vahelisest interaktsioonidest ja toimeaine lahustumiskiirusest (III).

MATERJALID JA MEETODID

- Füüsikaliste segude ja tahkete dispersioonide valmistamine
Füüsikalised segud valmistati erinevates toimeaine-abiaine vahekordades (3:1, 1:1, 1:3, 1:6, 1:9), mida kasutati tahkete dispersioonide võrdlusena.

Mudel toimeainena kasutati indometatsiini (IND). Abiaineteks valiti amorfne polümeer SOL ja kristalliline XYL. Modifitseeritud sulami kiirjahutamine toimus toimeaine ja polümeeride sulatamisel ja järgneval jahutamisel vedela lämmastikuga. Sulami-elektrospinnimine viidi läbi kõrge niiskuse juures (>90%) säilitatud mudel toimeaine ja SOL-i füüsikalise seguga. Võrdluseks valmistati toimeaine vaba puhta polümeeriga fiiber.

- Morfoloogiline ja topograafiline analüüs

Skaneerivat elektromikroskoopi kasutati morfoloogiliseks ja topograafiliseks analüüsiks. Uuriti puhtaid aineid, füüsikalisi segusid ja tahkeid dispersioone valmistatud sulami-kiirjahutamisel.

- Kristallograafia

Pulber-röntgendifraktomeetriat kasutati tahke faasi määramiseks. Uuriti mudeltoimeainet, abiaineid (SOL, XYL), füüsikalisi segusid ja tahkeid dispersioone. Eesmärgiks oli kindlaks määrata toimeaine amorfne vorm tahketes dispersioonides võrreldes difraktogramme vastavate füüsikaliste segudega.

- Pulbri voolavus, niiskuse sisaldus, märgumine

Pulbri voolavuse uurimiseks kasutati Helsingi Ülikoolis valmistatud uudet seadet, vee sisalduse määramiseks kasutati Karl-Fischeri titrimetriat. Analüüsid teostati IND, SOL ja XYL, füüsikaliste segudega ja tahkete dispersioonidega. Pulbrite veeauru imamisvõimet/sorptsiooni uuriti mõõtes pulbri kõrge niiskuse tingimuste juures (>90%) säilitamisel tema massi muutust ajas Pulbrite hüdrofoobsust ja hüdrofiilsust määrati veetilga kontaktnurga määramisel tablettide pinnal.

- Spektroskoopiline analüüs

Infrapuna, lähiinfrapuna ja tuumamagnetresonants spektroskoopiat kasutati IND, SOL ja XYL, füüsikaliste segude ja tahkete dispersioonide uurimiseks. Eesmärk oli uurida toimeainete ja abiainete vahelisi interaktsioone (H-sidemete teket) ja toimeaine domeeni suurust polümeeri maatriksis.

- Termiline analüüs

Diferentsiaalset skaneerivat kalorimeetriat ja termogravimeetrilist analüüsi kasutati termiliste sündmuste registreerimiseks, vee sisalduse määramiseks ja termilist stabiilsust IND, SOL ja XYL, füüsikalistel segudel ja tahketel dispersioonidel.

- Dissolutsioonitestid

In vitro test lahustumiskiiruse uurimiseks pH 1.2 ja 6.8 juures viidi läbi IND, füüsikaliste segude ja tahkete dispersioonidega. Vabanenud toimeaine kontsentratsioonid määrati spektrofotomeetriliselt ja kinnitati kõrgefektiivse vedelikkromatograafiaga.

- Stabiilsustestid

Tahkete dispersioonide füüsikaline stabiilsus (kuni kaks kuud) kahe erineva abiainega (SOL/XYL) viidi läbi toatemperatuuril kontrollitud niiskuse juures (0%, 50%, 90%) valguse eest kaitstult.

TULEMUSED JA ARUTELU

- Tahkete dispersioonide stabiilsuseuuringud näitasid, et kahefaasiline amorfse IND-i ja XYL-i süsteemis toimeaine kristalliseerus peale 4 päeva, kusjuures SOL-i sisaldav tahke dispersioon oli stabiilne vähemalt 2 kuud (**I**). SOL sisaldavad süsteimid inhibeerivad toimeaine kristallisatsiooni hoides IND amorfseks. Kristalliline XYL soodustab aga amorfse toimeaine kristallisatsiooni käitades kristallisatsiooni pinnana.
- Pulbriomaduste uurimine näitas, et füüsikalistes segudes on toimeaine kristallid kleepunud abiainete pinnale, agatahketes dispersioonides on nad kokku sulanud. Pulbri voolavus sõltus oluliselt abiainete omadustest. Mõlemad abiained (SOL/XYL), sõltuvalt kogusest parandasid füüsikaliste segude ja tahkete dispersionide voolavust. Füüsikaliste segude ja tahkete dispersioonide voolavus statistiliselt ei erinenud ($p < 0.05$). XYL-i sisaldavad segud näitasid paremat märgumist võrreldes vastavate SOL-i sisaldavate segudega ja kristallilise IND-ga. Abiained vähendasid ka IND-i ja vastavate füüsikaliste segude ning tahkete dispersioonide veetilga kontaktnurka, parandades süsteemi hüdrofiilsust.
- Sulami-kiirjahutamise meetodil said valmistatud kahefaasilised süsteimid, kus SOL-i sisaldavas tahkes dispersioonis oli tegu amorfse IND-ga dispergeeritud amorfses polümeeri-maatriksis ning XYL-i sisaldavas tahkes dispersioonis amorfse IND-ga sadenenud kristallilise suhkru-maatriksis. Mõlemad kahefaasilised süsteimid erinevate abinetega näitasid kiiremat toimeaine vabanemist võrreldes kristallilise IND-ga. Erandiks oli IND-i ja SOL-i füüsikaline segu, millest toimeaine vabanemine oli isegi aeglasem võrreldes puhta IND-ga. Põhjuseks võib olla polümeeri geelistumine, mis takistab toimeaine vabanemist.
- Edukas fiibri valmistamine sulami-elektrospinnimisel oli võimalik tänu vee kui plastifikaatori lisamisele. Selleks hoiti IND-i ja SOL-i füüsikaline segu kõrge niiskuse (90%) juures enne sulami-elektrospinnimist. Tänu vee olemasolule süsteemis õnnestus tööprotsessi temperatuuri langetada ca 40 °C. Võrdluseks oli valmistatud toimeaine vaba puhas polümeeri fiiber, mida samuti hoiti eelnevalt kõrge niiskuse juures (**III**).
- Sulami-elektrospinnimise teel valmistatud fiibrid olid siledad, kurrulise pinnaga, ristlõikes täheldati avausi (kanaleid), mis olid tekkinud tänu vee arustumisele. Fiibri komponendid IND ja SOL näitasid molekulaarsel tasemel efektiivset omavahelist segunevust. HPLC kinnitas minimaalset toimeaine lagunemist elektrospinnimine ajal, kinnitades seega protsessi stabiilsust. Tahke faasi analüüs näitas, et IND on fiibris amorfses vormis. NMR näitas ka 25–100 nm suuruseid IND-i domeene tahkes dispersioonis. Vees halvasti lahustuva toimeaine lahustumiskiirus fiibrist oli märgatavalt suurem võrreldes füüsikaliste segude (kristalliline/amorfne IND + polümeerne abiaine, SOL) ja kristallilise IND-ga. Esimese 30 min jooksul vabanes >90% toimeainest. Antud nähtuse põhjusteks on suurem fiiber-materjali eripind ja materjali poorsus ning toimeaine amorfse vormi olemasolu (**III**).

KOKKUVÕTE

Sulatamise meetodil valmistatud kahefaasilised tahked dispersioonid vees halvasti lahustuva toimeainega (indometatsiin, IND) ja kahe erineva abiainega (amorfne kopolümeer vs. kristalliline suhkur alkohol). Mõlemad abiained parandavad kohesiivse IND-i pulbri voolavust, mis on otseselt seotud abiaine kogusega füüsikalistes segudes või tahketes dispersioonides. Samuti paraneb mõlema abiaine (SOL/XYL) ja IND-i segude märguvus, aga XYL-i sisaldavad segud omavad kõrgemaid sorptsiooninäitajaid võrreldes SOL-ga. Toimeaine vabanemine *in vitro* tingimustes pH 6.8 juures füüsikalisest ja tahketest dispersioonidest sõltus suuresti kasutatavast abiaainest. Toimeaine suurem lahustumiskiirus SOL-i sisaldavatest tahketest dispersioonidest on seotud parema märgumisega ja inhibeeritud IND-i kristallisatsiooniga. Seega on IND tahkes dispersioonis amorfses vormis. XYL on vees kergesti lahustuv polüalkohol, mis parandab IND-i lahustumiskiirust suure tõenäosusega läbi parema märgumise ja hüdrofiilsema keskkonna tekitamise, sest IND ei püsi neis süsteemides amorfseks.

Lisaks sellele, sulami-elektrospinnimine tõestas end uudse võimalusena tahkete amorfsete dispersioonide valmistamisemeetodina vees halvasti lahustuvale toimeainele. Sulami-kiirjahutamisel ja sulami-elektrospinnimisel toimus ainult minimaalne toimeaine (IND-i) termiline lagunemine. Sulami-elektrospinnimise fiibri tahke-faasi analüüs näitab IND-i ja amorfse stabiliseeriva SOL-i molekularsel tasemel homogeenset segu. Sulami-elektrospinnimisel valmistatud IND-i ja SOL-i fiiber näitasid kiiremat lahustumist kui vastavad sulami kiirjahutamise meetodil valmistatud tahked dispersioonid, füüsikalised segud ja kristalliline toimeaine. Kokkuvõtteks, sulami-elektrospinnimist võib käsitleda alternatiivse meetodina traditsioonilisele või modifitseeritud sulami-kiirjahutamisele ja sulami ekstrusioonile, mis võimaldab valmistada amorfseid tahkeid dispersioone ja parandada seega toimeaine lahustumiskiirust ja seega vees halvasti lahustuvate toimeainete biosaadavust. Antud töö vajab edasist uurimist, kinnitamaks kas antud tulemused väljenduvad paremas absorptsioonis ja biosaadavuses *in vivo* uuringutes.

ACKNOWLEDGEMENTS

This work was carried out at Institute of Pharmacy, Faculty of Medicine, University of Tartu, Estonia during the years 2014–2018.

Estonian Research Council grants ETF7980, PUT1088, targeted financing funding (no SF0180042s09), institutional research funding IUT-34-18 of Estonian Ministry of Education and Research and European Regional Development Fund and Estonian government are acknowledged for research and mobility funding.

Professor Jyrki Heinämäki and Associate Professor Karin Kogermann are deeply acknowledged for their guidance, advice and endless support through my studies. You are a very hard working scientist, clear example of those who do their things with a passion in the heart. I appreciate sharing with me your expertise and cheering me up. It was my honour to work under your supervisor!

Professor Kalle Kirsimäe, Jaan Aruväli, Marian Külaviir and other great colleagues from Institute of Ecology and Earth Science at University of Tartu are thanked for helping getting me results and sharing their expertise.

I would like to acknowledge all co-authors from University of Tartu, University of Helsinki for their contribution in present research work.

My co-workers at University of Tartu and University of Helsinki are thanked for their thoughts and ideas shared with me, creation of warm working environment.

I am grateful to my family and friends for their emotional support throughout all those years.

PUBLICATIONS

CURRICULUM VITAE

Name Kristian Semjonov
Date of birth 7. august 1990
Aadress Institute of Pharmacy, Faculty of Medicine, University of Tartu
Nooruse 1, 50411, Tartu, Eesti
Phone +372 737 5286
E-mail kristian.semjonov@ut.ee

Education

2006–2009 Jõhvi Gymnasium
2009–2014 University of Tartu, Faculty of Medicine, Institute of Pharmacy (MSc)
2014– University of Tartu, Faculty of Medicine, PhD studies in pharmacy (PhD)

Scientific awards

2017 Faculty of Medicine 385th anniversary conference best oral presentation award among doctoral students

Professional employment

2017–2018 University of Tartu, Institute of Pharmacy, Junior Research Fellow

Scientific work

A total of 4 publications have been prepared, 8 oral talks and 9 poster presentation have been held on international conferences.

Research activity

Solid-state physicochemical properties, pharmaceutical excipients characterization and functionality investigation, drug release from drug delivery systems.

ELULOOKIRJELDUS

Nimi Kristian Semjonov
Sünniaeg 7. august 1990
Aadress Farmaatsia instituut, Meditsiiniteaduste valdkond, Tartu Ülikool
Nooruse 1, 50411, Tartu, Eesti
Telefon +372 737 5286
E-mail kristian.semjonov@ut.ee

Hariduskäik

2006–2009 Jõhvi Gümnaasium
2009–2014 Tartu Ülikool, Meditsiiniteaduste valdkond, farmaatsia instituut (MSc)
2014– Tartu Ülikool, Meditsiiniteaduste valdkond, doktorant farmaatsia erialal (PhD)

Teaduspreemiad ja tunnustused

2017 Meditsiiniteaduste valdkonna 385. aastapäeva teaduskonverentsi parim doktorantide suuline ettekanne

Erialane teenistuskäik

2017–2018 Tartu Ülikool, farmaatsia instituut, nooremteadur

Teadustegevus

Kokku on ilmunud 4 publikatsiooni, peetud 8 suulist ja 9 stendiettekannet rahvusvahelistel konverentsidel.

Uurimisvaldkond

Tahkete toimeainete füsikokeemilised omadused, abiainetete karakteriseerimine ja funktsionaalsuse uurimine, toimeaine vabanemine ravimkandursüsteemidest

DISSERTATIONES MEDICINAE UNIVERSITATIS TARTUENSIS

1. **Heidi-Ingrid Maaroos.** The natural course of gastric ulcer in connection with chronic gastritis and *Helicobacter pylori*. Tartu, 1991.
2. **Mihkel Zilmer.** Na-pump in normal and tumorous brain tissues: Structural, functional and tumorigenesis aspects. Tartu, 1991.
3. **Eero Vasar.** Role of cholecystokinin receptors in the regulation of behaviour and in the action of haloperidol and diazepam. Tartu, 1992.
4. **Tiina Talvik.** Hypoxic-ischaemic brain damage in neonates (clinical, biochemical and brain computed tomographical investigation). Tartu, 1992.
5. **Ants Peetsalu.** Vagotomy in duodenal ulcer disease: A study of gastric acidity, serum pepsinogen I, gastric mucosal histology and *Helicobacter pylori*. Tartu, 1992.
6. **Marika Mikelsaar.** Evaluation of the gastrointestinal microbial ecosystem in health and disease. Tartu, 1992.
7. **Hele Everaus.** Immuno-hormonal interactions in chronic lymphocytic leukaemia and multiple myeloma. Tartu, 1993.
8. **Ruth Mikelsaar.** Etiological factors of diseases in genetically consulted children and newborn screening: dissertation for the commencement of the degree of doctor of medical sciences. Tartu, 1993.
9. **Agu Tamm.** On metabolic action of intestinal microflora: clinical aspects. Tartu, 1993.
10. **Katrin Gross.** Multiple sclerosis in South-Estonia (epidemiological and computed tomographical investigations). Tartu, 1993.
11. **Oivi Uiho.** Childhood coeliac disease in Estonia: occurrence, screening, diagnosis and clinical characterization. Tartu, 1994.
12. **Viiu Tuulik.** The functional disorders of central nervous system of chemistry workers. Tartu, 1994.
13. **Margus Viigimaa.** Primary haemostasis, antiaggregative and anticoagulant treatment of acute myocardial infarction. Tartu, 1994.
14. **Rein Kolk.** Atrial versus ventricular pacing in patients with sick sinus syndrome. Tartu, 1994.
15. **Toomas Podar.** Incidence of childhood onset type 1 diabetes mellitus in Estonia. Tartu, 1994.
16. **Kiira Subi.** The laboratory surveillance of the acute respiratory viral infections in Estonia. Tartu, 1995.
17. **Irja Lutsar.** Infections of the central nervous system in children (epidemiologic, diagnostic and therapeutic aspects, long term outcome). Tartu, 1995.
18. **Aavo Lang.** The role of dopamine, 5-hydroxytryptamine, sigma and NMDA receptors in the action of antipsychotic drugs. Tartu, 1995.
19. **Andrus Arak.** Factors influencing the survival of patients after radical surgery for gastric cancer. Tartu, 1996.

20. **Tõnis Karki.** Quantitative composition of the human lactoflora and method for its examination. Tartu, 1996.
21. **Reet Mändar.** Vaginal microflora during pregnancy and its transmission to newborn. Tartu, 1996.
22. **Triin Remmel.** Primary biliary cirrhosis in Estonia: epidemiology, clinical characterization and prognostication of the course of the disease. Tartu, 1996.
23. **Toomas Kivastik.** Mechanisms of drug addiction: focus on positive reinforcing properties of morphine. Tartu, 1996.
24. **Paavo Pokk.** Stress due to sleep deprivation: focus on GABA_A receptor-chloride ionophore complex. Tartu, 1996.
25. **Kristina Allikmets.** Renin system activity in essential hypertension. Associations with atherothrombogenic cardiovascular risk factors and with the efficacy of calcium antagonist treatment. Tartu, 1996.
26. **Triin Parik.** Oxidative stress in essential hypertension: Associations with metabolic disturbances and the effects of calcium antagonist treatment. Tartu, 1996.
27. **Svetlana Päi.** Factors promoting heterogeneity of the course of rheumatoid arthritis. Tartu, 1997.
28. **Maarike Sallo.** Studies on habitual physical activity and aerobic fitness in 4 to 10 years old children. Tartu, 1997.
29. **Paul Naaber.** *Clostridium difficile* infection and intestinal microbial ecology. Tartu, 1997.
30. **Rein Pähkla.** Studies in pinoline pharmacology. Tartu, 1997.
31. **Andrus Juhan Voitk.** Outpatient laparoscopic cholecystectomy. Tartu, 1997.
32. **Joel Starkopf.** Oxidative stress and ischaemia-reperfusion of the heart. Tartu, 1997.
33. **Janika Kõrv.** Incidence, case-fatality and outcome of stroke. Tartu, 1998.
34. **Ülla Linnamägi.** Changes in local cerebral blood flow and lipid peroxidation following lead exposure in experiment. Tartu, 1998.
35. **Ave Minajeva.** Sarcoplasmic reticulum function: comparison of atrial and ventricular myocardium. Tartu, 1998.
36. **Oleg Milenin.** Reconstruction of cervical part of esophagus by revascularised ileal autografts in dogs. A new complex multistage method. Tartu, 1998.
37. **Sergei Pakriev.** Prevalence of depression, harmful use of alcohol and alcohol dependence among rural population in Udmurtia. Tartu, 1998.
38. **Allen Kaasik.** Thyroid hormone control over β -adrenergic signalling system in rat atria. Tartu, 1998.
39. **Vallo Matto.** Pharmacological studies on anxiogenic and antiaggressive properties of antidepressants. Tartu, 1998.
40. **Maire Vasar.** Allergic diseases and bronchial hyperreactivity in Estonian children in relation to environmental influences. Tartu, 1998.
41. **Kaja Julge.** Humoral immune responses to allergens in early childhood. Tartu, 1998.

42. **Heli Grünberg**. The cardiovascular risk of Estonian schoolchildren. A cross-sectional study of 9-, 12- and 15-year-old children. Tartu, 1998.
43. **Epp Sepp**. Formation of intestinal microbial ecosystem in children. Tartu, 1998.
44. **Mai Ots**. Characteristics of the progression of human and experimental glomerulopathies. Tartu, 1998.
45. **Tiina Ristimäe**. Heart rate variability in patients with coronary artery disease. Tartu, 1998.
46. **Leho Kõiv**. Reaction of the sympatho-adrenal and hypothalamo-pituitary-adrenocortical system in the acute stage of head injury. Tartu, 1998.
47. **Bela Adojaan**. Immune and genetic factors of childhood onset IDDM in Estonia. An epidemiological study. Tartu, 1999.
48. **Jakov Shlik**. Psychophysiological effects of cholecystokinin in humans. Tartu, 1999.
49. **Kai Kisand**. Autoantibodies against dehydrogenases of α -ketoacids. Tartu, 1999.
50. **Toomas Marandi**. Drug treatment of depression in Estonia. Tartu, 1999.
51. **Ants Kask**. Behavioural studies on neuropeptide Y. Tartu, 1999.
52. **Ello-Rahel Karelson**. Modulation of adenylate cyclase activity in the rat hippocampus by neuropeptide galanin and its chimeric analogs. Tartu, 1999.
53. **Tanel Laisaar**. Treatment of pleural empyema — special reference to intrapleural therapy with streptokinase and surgical treatment modalities. Tartu, 1999.
54. **Eve Pihl**. Cardiovascular risk factors in middle-aged former athletes. Tartu, 1999.
55. **Katrin Õunap**. Phenylketonuria in Estonia: incidence, newborn screening, diagnosis, clinical characterization and genotype/phenotype correlation. Tartu, 1999.
56. **Siiri Kõljalg**. *Acinetobacter* – an important nosocomial pathogen. Tartu, 1999.
57. **Helle Karro**. Reproductive health and pregnancy outcome in Estonia: association with different factors. Tartu, 1999.
58. **Heili Varendi**. Behavioral effects observed in human newborns during exposure to naturally occurring odors. Tartu, 1999.
59. **Anneli Beilmann**. Epidemiology of epilepsy in children and adolescents in Estonia. Prevalence, incidence, and clinical characteristics. Tartu, 1999.
60. **Vallo Volke**. Pharmacological and biochemical studies on nitric oxide in the regulation of behaviour. Tartu, 1999.
61. **Pilvi Ilves**. Hypoxic-ischaemic encephalopathy in asphyxiated term infants. A prospective clinical, biochemical, ultrasonographical study. Tartu, 1999.
62. **Anti Kalda**. Oxygen-glucose deprivation-induced neuronal death and its pharmacological prevention in cerebellar granule cells. Tartu, 1999.
63. **Eve-Irene Lepist**. Oral peptide prodrugs – studies on stability and absorption. Tartu, 2000.

64. **Jana Kivastik.** Lung function in Estonian schoolchildren: relationship with anthropometric indices and respiratory symptoms, reference values for dynamic spirometry. Tartu, 2000.
65. **Karin Kull.** Inflammatory bowel disease: an immunogenetic study. Tartu, 2000.
66. **Kaire Innos.** Epidemiological resources in Estonia: data sources, their quality and feasibility of cohort studies. Tartu, 2000.
67. **Tamara Vorobjova.** Immune response to *Helicobacter pylori* and its association with dynamics of chronic gastritis and epithelial cell turnover in antrum and corpus. Tartu, 2001.
68. **Ruth Kalda.** Structure and outcome of family practice quality in the changing health care system of Estonia. Tartu, 2001.
69. **Annika Krüüner.** *Mycobacterium tuberculosis* – spread and drug resistance in Estonia. Tartu, 2001.
70. **Marlit Veldi.** Obstructive Sleep Apnoea: Computerized Endopharyngeal Myotonometry of the Soft Palate and Lingual Musculature. Tartu, 2001.
71. **Anneli Uusküla.** Epidemiology of sexually transmitted diseases in Estonia in 1990–2000. Tartu, 2001.
72. **Ade Kallas.** Characterization of antibodies to coagulation factor VIII. Tartu, 2002.
73. **Heidi Annuk.** Selection of medicinal plants and intestinal lactobacilli as antimicrobial components for functional foods. Tartu, 2002.
74. **Aet Lukmann.** Early rehabilitation of patients with ischaemic heart disease after surgical revascularization of the myocardium: assessment of health-related quality of life, cardiopulmonary reserve and oxidative stress. A clinical study. Tartu, 2002.
75. **Maigi Eisen.** Pathogenesis of Contact Dermatitis: participation of Oxidative Stress. A clinical – biochemical study. Tartu, 2002.
76. **Piret Hussar.** Histology of the post-traumatic bone repair in rats. Elaboration and use of a new standardized experimental model – bicortical perforation of tibia compared to internal fracture and resection osteotomy. Tartu, 2002.
77. **Tõnu Rätsep.** Aneurysmal subarachnoid haemorrhage: Noninvasive monitoring of cerebral haemodynamics. Tartu, 2002.
78. **Marju Herodes.** Quality of life of people with epilepsy in Estonia. Tartu, 2003.
79. **Katre Maasalu.** Changes in bone quality due to age and genetic disorders and their clinical expressions in Estonia. Tartu, 2003.
80. **Toomas Sillakivi.** Perforated peptic ulcer in Estonia: epidemiology, risk factors and relations with *Helicobacter pylori*. Tartu, 2003.
81. **Leena Puksa.** Late responses in motor nerve conduction studies. F and A waves in normal subjects and patients with neuropathies. Tartu, 2003.
82. **Krista Lõivukene.** *Helicobacter pylori* in gastric microbial ecology and its antimicrobial susceptibility pattern. Tartu, 2003.

83. **Helgi Kolk.** Dyspepsia and *Helicobacter pylori* infection: the diagnostic value of symptoms, treatment and follow-up of patients referred for upper gastrointestinal endoscopy by family physicians. Tartu, 2003.
84. **Helena Soomer.** Validation of identification and age estimation methods in forensic odontology. Tartu, 2003.
85. **Kersti Oselin.** Studies on the human MDR1, MRP1, and MRP2 ABC transporters: functional relevance of the genetic polymorphisms in the *MDR1* and *MRP1* gene. Tartu, 2003.
86. **Jaan Soplepmann.** Peptic ulcer haemorrhage in Estonia: epidemiology, prognostic factors, treatment and outcome. Tartu, 2003.
87. **Margot Peetsalu.** Long-term follow-up after vagotomy in duodenal ulcer disease: recurrent ulcer, changes in the function, morphology and *Helicobacter pylori* colonisation of the gastric mucosa. Tartu, 2003.
88. **Kersti Klaamas.** Humoral immune response to *Helicobacter pylori* a study of host-dependent and microbial factors. Tartu, 2003.
89. **Pille Taba.** Epidemiology of Parkinson's disease in Tartu, Estonia. Prevalence, incidence, clinical characteristics, and pharmacoepidemiology. Tartu, 2003.
90. **Alar Veraksitš.** Characterization of behavioural and biochemical phenotype of cholecystokinin-2 receptor deficient mice: changes in the function of the dopamine and endopioidergic system. Tartu, 2003.
91. **Ingrid Kalev.** CC-chemokine receptor 5 (CCR5) gene polymorphism in Estonians and in patients with Type I and Type II diabetes mellitus. Tartu, 2003.
92. **Lumme Kadaja.** Molecular approach to the regulation of mitochondrial function in oxidative muscle cells. Tartu, 2003.
93. **Aive Liigant.** Epidemiology of primary central nervous system tumours in Estonia from 1986 to 1996. Clinical characteristics, incidence, survival and prognostic factors. Tartu, 2004.
94. **Andres, Kulla.** Molecular characteristics of mesenchymal stroma in human astrocytic gliomas. Tartu, 2004.
95. **Mari Järvelaid.** Health damaging risk behaviours in adolescence. Tartu, 2004.
96. **Ülle Pechter.** Progression prevention strategies in chronic renal failure and hypertension. An experimental and clinical study. Tartu, 2004.
97. **Gunnar Tasa.** Polymorphic glutathione S-transferases – biology and role in modifying genetic susceptibility to senile cataract and primary open angle glaucoma. Tartu, 2004.
98. **Tuuli Käämbre.** Intracellular energetic unit: structural and functional aspects. Tartu, 2004.
99. **Vitali Vassiljev.** Influence of nitric oxide syntase inhibitors on the effects of ethanol after acute and chronic ethanol administration and withdrawal. Tartu, 2004.

100. **Aune Rehema.** Assessment of nonhaem ferrous iron and glutathione redox ratio as markers of pathogeneticity of oxidative stress in different clinical groups. Tartu, 2004.
101. **Evelin Seppet.** Interaction of mitochondria and ATPases in oxidative muscle cells in normal and pathological conditions. Tartu, 2004.
102. **Eduard Maron.** Serotonin function in panic disorder: from clinical experiments to brain imaging and genetics. Tartu, 2004.
103. **Marje Oona.** *Helicobacter pylori* infection in children: epidemiological and therapeutic aspects. Tartu, 2004.
104. **Kersti Kokk.** Regulation of active and passive molecular transport in the testis. Tartu, 2005.
105. **Vladimir Järv.** Cross-sectional imaging for pretreatment evaluation and follow-up of pelvic malignant tumours. Tartu, 2005.
106. **Andre Õun.** Epidemiology of adult epilepsy in Tartu, Estonia. Incidence, prevalence and medical treatment. Tartu, 2005.
107. **Piibe Muda.** Homocysteine and hypertension: associations between homocysteine and essential hypertension in treated and untreated hypertensive patients with and without coronary artery disease. Tartu, 2005.
108. **Küllli Kingo.** The interleukin-10 family cytokines gene polymorphisms in plaque psoriasis. Tartu, 2005.
109. **Mati Merila.** Anatomy and clinical relevance of the glenohumeral joint capsule and ligaments. Tartu, 2005.
110. **Epp Songisepp.** Evaluation of technological and functional properties of the new probiotic *Lactobacillus fermentum* ME-3. Tartu, 2005.
111. **Tiia Ainla.** Acute myocardial infarction in Estonia: clinical characteristics, management and outcome. Tartu, 2005.
112. **Andres Sell.** Determining the minimum local anaesthetic requirements for hip replacement surgery under spinal anaesthesia – a study employing a spinal catheter. Tartu, 2005.
113. **Tiia Tamme.** Epidemiology of odontogenic tumours in Estonia. Pathogenesis and clinical behaviour of ameloblastoma. Tartu, 2005.
114. **Triine Annus.** Allergy in Estonian schoolchildren: time trends and characteristics. Tartu, 2005.
115. **Tiia Voor.** Microorganisms in infancy and development of allergy: comparison of Estonian and Swedish children. Tartu, 2005.
116. **Priit Kasenõmm.** Indicators for tonsillectomy in adults with recurrent tonsillitis – clinical, microbiological and pathomorphological investigations. Tartu, 2005.
117. **Eva Zusinaite.** Hepatitis C virus: genotype identification and interactions between viral proteases. Tartu, 2005.
118. **Piret Köll.** Oral lactoflora in chronic periodontitis and periodontal health. Tartu, 2006.
119. **Tiina Stelmach.** Epidemiology of cerebral palsy and unfavourable neuro-developmental outcome in child population of Tartu city and county, Estonia Prevalence, clinical features and risk factors. Tartu, 2006.

120. **Katrin Pudersell.** Tropane alkaloid production and riboflavine excretion in the field and tissue cultures of henbane (*Hyoscyamus niger* L.). Tartu, 2006.
121. **Küllli Jaako.** Studies on the role of neurogenesis in brain plasticity. Tartu, 2006.
122. **Aare Märtson.** Lower limb lengthening: experimental studies of bone regeneration and long-term clinical results. Tartu, 2006.
123. **Heli Tähepõld.** Patient consultation in family medicine. Tartu, 2006.
124. **Stanislav Liskmann.** Peri-implant disease: pathogenesis, diagnosis and treatment in view of both inflammation and oxidative stress profiling. Tartu, 2006.
125. **Ruth Rudissaar.** Neuropharmacology of atypical antipsychotics and an animal model of psychosis. Tartu, 2006.
126. **Helena Andreson.** Diversity of *Helicobacter pylori* genotypes in Estonian patients with chronic inflammatory gastric diseases. Tartu, 2006.
127. **Katrin Pruus.** Mechanism of action of antidepressants: aspects of serotonergic system and its interaction with glutamate. Tartu, 2006.
128. **Priit Pöder.** Clinical and experimental investigation: relationship of ischaemia/reperfusion injury with oxidative stress in abdominal aortic aneurysm repair and in extracranial brain artery endarterectomy and possibilities of protection against ischaemia using a glutathione analogue in a rat model of global brain ischaemia. Tartu, 2006.
129. **Marika Tammaru.** Patient-reported outcome measurement in rheumatoid arthritis. Tartu, 2006.
130. **Tiia Reimand.** Down syndrome in Estonia. Tartu, 2006.
131. **Diva Eensoo.** Risk-taking in traffic and Markers of Risk-Taking Behaviour in Schoolchildren and Car Drivers. Tartu, 2007.
132. **Riina Vibo.** The third stroke registry in Tartu, Estonia from 2001 to 2003: incidence, case-fatality, risk factors and long-term outcome. Tartu, 2007.
133. **Chris Pruunsild.** Juvenile idiopathic arthritis in children in Estonia. Tartu, 2007.
134. **Eve Õiglane-Šlik.** Angelman and Prader-Willi syndromes in Estonia. Tartu, 2007.
135. **Kadri Haller.** Antibodies to follicle stimulating hormone. Significance in female infertility. Tartu, 2007.
136. **Pille Ööpik.** Management of depression in family medicine. Tartu, 2007.
137. **Jaak Kals.** Endothelial function and arterial stiffness in patients with atherosclerosis and in healthy subjects. Tartu, 2007.
138. **Priit Kampus.** Impact of inflammation, oxidative stress and age on arterial stiffness and carotid artery intima-media thickness. Tartu, 2007.
139. **Margus Punab.** Male fertility and its risk factors in Estonia. Tartu, 2007.
140. **Alar Toom.** Heterotopic ossification after total hip arthroplasty: clinical and pathogenetic investigation. Tartu, 2007.

141. **Lea Pehme.** Epidemiology of tuberculosis in Estonia 1991–2003 with special regard to extrapulmonary tuberculosis and delay in diagnosis of pulmonary tuberculosis. Tartu, 2007.
142. **Juri Karjagin.** The pharmacokinetics of metronidazole and meropenem in septic shock. Tartu, 2007.
143. **Inga Talvik.** Inflicted traumatic brain injury shaken baby syndrome in Estonia – epidemiology and outcome. Tartu, 2007.
144. **Tarvo Rajasalu.** Autoimmune diabetes: an immunological study of type 1 diabetes in humans and in a model of experimental diabetes (in RIP-B7.1 mice). Tartu, 2007.
145. **Inga Karu.** Ischaemia-reperfusion injury of the heart during coronary surgery: a clinical study investigating the effect of hyperoxia. Tartu, 2007.
146. **Peeter Padrik.** Renal cell carcinoma: Changes in natural history and treatment of metastatic disease. Tartu, 2007.
147. **Neve Vendt.** Iron deficiency and iron deficiency anaemia in infants aged 9 to 12 months in Estonia. Tartu, 2008.
148. **Lenne-Triin Heidmets.** The effects of neurotoxins on brain plasticity: focus on neural Cell Adhesion Molecule. Tartu, 2008.
149. **Paul Korrovits.** Asymptomatic inflammatory prostatitis: prevalence, etiological factors, diagnostic tools. Tartu, 2008.
150. **Annika Reintam.** Gastrointestinal failure in intensive care patients. Tartu, 2008.
151. **Kristiina Roots.** Cationic regulation of Na-pump in the normal, Alzheimer's and CCK₂ receptor-deficient brain. Tartu, 2008.
152. **Helen Puusepp.** The genetic causes of mental retardation in Estonia: fragile X syndrome and creatine transporter defect. Tartu, 2009.
153. **Kristiina Rull.** Human chorionic gonadotropin beta genes and recurrent miscarriage: expression and variation study. Tartu, 2009.
154. **Margus Eimre.** Organization of energy transfer and feedback regulation in oxidative muscle cells. Tartu, 2009.
155. **Maire Link.** Transcription factors FoxP3 and AIRE: autoantibody associations. Tartu, 2009.
156. **Kai Haldre.** Sexual health and behaviour of young women in Estonia. Tartu, 2009.
157. **Kaur Liivak.** Classical form of congenital adrenal hyperplasia due to 21-hydroxylase deficiency in Estonia: incidence, genotype and phenotype with special attention to short-term growth and 24-hour blood pressure. Tartu, 2009.
158. **Kersti Ehrlich.** Antioxidative glutathione analogues (UPF peptides) – molecular design, structure-activity relationships and testing the protective properties. Tartu, 2009.
159. **Anneli Rätsep.** Type 2 diabetes care in family medicine. Tartu, 2009.
160. **Silver Türk.** Etiopathogenetic aspects of chronic prostatitis: role of mycoplasmas, coryneform bacteria and oxidative stress. Tartu, 2009.

161. **Kaire Heilman.** Risk markers for cardiovascular disease and low bone mineral density in children with type 1 diabetes. Tartu, 2009.
162. **Kristi Rüütel.** HIV-epidemic in Estonia: injecting drug use and quality of life of people living with HIV. Tartu, 2009.
163. **Triin Eller.** Immune markers in major depression and in antidepressive treatment. Tartu, 2009.
164. **Siim Suutre.** The role of TGF- β isoforms and osteoprogenitor cells in the pathogenesis of heterotopic ossification. An experimental and clinical study of hip arthroplasty. Tartu, 2010.
165. **Kai Kliiman.** Highly drug-resistant tuberculosis in Estonia: Risk factors and predictors of poor treatment outcome. Tartu, 2010.
166. **Inga Villa.** Cardiovascular health-related nutrition, physical activity and fitness in Estonia. Tartu, 2010.
167. **Tõnis Org.** Molecular function of the first PHD finger domain of Auto-immune Regulator protein. Tartu, 2010.
168. **Tuuli Metsvaht.** Optimal antibacterial therapy of neonates at risk of early onset sepsis. Tartu, 2010.
169. **Jaanus Kahu.** Kidney transplantation: Studies on donor risk factors and mycophenolate mofetil. Tartu, 2010.
170. **Koit Reimand.** Autoimmunity in reproductive failure: A study on associated autoantibodies and autoantigens. Tartu, 2010.
171. **Mart Kull.** Impact of vitamin D and hypolactasia on bone mineral density: a population based study in Estonia. Tartu, 2010.
172. **Rael Laugesaar.** Stroke in children – epidemiology and risk factors. Tartu, 2010.
173. **Mark Braschinsky.** Epidemiology and quality of life issues of hereditary spastic paraplegia in Estonia and implementation of genetic analysis in everyday neurologic practice. Tartu, 2010.
174. **Kadri Suija.** Major depression in family medicine: associated factors, recurrence and possible intervention. Tartu, 2010.
175. **Jarno Habicht.** Health care utilisation in Estonia: socioeconomic determinants and financial burden of out-of-pocket payments. Tartu, 2010.
176. **Kristi Abram.** The prevalence and risk factors of rosacea. Subjective disease perception of rosacea patients. Tartu, 2010.
177. **Malle Kuum.** Mitochondrial and endoplasmic reticulum cation fluxes: Novel roles in cellular physiology. Tartu, 2010.
178. **Rita Teek.** The genetic causes of early onset hearing loss in Estonian children. Tartu, 2010.
179. **Daisy Volmer.** The development of community pharmacy services in Estonia – public and professional perceptions 1993–2006. Tartu, 2010.
180. **Jelena Lissitsina.** Cytogenetic causes in male infertility. Tartu, 2011.
181. **Delia Lepik.** Comparison of gunshot injuries caused from Tokarev, Makarov and Glock 19 pistols at different firing distances. Tartu, 2011.
182. **Ene-Renate Pähkla.** Factors related to the efficiency of treatment of advanced periodontitis. Tartu, 2011.

183. **Maarja Krass.** L-Arginine pathways and antidepressant action. Tartu, 2011.
184. **Taavi Lai.** Population health measures to support evidence-based health policy in Estonia. Tartu, 2011.
185. **Tiit Salum.** Similarity and difference of temperature-dependence of the brain sodium pump in normal, different neuropathological, and aberrant conditions and its possible reasons. Tartu, 2011.
186. **Tõnu Vooder.** Molecular differences and similarities between histological subtypes of non-small cell lung cancer. Tartu, 2011.
187. **Jelena Štšepetova.** The characterisation of intestinal lactic acid bacteria using bacteriological, biochemical and molecular approaches. Tartu, 2011.
188. **Radko Avi.** Natural polymorphisms and transmitted drug resistance in Estonian HIV-1 CRF06_cpx and its recombinant viruses. Tartu, 2011, 116 p.
189. **Edward Laane.** Multiparameter flow cytometry in haematological malignancies. Tartu, 2011, 152 p.
190. **Triin Jagomägi.** A study of the genetic etiology of nonsyndromic cleft lip and palate. Tartu, 2011, 158 p.
191. **Ivo Laidmäe.** Fibrin glue of fish (*Salmo salar*) origin: immunological study and development of new pharmaceutical preparation. Tartu, 2012, 150 p.
192. **Ülle Parm.** Early mucosal colonisation and its role in prediction of invasive infection in neonates at risk of early onset sepsis. Tartu, 2012, 168 p.
193. **Kaupo Teesalu.** Autoantibodies against desmin and transglutaminase 2 in celiac disease: diagnostic and functional significance. Tartu, 2012, 142 p.
194. **Maksim Zagura.** Biochemical, functional and structural profiling of arterial damage in atherosclerosis. Tartu, 2012, 162 p.
195. **Vivian Kont.** Autoimmune regulator: characterization of thymic gene regulation and promoter methylation. Tartu, 2012, 134 p.
196. **Pirje Hütt.** Functional properties, persistence, safety and efficacy of potential probiotic lactobacilli. Tartu, 2012, 246 p.
197. **Innar Tõru.** Serotonergic modulation of CCK-4- induced panic. Tartu, 2012, 132 p.
198. **Sigrid Vorobjov.** Drug use, related risk behaviour and harm reduction interventions utilization among injecting drug users in Estonia: implications for drug policy. Tartu, 2012, 120 p.
199. **Martin Serg.** Therapeutic aspects of central haemodynamics, arterial stiffness and oxidative stress in hypertension. Tartu, 2012, 156 p.
200. **Jaanika Kumm.** Molecular markers of articular tissues in early knee osteoarthritis: a population-based longitudinal study in middle-aged subjects. Tartu, 2012, 159 p.
201. **Kertu Rünkorg.** Functional changes of dopamine, endopioid and endocannabinoid systems in CCK2 receptor deficient mice. Tartu, 2012, 125 p.
202. **Mai Blöndal.** Changes in the baseline characteristics, management and outcomes of acute myocardial infarction in Estonia. Tartu, 2012, 127 p.

203. **Jana Lass.** Epidemiological and clinical aspects of medicines use in children in Estonia. Tartu, 2012, 170 p.
204. **Kai Truusalu.** Probiotic lactobacilli in experimental persistent *Salmonella* infection. Tartu, 2013, 139 p.
205. **Oksana Jagur.** Temporomandibular joint diagnostic imaging in relation to pain and bone characteristics. Long-term results of arthroscopic treatment. Tartu, 2013, 126 p.
206. **Katrin Sikk.** Manganese-ephedrone intoxication – pathogenesis of neurological damage and clinical symptomatology. Tartu, 2013, 125 p.
207. **Kai Blöndal.** Tuberculosis in Estonia with special emphasis on drug-resistant tuberculosis: Notification rate, disease recurrence and mortality. Tartu, 2013, 151 p.
208. **Marju Puurand.** Oxidative phosphorylation in different diseases of gastric mucosa. Tartu, 2013, 123 p.
209. **Aili Tagoma.** Immune activation in female infertility: Significance of autoantibodies and inflammatory mediators. Tartu, 2013, 135 p.
210. **Liis Sabre.** Epidemiology of traumatic spinal cord injury in Estonia. Brain activation in the acute phase of traumatic spinal cord injury. Tartu, 2013, 135 p.
211. **Merit Lamp.** Genetic susceptibility factors in endometriosis. Tartu, 2013, 125 p.
212. **Erik Salum.** Beneficial effects of vitamin D and angiotensin II receptor blocker on arterial damage. Tartu, 2013, 167 p.
213. **Maire Karelson.** Vitiligo: clinical aspects, quality of life and the role of melanocortin system in pathogenesis. Tartu, 2013, 153 p.
214. **Kuldar Kaljurand.** Prevalence of exfoliation syndrome in Estonia and its clinical significance. Tartu, 2013, 113 p.
215. **Raido Paasma.** Clinical study of methanol poisoning: handling large outbreaks, treatment with antidotes, and long-term outcomes. Tartu, 2013, 96 p.
216. **Anne Kleinberg.** Major depression in Estonia: prevalence, associated factors, and use of health services. Tartu, 2013, 129 p.
217. **Triin Eglit.** Obesity, impaired glucose regulation, metabolic syndrome and their associations with high-molecular-weight adiponectin levels. Tartu, 2014, 115 p.
218. **Kristo Ausmees.** Reproductive function in middle-aged males: Associations with prostate, lifestyle and couple infertility status. Tartu, 2014, 125 p.
219. **Kristi Huik.** The influence of host genetic factors on the susceptibility to HIV and HCV infections among intravenous drug users. Tartu, 2014, 144 p.
220. **Liina Tserel.** Epigenetic profiles of monocytes, monocyte-derived macrophages and dendritic cells. Tartu, 2014, 143 p.
221. **Irina Kerna.** The contribution of *ADAM12* and *CILP* genes to the development of knee osteoarthritis. Tartu, 2014, 152 p.

222. **Ingrid Liiv.** Autoimmune regulator protein interaction with DNA-dependent protein kinase and its role in apoptosis. Tartu, 2014, 143 p.
223. **Liivi Maddison.** Tissue perfusion and metabolism during intra-abdominal hypertension. Tartu, 2014, 103 p.
224. **Krista Ress.** Childhood coeliac disease in Estonia, prevalence in atopic dermatitis and immunological characterisation of coexistence. Tartu, 2014, 124 p.
225. **Kai Muru.** Prenatal screening strategies, long-term outcome of children with marked changes in maternal screening tests and the most common syndromic heart anomalies in Estonia. Tartu, 2014, 189 p.
226. **Kaja Rahu.** Morbidity and mortality among Baltic Chernobyl cleanup workers: a register-based cohort study. Tartu, 2014, 155 p.
227. **Klari Noormets.** The development of diabetes mellitus, fertility and energy metabolism disturbances in a Wfs1-deficient mouse model of Wolfram syndrome. Tartu, 2014, 132 p.
228. **Liis Toome.** Very low gestational age infants in Estonia. Tartu, 2014, 183 p.
229. **Ceith Nikkolo.** Impact of different mesh parameters on chronic pain and foreign body feeling after open inguinal hernia repair. Tartu, 2014, 132 p.
230. **Vadim Brjalin.** Chronic hepatitis C: predictors of treatment response in Estonian patients. Tartu, 2014, 122 p.
231. **Vahur Metsna.** Anterior knee pain in patients following total knee arthroplasty: the prevalence, correlation with patellar cartilage impairment and aspects of patellofemoral congruence. Tartu, 2014, 130 p.
232. **Marju Kase.** Glioblastoma multiforme: possibilities to improve treatment efficacy. Tartu, 2015, 137 p.
233. **Riina Runnel.** Oral health among elementary school children and the effects of polyol candies on the prevention of dental caries. Tartu, 2015, 112 p.
234. **Made Laanpere.** Factors influencing women's sexual health and reproductive choices in Estonia. Tartu, 2015, 176 p.
235. **Andres Lust.** Water mediated solid state transformations of a polymorphic drug – effect on pharmaceutical product performance. Tartu, 2015, 134 p.
236. **Anna Klugman.** Functionality related characterization of pretreated wood lignin, cellulose and polyvinylpyrrolidone for pharmaceutical applications. Tartu, 2015, 156 p.
237. **Triin Laisk-Podar.** Genetic variation as a modulator of susceptibility to female infertility and a source for potential biomarkers. Tartu, 2015, 155 p.
238. **Mailis Tõnisson.** Clinical picture and biochemical changes in blood in children with acute alcohol intoxication. Tartu, 2015, 100 p.
239. **Kadri Tamme.** High volume haemodiafiltration in treatment of severe sepsis – impact on pharmacokinetics of antibiotics and inflammatory response. Tartu, 2015, 133 p.

240. **Kai Part.** Sexual health of young people in Estonia in a social context: the role of school-based sexuality education and youth-friendly counseling services. Tartu, 2015, 203 p.
241. **Urve Paaver.** New perspectives for the amorphization and physical stabilization of poorly water-soluble drugs and understanding their dissolution behavior. Tartu, 2015, 139 p.
242. **Aleksandr Peet.** Intrauterine and postnatal growth in children with HLA-conferred susceptibility to type 1 diabetes. Tartu. 2015, 146 p.
243. **Piret Mitt.** Healthcare-associated infections in Estonia – epidemiology and surveillance of bloodstream and surgical site infections. Tartu, 2015, 145 p.
244. **Merli Saare.** Molecular Profiling of Endometriotic Lesions and Endometriosis of Endometriosis Patients. Tartu, 2016, 129 p.
245. **Kaja-Triin Laisaar.** People living with HIV in Estonia: Engagement in medical care and methods of increasing adherence to antiretroviral therapy and safe sexual behavior. Tartu, 2016, 132 p.
246. **Eero Merilind.** Primary health care performance: impact of payment and practice-based characteristics. Tartu, 2016, 120 p.
247. **Jaanika Kärner.** Cytokine-specific autoantibodies in AIRE deficiency. Tartu, 2016, 182 p.
248. **Kaido Paapstel.** Metabolomic profile of arterial stiffness and early biomarkers of renal damage in atherosclerosis. Tartu, 2016, 173 p.
249. **Liidia Kiisk.** Long-term nutritional study: anthropometrical and clinico-laboratory assessments in renal replacement therapy patients after intensive nutritional counselling. Tartu, 2016, 207 p.
250. **Georgi Nellis.** The use of excipients in medicines administered to neonates in Europe. Tartu, 2017, 159 p.
251. **Aleksei Rakitin.** Metabolic effects of acute and chronic treatment with valproic acid in people with epilepsy. Tartu, 2017, 125 p.
252. **Eveli Kallas.** The influence of immunological markers to susceptibility to HIV, HBV, and HCV infections among persons who inject drugs. Tartu, 2017, 138 p.
253. **Tiina Freimann.** Musculoskeletal pain among nurses: prevalence, risk factors, and intervention. Tartu, 2017, 125 p.
254. **Evelyn Aaviksoo.** Sickness absence in Estonia: determinants and influence of the sick-pay cut reform. Tartu, 2017, 121 p.
255. **Kalev Nõupuu.** Autosomal-recessive Stargardt disease: phenotypic heterogeneity and genotype-phenotype associations. Tartu, 2017, 131 p.
256. **Ho Duy Binh.** Osteogenesis imperfecta in Vietnam. Tartu, 2017, 125 p.
257. **Uku Haljasorg.** Transcriptional mechanisms in thymic central tolerance. Tartu, 2017, 147 p.
258. **Živile Riispere.** IgA Nephropathy study according to the Oxford Classification: IgA Nephropathy clinical-morphological correlations, disease progression and the effect of renoprotective therapy. Tartu, 2017, 129 p.

259. **Hiie Soeorg.** Coagulase-negative staphylococci in gut of preterm neonates and in breast milk of their mothers. Tartu, 2017, 216 p.
260. **Anne-Mari Anton Willmore.** Silver nanoparticles for cancer research. Tartu, 2017, 132 p.
261. **Ott Laius.** Utilization of osteoporosis medicines, medication adherence and the trend in osteoporosis related hip fractures in Estonia. Tartu, 2017, 134 p.
262. **Alar Aab.** Insights into molecular mechanisms of asthma and atopic dermatitis. Tartu, 2017, 164 p.
263. **Sander Pajusalu.** Genome-wide diagnostics of Mendelian disorders: from chromosomal microarrays to next-generation sequencing. Tartu, 2017, 146 p.
264. **Mikk Jürisson.** Health and economic impact of hip fracture in Estonia. Tartu, 2017, 164 p.
265. **Kaspar Tootsi.** Cardiovascular and metabolomic profiling of osteoarthritis. Tartu, 2017, 150 p.
266. **Mario Saare.** The influence of AIRE on gene expression – studies of transcriptional regulatory mechanisms in cell culture systems. Tartu, 2017, 172 p.
267. **Piia Jõgi.** Epidemiological and clinical characteristics of pertussis in Estonia. Tartu, 2018, 168 p.
268. **Elle Põldoja.** Structure and blood supply of the superior part of the shoulder joint capsule. Tartu, 2018, 116 p.
269. **Minh Son Nguyen.** Oral health status and prevalence of temporomandibular disorders in 65–74-year-olds in Vietnam. Tartu, 2018, 182 p.